

## MAGISTERARBEIT

Titel der Magisterarbeit

# **Strong Conservation Form and Grid Generation in Nonsteady Curvilinear Coordinates**

**Numerical Methods  
for Implicit Radiation Hydrodynamics in 2D and 3D**

angestrebter akademischer Grad:  
Magister der Naturwissenschaften (Mag.rer.nat.)

Verfasser: Harald Höller, Bakk.rer.nat.  
Matrikelnummer: 0104177  
Studienrichtung: Astronomie A 066 861  
Betreut von: Ao.Univ.-Prof.Dr. Ernst Dorfi

Wien, 25. März 2010



## Danksagung

Allen Menschen, Tieren und Behörden, die mich im Laufe des Studiums unterstützt haben, möchte ich herzlich danken und vielen davon ein Bussi geben.

Ich verneige mich vor meinem Betreuer Prof. Ernst Dorfi für die geduldigen und wegweisenden Diskussionen, seine fordernde Hartnäckigkeit und die vielen motivierenden Anekdoten aus der Welt der Wissenschaft.

Diese Arbeit ist *Kollegen Nonius Skala* gewidmet.

## **Erklärung**

Ich erkläre ehrenwörtlich, dass ich die vorliegende Arbeit selbständig und ohne fremde Hilfe verfasst, andere als die angegebenen Quellen nicht benutzt und die den benutzten Quellen wörtlich oder inhaltlich entnommenen Stellen als solche kenntlich gemacht habe.

Wien, am 25. März 2010

# Contents

<b>1</b>	<b>Fundamental Mathematics of RHD</b>	<b>9</b>
1.1	The Hyperbolic Part . . . . .	9
1.1.1	Hyperbolic Conservation Laws . . . . .	9
1.1.2	Weak Solutions . . . . .	11
1.1.3	Rankine-Hugoniot and Entropy Conditions . . . . .	12
1.2	The Elliptic Part . . . . .	14
1.2.1	The Poisson Equation . . . . .	15
1.2.2	Harmonic Functions and the Maximum Principle . . . . .	16
<b>2</b>	<b>Fundamental Physics of RHD</b>	<b>17</b>
2.1	Hydrodynamics . . . . .	17
2.1.1	Continuity Equation . . . . .	18
2.1.2	Equation of Motion . . . . .	18
2.1.3	Energy Equation . . . . .	19
2.2	Radiation . . . . .	20
2.2.1	The Radiation Field and its Momenta . . . . .	20
2.2.2	Interaction with Matter . . . . .	21
2.2.3	Radiation Closure Relation . . . . .	23
2.2.4	Fluid Frame . . . . .	25
2.3	Gravitation . . . . .	27
2.3.1	Self-Gravitation in 2D and 3D . . . . .	27
2.3.2	Non-Static Gravitation Equation . . . . .	28
2.4	Full Set of RHD Equations with Self-Gravitation . . . . .	30
<b>3</b>	<b>Conservative Numerics</b>	<b>31</b>
3.1	Numerical Methods for Conservation Laws . . . . .	31
3.1.1	Introduction to Discretization Methods . . . . .	31
3.1.2	Error and Stability in the Linear Case . . . . .	32
3.1.3	Conservative Methods and Lax Wendroff Theorem . . . . .	34
3.1.4	Artificial Viscosity . . . . .	37
3.1.5	Flux Limiters . . . . .	38
3.2	Conservative Methods in General Curvilinear Coordinates . . . . .	39
3.2.1	Tensor Calculus and Elementary Differential Geometry . . . . .	40

3.2.2	Strong Conservation Form . . . . .	43
3.2.3	Adaptive Grids . . . . .	47
3.2.4	Artificial Viscosity . . . . .	48
3.3	Strong Conservation Form of RHD in Spherical and Polar Coordinates . .	49
3.3.1	Continuity Equation . . . . .	50
3.3.2	Equation of Motion . . . . .	51
3.3.3	Equation of Internal Energy . . . . .	57
3.3.4	Equation of Radiation Energy . . . . .	58
3.3.5	Radiative Flux Equation . . . . .	59
<b>4</b>	<b>Orthogonal and Nonorthogonal Adaptive Grids</b>	<b>63</b>
4.1	Basic Principles of Grid Generation . . . . .	63
4.2	The Grid We Are Looking For . . . . .	64
4.3	Remarks on Grid Generation Methods . . . . .	65
4.3.1	Differential Methods . . . . .	66
4.3.2	Laplace Systems . . . . .	66
4.3.3	Conformal Mapping . . . . .	67
4.3.4	Algebraic Methods . . . . .	68
4.3.5	Equidistribution . . . . .	68
4.4	Equidistribution and Interpolation Attempt . . . . .	69
4.4.1	Toy Model . . . . .	69
4.4.2	Analysis . . . . .	71
4.5	On the Peculiarity of Orthogonal Coordinates . . . . .	72
4.6	Quasi-Polar Coordinates Attempt . . . . .	73
4.6.1	Toy Model . . . . .	73
4.6.2	Analysis . . . . .	74
4.7	Strong Conservation Form in Nonorthogonal Coordinates . . . . .	75
<b>5</b>	<b>Conclusions and Prospective</b>	<b>77</b>
<b>6</b>	<b>Appendix</b>	<b>79</b>
6.1	Arguments and Details . . . . .	79
6.1.1	Symmetry of the Stress Tensor . . . . .	79
6.1.2	Rankine-Hugoniot Conditions . . . . .	79
6.1.3	Diffusion Approximation . . . . .	81
6.1.4	Strong Conservation Form on Adaptive Grids . . . . .	81
6.2	Mathematica Files . . . . .	84

# Prologue

## Motivation

In astrophysics a multitude of systems and configurations are described with concepts from hydrodynamics coupled with gravitation, radiation and magnetism. Mathematically radiation hydrodynamics (RHD) and magnetohydrodynamics (MHD) are systems of coupled nonlinear partial differential equations. Multiple fields in astrophysics have been adopting and developing sophisticated numerical methods for solving these PDEs in various applications.

Explicit numerical schemes in computational fluid dynamics have been popular for many years and received substantial boosts due to advances in technology and parallelizing techniques. Riemann solvers and related methods are extensively adapted in 2D and 3D computations however they have one main disadvantage. An inherent limitation for time steps in explicit schemes impedes applications where various time scales are of interest. Hence a majority of these calculations emphasize on small temporal and spatial scales but fail to treat phenomena properly on very diverse scales.

Techniques for implicit numerics are computationally more expensive since they are hardly parallelizable but do not limit the increments of the scheme intrinsically. Implicit RHD in 1D has proven favorable for describing astrophysical processes on large spatial and temporal scales like nonlinear pulsation or long term development of supernovae. The idea of this thesis was to study suitable generalizations of these concepts to 2D and 3D. Additional degrees of freedom in multi-dimensional implicit RHD would disclose the treatment of large scale convection and how it interacts with rotation, mixing, the coupling of rotation and pulsation, transport of angular momentum and mass loss, interactions of discs and stars during star formation processes etc. The target of this thesis was to find the strong conservation form of the equations of radiation hydrodynamics in non-steady curvilinear coordinates and to study multi-dimensional adaptive grid generation.

## Synopsis

The Euler equations of hydrodynamics, the Maxwell equations as well as radiative transport equations are hyperbolic PDEs that connect certain densities and fluxes via conservation laws. Generally they emerge from natural symmetries that constitute major principles in mathematical physics. The numerical implementation of these equations essentially needs to comprise these qualities. Applied mathematics have developed an articulate framework of numerical methods for conservation laws that ensure the conservation of mass, momentum, energy etc. if applied properly. The main challenge is to compute the fluxes correctly which indeed will be the issue of the first three chapters in this paper. Self gravitation is described via the Poisson equation that poses an extra challenge due to its elliptic nature. While 1D computations avoid solving this pure boundary value problem by considering an integrated form we will have to design a different approach to self gravitation in 2D and 3D.

A generalization of implicit conservative numerics to multiple dimensions requires advanced concepts of tensor analysis and differential geometry and hence a more thorough dedication to mathematical fundamentals than maybe expected at first glance. Hence we begin to discuss fundamental mathematics and physics of RHD with special focus on differential geometric consistency and study numerical methods for nonlinear conservation laws to gain a solid definition of the term *conservative*. The efforts in tensor analysis will be needed when applying *Vinokurs theorem* to gain the *strong conservation form* for conservation laws in general curvilinear coordinates. Moreover, it will be required to slightly reformulate the *artificial viscosity* for such nonlinear coordinates.

Astronomical objects are characterized by fast flows and high propagation speeds on the one hand but *astronomical* length and time scales on the other hand. Implicit numerical schemes are not affected by the *Courant Friedrichs Levy condition* which limits explicit schemes to rather impracticably small time steps. Implicit methods however produce algebraic problems that require matrix inversion which is computationally expensive. In order to achieve viable resolution, *adaptive grid techniques* have been developed. It is desired to treat processes on small length scales like shocks and ionization fronts as well as physics at the extent of the objects dimension itself like large scale convection flows and pulsations. The combination of implicit schemes and adaptive grids allows to resolve astrophysics appropriately at various scales.

In the last chapter of this paper we study problem oriented *adaptive grid generation in 2D and 3D*. We establish three main postulations for an ideal grid and analyze several feasible approaches.



# 1 Fundamental Mathematics of RHD

The equations of radiation hydrodynamics (RHD) are a system of nonlinear second order partial differential equations with hyperbolic and elliptic parts. Generally they are posed as an initial value problem with boundary conditions. The simultaneous solution of hyperbolic terms, as coming from the dynamics and the strictly elliptical Poisson equation constitute one major problem for finding suitable solution methods. In the following chapter we will retrieve the fundamental mathematics of hyperbolic conservation laws as they appear in hydrodynamics and radiation transfer as well as some basic concepts for elliptic partial differential equations like the Poisson equation in order to motivate certain numerical concepts that will arise in chapter 3. As we will see, accurate analysis provides expedient approaches to our numerical problem.

## 1.1 The Hyperbolic Part

Dynamical physical processes are mathematically described via hyperbolic partial differential equations<sup>1</sup>. The wave equation, the Burgers' equation, the equations of hydrodynamics and the Dirac equation are prominent examples of hyperbolic evolution equations. They always characterize systems with finite propagation speeds, a quality often referred to as *causality*. Information from a point in space and time is causally associated solely with a finite region, a domain of dependence. In chapter 3 we will resort to this important issue when we discuss stability and convergence of numerical methods.

In the following section we want to define some fundamental mathematical terms and present important concepts that will accompany the entire paper.

### 1.1.1 Hyperbolic Conservation Laws

The Euler equations of hydrodynamics as well as the angular moment equations of radiative transfer can be derived from conservation laws originating from one of the most fundamental theorems of mathematical physics, the Noether Theorem (see e.g. Bhutani (1981) [4], Kambe (2007) [21]). In hydrodynamics, the conservation of mass, momentum and energy leads to the continuity equation, the equation of motion and the energy equation. Analog correspondences are derived for radiation. Mathematically

---

<sup>1</sup>The Schrödinger equation of quantum mechanics is excepted.

## 1 Fundamental Mathematics of RHD

the equations of radiation hydrodynamics form a system of *hyperbolic conservation laws* that describe the interaction of a *density function*  $\mathbf{d}$

$$\mathbf{d} : \mathbb{R}^n \times [0, \infty) \rightarrow \mathbb{R}^m$$

and its *flux*  $\mathbf{f}$

$$\mathbf{f} : U \rightarrow \mathbb{R}^m, \quad U \subseteq \mathbb{R}^m, \quad U \text{ open.}$$

The temporal and spatial change of the integrated density in a connected space  $\Omega \in \mathbb{R}^n$  then equals the flux over the boundary  $\partial\Omega$ , where  $\mathbf{S}$  is the outward oriented surface element.

$$\partial_t \int_{\Omega} \mathbf{d} dV + \int_{\partial\Omega} \mathbf{f} \cdot d\mathbf{S} = \mathbf{0} \quad \forall t > 0 \quad (1.1)$$

*Hyperbolicity* is granted if the Jacobian matrix associated with the fluxes  $\nabla_{\mathbf{d}}\mathbf{f}$  has real eigenvalues and there exists a complete set of eigenvectors. Provided it is physically justified, demanding this quality on a set of equations even can help to formulate constraints to the solutions (see subsection 2.2.3).

For the in section 2.1 further motivated physical problem of hydrodynamics this system gains the following form as an example<sup>2</sup>.

$$\mathbf{d}(\mathbf{x}, t) = \begin{pmatrix} \rho(\mathbf{x}, t) \\ (\rho\mathbf{u})(\mathbf{x}, t) \\ (\rho\epsilon)(\mathbf{x}, t) \end{pmatrix}, \quad \mathbf{f}(\mathbf{d}) = \begin{pmatrix} \rho\mathbf{u} \\ \mathbf{u}\rho\mathbf{u} + \mathbf{P} \\ \rho\epsilon\mathbf{u} + \mathbf{P} \cdot \mathbf{u} \end{pmatrix} \quad (1.2)$$

$$\begin{aligned} \partial_t \int_{\Omega} \rho dV + \int_{\partial\Omega} \rho\mathbf{u} \cdot d\mathbf{S} &= 0 \\ \partial_t \int_{\Omega} \mathbf{u}\rho dV + \int_{\partial\Omega} (\mathbf{u}\rho\mathbf{u} + \mathbf{P}) \cdot d\mathbf{S} &= \mathbf{0} \\ \partial_t \int_{\Omega} \rho\epsilon dV + \int_{\partial\Omega} (\rho\epsilon\mathbf{u} + \mathbf{P} \cdot \mathbf{u}) \cdot d\mathbf{S} &= 0 \end{aligned} \quad (1.3)$$

Let  $\mathbf{f}$  be a continuously differentiable function, then we can rewrite equation (1.1) via the divergence theorem as follows.

$$\int_t \int_{\Omega} (\partial_t \mathbf{d} + \text{div } \mathbf{f}(\mathbf{d})) dV dt = \mathbf{0} \quad \forall t > 0, \Omega \subset \mathbb{R}^n \quad (1.4)$$

---

<sup>2</sup>Notation: Summations respectively projections of tensorial quantities are always denoted by  $\cdot$  or  $:$  whereas tensor products  $\otimes$  are omitted, i.e.  $\mathbf{u}\mathbf{u} = \mathbf{u} \otimes \mathbf{u}$ .

Locally the system of partial differential equations

$$\partial_t \mathbf{d} + \operatorname{div} \mathbf{f}(\mathbf{d}) = \mathbf{0} \quad (1.5)$$

gives pointwise solutions for our vector field  $\mathbf{d}$  that describes the conserved densities or state variables of mass, momentum and energy. With initial condition (or the initial state of the density function)  $\mathbf{d}_0$

$$\mathbf{d}(\mathbf{x}, 0) = \mathbf{d}_0(\mathbf{x}) \quad \forall \mathbf{x} \in \mathbb{R}^n \quad (1.6)$$

Equation (1.5) with initial condition (1.6) is called *Cauchy problem*. The main theorem for this class of partial differential equations associated with analytic initial conditions is the theorem of Cauchy-Kovalevskaja which states local existence and uniqueness also for nonlinear Cauchy problems. However, with analyticity demanded this theorem has hardly any practical relevance. Questions of local and global well-posedness for general nonlinear Cauchy problems require sophisticated concepts of functional analysis (see e.g. Adams [1], Evans [14]). We want to mention some basic concepts of these variational formulations of partial differential equations in an extent that they arise in the context of radiation hydrodynamics and accordingly numerics.

### 1.1.2 Weak Solutions

Since even the simplest examples of one-dimensional scalar conservation laws like the Burgers' equation have classical solutions only in some special cases, one has to broaden the considered function space of possible solutions (the adequate function spaces are Sobolev spaces, see Evans [14]). For so called *weak solutions*, we appeal to generalized functions where also discontinuities can be dealt with. The generalized concept of differentiation of distributions shifts operations to *test functions*  $\gamma(\mathbf{x}, t)$ . These test functions  $\gamma : G \in \mathbb{R}^n \times \mathbb{R}^+ \rightarrow \mathbb{R}$  have compact support, meaning that there exists a compact subset (here i.e. closed and bounded)  $K$  such that  $\gamma(\mathbf{x}, t) = 0 \quad \forall \mathbf{x} \in G \setminus K(\gamma)$ .

$$\int_{t \geq 0} \int_{\mathbb{R}^n} (\partial_t \mathbf{d} + \operatorname{div} \mathbf{f}(\mathbf{u})) \gamma \, dV \, dt = 0 \quad \forall \gamma \in G \quad (1.7)$$

To simplify matters, we let these test functions be continuously differentiable. Then with partial integration and our postulations for  $\gamma$

$$\begin{aligned} \int_{t \geq 0} \partial_t \mathbf{d} \gamma dt &= \gamma \mathbf{d} \Big|_0^\infty - \int_0^\infty \mathbf{d} \partial_t \gamma dt \\ &= \gamma(\mathbf{x}, 0) \mathbf{d}_0(\mathbf{x}) - \int_0^\infty \mathbf{d} \partial_t \gamma dt \\ \int_{\mathbb{R}^n} \operatorname{div} \mathbf{f}(\mathbf{d}) \gamma dV &= \underbrace{\gamma \mathbf{f} \Big|_{-\infty}^\infty}_{=0} - \int_{\mathbb{R}^n} \mathbf{f} \operatorname{grad} \gamma dV \end{aligned} \quad (1.8)$$

we derive the weak formulation of our conservation law (1.4).

$$\int_{t \geq 0} \int_{\mathbb{R}^n} (\mathbf{d} \partial_t \gamma + \mathbf{f}(\mathbf{d}) \operatorname{grad} \gamma) dV dt = - \int_{\mathbb{R}^n} \gamma(\mathbf{x}, 0) \mathbf{d}_0(\mathbf{x}) dV \quad (1.9)$$

The function  $\mathbf{d} \in \mathcal{L}^\infty$  is called *weak solution of the Cauchy problem* (1.4), if it satisfies (1.9) and  $\mathbf{d} \in U$  with  $\mathbf{d}_0 \in \mathcal{L}^\infty$ . This weak solution is not necessarily unique and normally further constraints have to be imposed.

### 1.1.3 Rankine-Hugoniot and Entropy Conditions

For the most physical problems it will be sufficient to look for weak solutions in the function space of piecewise continuously differentiable functions. The physical variables  $\mathbf{d}$  are weak solutions, if they are a classical solutions wherever they are  $\mathcal{C}^1$  and at discontinuities (shocks) they need to satisfy additional conditions. As we will see in chapter 2, these conditions posses direct physical relevance when applied to a physical system like radiation hydrodynamics. The full derivation of the one-dimensional *Riemann-problem* for (1.4) considered can be found in the Appendix 6.1.2.

We conclude,

$$\begin{aligned} \int_0^\infty \int_{-\infty}^\infty (d \partial_t \gamma + f(d) \partial_x \gamma) dx dt &= - \int_{-\infty}^\infty \gamma(x, 0) d_0(x) dx + \\ &+ \int_0^\infty \gamma(x, x/u_s) \left( \frac{f(d_l) - f(d_r)}{u_s} - (d_l - d_r) \right) dx \end{aligned} \quad (1.10)$$

is weak solution of the Riemann-problem, if

$$\frac{f(d_l) - f(d_r)}{u_s} - (d_l - d_r) = 0 \quad (1.11)$$

respectively

$$u_s = \frac{f(d_l) - f(d_r)}{d_l - d_r}. \quad (1.12)$$

We call  $u_s$  *shock velocity* and (1.12) *Rankine-Hugoniot condition*.

As already mentioned, weak solutions of the Cauchy problem are not necessarily unique and thus may be physically pointless. However, there is a way to pick physically valuable solutions out of multiple. One method is to implement an artificial viscosity term

$$\partial_t \mathbf{d}^* + \operatorname{div} \mathbf{f}(\mathbf{d}^*) = \varepsilon \nu \Delta \mathbf{d}^*, \quad \varepsilon > 0 \quad (1.13)$$

and evaluate the equation for  $\varepsilon \rightarrow 0$  as limit case of the original one. The idea is motivated from physical diffusion, which broadens sincere discontinuities to differentiable steep gradients. The physical solution of the weakly formulated problem has to be the zero diffusion limit of the diffusive problem. However, in analytical practice this limit is rather bulky to calculate, hence simpler conditions have to be found. The common technique to do this is motivated from continuum physics as well, where an additional conservation law holds for the entropy of the fluid flow as long as the solutions remain smooth. Moreover, it is known, that along admissible shocks this *physical* variable never decreases, so the conservation law for the entropy can be reformulated as inequality.

We regard a scalar entropy function  $\sigma(\mathbf{d})$  and an entropy flux  $\phi(\mathbf{d})$  which satisfy

$$\partial_t \sigma(\mathbf{d}) + \operatorname{div} \phi(\mathbf{d}) = 0. \quad (1.14)$$

Assuming differentiable functions, we rewrite that conservation law via the chain rule and compare it to (1.5) multiplied with  $\nabla_{\mathbf{d}} \sigma$  to obtain

$$\begin{aligned} \nabla_{\mathbf{d}} \sigma \partial_t \mathbf{d} + \nabla_{\mathbf{d}} \phi \nabla_{\mathbf{x}} \mathbf{d} &= 0 \\ \nabla_{\mathbf{d}} \sigma \partial_t \mathbf{d} + \nabla_{\mathbf{d}} \sigma \nabla_{\mathbf{d}} \mathbf{f} \nabla_{\mathbf{x}} \mathbf{d} &= 0 \\ \nabla_{\mathbf{d}} \sigma \operatorname{div} \mathbf{f} &= \operatorname{div} \phi \end{aligned} \quad (1.15)$$

where in the more dimensional case the appearing matrices of gradients have to fulfill some further constraints (see e.g. Godlewski and Raviart (1992) [16]). For scalar equations, it is always possible to find an entropy function of that kind. Furthermore we postulate convexity for the entropy function.<sup>3</sup>

$$\nabla_{\mathbf{d}}^2 \sigma > 0, \quad \forall \mathbf{d} \quad (1.16)$$

---

<sup>3</sup>In physical entropy one would require an eventual inequality with  $\geq$  in place of  $\leq$  but mathematical literature commonly chooses  $\sigma'' > 0$ .

To get our actual entropy condition, we rewrite (1.14) in the viscous form

$$\partial_t \sigma(\mathbf{d}^*) + \operatorname{div} \phi(\mathbf{d}^*) = \varepsilon \nu \nabla_{\mathbf{d}} \sigma(\mathbf{d}^*) \Delta \mathbf{d}^* \quad (1.17)$$

and integrate over an arbitrary time interval  $[t_0, t_1]$ .

$$\begin{aligned} \int_{t_0}^{t_1} \int_{\Omega} \left( \partial_t \sigma(\mathbf{d}^*) + \operatorname{div} \phi(\mathbf{d}^*) \right) dV dt &= \varepsilon \nu \int_{t_0}^{t_1} \int_{\Omega} \nabla_{\mathbf{d}} \sigma(\mathbf{d}^*) \Delta \mathbf{d}^* dV dt = \\ &= \varepsilon \nu \int_{t_0}^{t_1} \int_{\partial \Omega} \left( \nabla_{\mathbf{x}} \mathbf{d}^* \nabla_{\mathbf{d}} \sigma(\mathbf{d}^*) \right) \cdot d\mathbf{S} dt - \varepsilon \nu \int_{t_0}^{t_1} \int_{\Omega} \nabla_{\mathbf{x},i} \mathbf{d}^* \underbrace{\nabla^2 \sigma(\mathbf{d}^*)}_{>0} \nabla_{\mathbf{x},i} \mathbf{d}^* dV dt \end{aligned} \quad (1.18)$$

When we now consider our non diffusive limit for  $\varepsilon \rightarrow 0$ , the first term on the right hand side vanishes without further restriction whereas the second term has to remain non positive. With partial integration and divergence theorem we get our entropy condition (1.19).

$$\begin{aligned} \int_{t_0}^{t_1} \int_{\Omega} \left( \partial_t \sigma(\mathbf{d}) + \operatorname{div} \phi(\mathbf{d}) \right) dV dt &\leq 0 \\ \int_{\Omega} \sigma(\mathbf{d}(\mathbf{x}, t_1)) dV &\leq \int_{\Omega} \sigma(\mathbf{d}(\mathbf{x}, t_0)) dV - \int_{t_0}^{t_1} \int_{\partial \Omega} \phi(\mathbf{d}) d\mathbf{S} dt \end{aligned} \quad (1.19)$$

For bounded, continuous pointwise solutions  $\mathbf{d}^*$  with  $\mathbf{d}^* \rightarrow \mathbf{d}$  for  $\varepsilon \rightarrow 0$ , the *vanishing viscosity solution*  $\mathbf{d}$  is weak solution of the initial value problem (1.4) and fulfills entropy condition (1.19). Generally spoken, applying the entropy condition systems with shock solutions unveils those propagation velocities that ensure that no characteristics rise from discontinuities which would be non-physical. For details and proofs we refer to LeVeque [26].

In chapter 3 we will discuss these analytic concepts in numerical context and work out its concrete applications for (radiation) hydrodynamics.

## 1.2 The Elliptic Part

As already elaborated radiation hydrodynamics are partial differential equations of the hyperbolic type. However, the dynamics are only one part of the challenge emerging in astrophysical applications. Self gravitation in classical astronomical objects is described

via the Poisson equation, an elliptical partial differential equation which emerges as pure boundary value problem for the gravitational potential. Unlike hyperbolic PDEs elliptical problems mostly describe equilibrium physics and their solutions are typically quite smooth as we will see.

### 1.2.1 The Poisson Equation

The *Poisson equation* describes the spatial distribution of a scalar field  $\Phi$

$$\Phi : \bar{U} \subseteq \mathbb{R}^n \rightarrow \mathbb{R} \quad (1.20)$$

induced by a source  $\rho$

$$\rho : U \subseteq \mathbb{R}^n \rightarrow \mathbb{R} \quad (1.21)$$

and has the following form; the choice of the minus sign originates from the customary definition for ellipticity of differential operators.

$$-\Delta\Phi = \rho. \quad (1.22)$$

When it comes to our physical application of self-gravitation, we will pull the sign into the definition of the gravitational potential and consider  $\Delta\Phi_{\text{grav}} = 4\pi G\rho_{\text{m}}$ .

The Poisson equation is posed with Dirichlet or Neumann boundary conditions which means either boundary values or their derivatives are given. Often it is useful to impose mixed boundary conditions, where the boundary of the region  $\partial\Omega$  is separated in a part with Dirichlet conditions  $\partial\Omega^{\text{Dir}}$  and a part with Neumann boundary conditions  $\partial\Omega^{\text{Neu}}$  and  $\partial\Omega = \partial\Omega^{\text{Dir}} \cup \partial\Omega^{\text{Neu}}$ .

$$\begin{aligned} \Phi &= \psi^{\text{Dir}} && \text{in } \partial\Omega^{\text{Dir}} \\ \mathbf{n} \cdot \nabla\Phi &= \psi^{\text{Neu}} && \text{in } \partial\Omega^{\text{Neu}} \end{aligned} \quad (1.23)$$

The Poisson equation can be understood as the inhomogeneous generalization of the *Laplace equation*  $\Delta\tilde{\Phi} = 0$ . Physically, latter equation describes a solenoidal, irrotational vector field  $\mathbf{u} = \nabla\tilde{\Phi}$  with  $\text{div } \mathbf{u} = \text{rot } \mathbf{u} = 0$ . This circumstance implies that  $\tilde{\Phi}$  must be invariant under rotation and can be used to derive the fundamental solution. With Green's function and convolution of the inhomogeneous term  $\rho$  we derive the analytical solution of the Laplace equation<sup>4</sup>. In the light of these presumptions, we can investigate fundamental attributes of solutions of the Laplace equation in order to learn something about the solutions of the Poisson equation.

---

<sup>4</sup> $\tilde{\Phi}(\mathbf{x}) = \tilde{\Phi}(r)$ ,  $\partial_i r = \frac{x^i}{r}$  ...  $\rightarrow$  Green's functions of the fundamental solution of the Laplace equation in 3D is  $\Delta^{(3)}\left(-\frac{1}{4\pi r}\right) = \delta^{(3)}(\mathbf{x})$  and  $\Phi = \int G(\mathbf{x}, \mathbf{x}')\rho(\mathbf{x}') dV$  is solution of  $\Delta\Phi = \rho$ .

### 1.2.2 Harmonic Functions and the Maximum Principle

One important aspect of the Laplace operator as it emerges in Poisson and Laplace equation is the fact that it acts regularizing; the according theorem follows. Hence it will be adequate to deal with differentiable functions when we look for solutions of (1.22). Any function satisfying  $\Delta\tilde{\Phi} = 0$  in  $U$  and  $\mathcal{C}^2$  is called *harmonic function*.

Given  $\tilde{\Phi}$  is harmonic, we can derive a mean-value formula which states that on a spherical subset<sup>5</sup>  $B(\mathbf{x}, r) \subset U$ , a solution  $\tilde{\Phi}(\mathbf{x})$  equals both the average of  $\tilde{\Phi}$  over the sphere  $\partial B$  and the average of  $\tilde{\Phi}$  on the entire ball  $B$ .

$$\tilde{\Phi}(\mathbf{x}) = \frac{\Gamma(\frac{n}{2} + 1)}{n\pi^{n/2}r^{n-1}} \int_{\partial B(\mathbf{x}, r)} \tilde{\Phi} dS = \frac{\Gamma(\frac{n}{2} + 1)}{\pi^{n/2}r^n} \int_{B(\mathbf{x}, r)} \tilde{\Phi} dV \quad (1.24)$$

In 3 dimensions this simply yields  $\tilde{\Phi}(\mathbf{x}) = \frac{1}{4\pi r^2} \int \tilde{\Phi} dS = \frac{3}{4\pi r^3} \int \tilde{\Phi} dV$  with corresponding integration ranges. In the light of these conclusions, we deduce some interesting properties of harmonic functions.

The (*strong*) *maximum principle* states for a  $\tilde{\Phi} \in \mathcal{C}^2(U) \cap \mathcal{C}(\bar{U})$  harmonic within  $U$ ,

*i.)*  $\max_{\bar{U}} \tilde{\Phi} = \max_{\partial U} \tilde{\Phi}$ .

*ii.)* Furthermore, if  $U$  is connected and  $\exists x_0 \in U$  such that  $u(x_0) = \max_U \tilde{\Phi}$ , it follows that  $\tilde{\Phi}$  is constant within all  $U$ .

Assertion *i.)* implies that the maximum will be found at the boundary of the domain and *ii.)* states that if a maximum is on the inside of the boundary the function  $\tilde{\Phi}$  consequently is constant within  $U$ . Another important conclusion of this theorem concerns the Poisson equation. It can be shown that for the boundary value problem

$$\begin{aligned} -\Delta\Phi &= \rho \quad \text{in } U \\ \Phi &= g \quad \text{in } \partial U \end{aligned} \quad (1.25)$$

there exists at most one solution  $\Phi \in \mathcal{C}^2(U) \cap \mathcal{C}(\bar{U})$ . With this *uniqueness theorem* we gain at least some comfort for the gravitational part of our numerical problem. As a further side note we mention the *regularity theorem*. It reveals that if  $\tilde{\Phi} \in \mathcal{C}^2$  is harmonic then it automatically is infinitely differentiable, i.e.  $\tilde{\Phi} \in \mathcal{C}^\infty$ .

Without dwelling on the Laplace equation any further, we recapitulate that mathematical analysis of the elliptical part of our system of equations brings forward less sophisticated problems than the hyperbolic part. Obviously, uniqueness and regularity are soothing qualities when it comes to solving partial differential equations. All theorems and proofs of this section can be found in Lawrence C. Evans (1998), p.17 ff. [14].

<sup>5</sup>Closed  $n$ -dimensional ball  $B(\mathbf{x}, r)$  with center  $\mathbf{x}$ , radius  $r > 0$ .



## 2 Fundamental Physics of RHD

Astronomical objects are basically self-gravitating aggregations of (gaseous) material with magnetic fields and radiation. Radiation hydrodynamics as we will discuss them, factor out magnetic effects and solely consider radiative contributions through photons.

The fundamental equations of hydrodynamics describe the motion of fluids in terms of continuous quantities. The dynamics and kinetics of fluid particles are described by macroscopic functions like the mass density  $\rho$ , its velocity  $\mathbf{u}$ , internal energy and gaseous pressure as primary variables mostly. In this model, infinitesimal volume elements of the fluid are still big enough that intermolecular forces can be neglected, meaning that they contain a sufficient number of molecules. The thermodynamic variables intrinsically are assumed to be well defined (equilibrium thermodynamics) and characterized by an equation of state.

The radiative transfer equation describes energy transfer in form of electromagnetic radiation, affected by absorption, emission and scattering. The fundamental quantity to describe the radiative field is the spectral intensity  $I_\gamma$ , which can be understood as macroscopic quantity to describe the photonic energy flow. The mass density  $\rho$  is also source for the gravitational potential  $\Phi$ . In the following sections we will physically motivate the set of equations of radiation hydrodynamics with gravitation bit by bit.

One major intention in the upcoming paragraphs will be rigorous and consistent (in terms of differential geometry) definitions of the physical variables which will be crucial for the numerical methods in general curvilinear coordinates investigated in section 3.2.

### 2.1 Hydrodynamics

As anticipated, the equations of hydrodynamics can be derived from conservation laws of mass, momentum and energy. Since the fundamentals of hydrodynamics are more than well documented (e.g. in Landau, Lifschitz [23]) we confine our portrayal to a brief synopsis and concentrate on a few interesting details.

### 2.1.1 Continuity Equation

The conservation of mass is physically justified as long as no mass is generated or annihilated

$$\frac{dm}{dt} = \frac{d}{dt} \int_{V(t)} \rho dV = 0 \quad (2.1)$$

and leads to the continuity equation.

$$\begin{aligned} \int_{V(t)} \left( \partial_t \rho + \operatorname{div}(\rho \mathbf{u}) \right) dV &= 0 \\ \int_{V(t)} \partial_t \rho + \int_{\partial V(t)} (\rho \mathbf{u}) \cdot d\mathbf{S} &= 0 \end{aligned} \quad (2.2)$$

Clearly the domain  $\Omega$  of the conservation law, introduced in section 1.1 is an  $n$ -dimensional Volume that is a bounded subset of the  $\mathbb{R}^n$ ,  $n = 1, 2, 3$ . The mass density  $\rho$  is a non negative scalar field  $\rho(\mathbf{x}, t) : \mathbb{R}^{n+1} \rightarrow \mathbb{R}^+$  and the velocity  $\mathbf{u}$  a vector field  $\mathbf{u}(\mathbf{x}, t) : \mathbb{R}^{n+1} \rightarrow \mathbb{R}^{n+1}$ . Solutions of these primary variables  $\rho, \mathbf{u}$ , that is densities of the conservation laws, will emerge as piecewise continuous functions.

As a side note the flow is called stationary if  $\partial_t \rho = 0$  and incompressible if  $\operatorname{div} \mathbf{u} = 0$ . However, in astrophysical applications these special cases will fail to describe the physics appropriately.

### 2.1.2 Equation of Motion

In order to yield the equation of motion from the conservation of momentum it is required to specify which forces act upon the fluid. Now we are concerned with a non-scalar conservation law and as we will see in chapter 3, in this case we will have to avail ourselves of general tensorial notation. Thus, at this point we introduce one main tensorial quantity (and secondary physical variable), the non-relativistic viscous stress tensor.

$$\begin{aligned} \mathbf{T} &= \rho \mathbf{u} \mathbf{u} + \mathbf{P} - \sigma \\ T^{ij} &= \rho u^i u^j + P^{ij} - \sigma^{ij} \end{aligned} \quad (2.3)$$

$\mathbf{T}(\mathbf{x}, t) : \mathbb{R}^{n+1} \times \mathbb{R}^{n+1} \rightarrow \mathbb{R}^{n+1} \times \mathbb{R}^{n+1}$ . This symmetric<sup>1</sup> tensor ( $T^{ij} = T^{ji}$ ) describes contributions from momentum  $\rho u^i$  in  $j$ -direction, generally anisotropic pressure  $P^{ij}$  and friction  $\sigma^{ij}$  forces. Diagonal elements express pressure and off-diagonal elements shear

---

<sup>1</sup> $\mathbf{T}$  is symmetric, if conservation of angular momentum  $\rho \mathbf{x} \times \mathbf{u}$  is invoked, see derivation in the Appendix 6.1.1.

stresses. The equation of motion in then yields<sup>2</sup>

$$\begin{aligned} \int_{V(t)} \left( \partial_t(\rho \mathbf{u}) + \operatorname{div} \mathbf{T} \right) dV &= 0 \\ \int_{V(t)} \partial_t(\rho \mathbf{u}) dV + \int_{\partial V(t)} (\rho \mathbf{u} \mathbf{u} + \mathbf{P} - \sigma) \cdot d\mathbf{S} &= 0. \end{aligned} \quad (2.4)$$

Special cases for the energy-stress tensor in fluid dynamics are e.g. the dust model where no particle interaction is assumed  $\mathbf{P} = \sigma = 0$ . Anyway, in numerous physical applications the pressure forces can be expected to be isotropic. If so, the pressure tensor simplifies to a diagonal tensor which consists of the scalar gaseous pressure  $p$  and a *measure of uniformity*, the the metric tensor  $\mathbf{g}$ , which yields  $\mathbf{P} = p\mathbf{g}$ . The divergence of that tensor can be further simplified to the well known gradient of the gaseous pressure. We will extensively occupy ourselves with the viscous pressure tensor  $\sigma$  in succession, especially in section 3.2.4. At this point it shall only be mentioned that we neglect physical viscosity since the gas of a star is easily approximated as ideal fluid. As indicated in section 1.1.3, we will impose artificial dynamic viscosity when we concern ourselves with mathematical methods for solving nonlinear conservation laws.

Implicitly we already have defined a thermodynamic equation of state which describes the state of the fluid in terms of pressure  $p$ , volume  $V$  and temperature  $T$  by imposing an ideal fluid. Since stars are largely composed of hot, low-pressure hydrogen gas, it is quite reasonable to apply this model.

### 2.1.3 Energy Equation

The energy balance of a fluid includes kinetic and pressure parts as well as inner energy. Latter is once more a thermodynamic quantity which is associated with the equation of state. We define a new non-negative scalar field, the specific inner energy  $\epsilon(\mathbf{x}, t) : \mathbb{R}^{n+1} \rightarrow \mathbb{R}^+$  which in case of an ideal fluid equals its thermic energy. The conservation of the total energy of a bounded fluid element in this strictly hydrodynamic case yields<sup>3</sup>

$$\begin{aligned} \int_{V(t)} \left( \partial_t \left( \frac{1}{2} \rho \mathbf{u}^2 + \rho \epsilon \right) + \operatorname{div} (\mathbf{T} \cdot \mathbf{u} + \rho \epsilon \mathbf{u}) \right) dV &= 0 \\ \int_{V(t)} \partial_t \left( \frac{1}{2} \rho \mathbf{u}^2 + \rho \epsilon \right) dV + \int_{\partial V(t)} \left( \left( \frac{1}{2} \rho \mathbf{u}^2 + \rho \epsilon \right) \mathbf{u} + (\mathbf{P} - \sigma) \cdot \mathbf{u} \right) \cdot d\mathbf{S} &= 0. \end{aligned} \quad (2.5)$$

<sup>2</sup>In general relativity the conservation of momentum can be found in its most elegant form  $\nabla \cdot \mathbf{T} = 0$ .

In this case all variables are defined in a four-dimensional spacetime, where the 0-component of the covariant nabla operator contains the temporal derivative.

<sup>3</sup>Using  $\nabla(\frac{1}{2} \mathbf{u}^2) = \mathbf{u} \nabla \cdot \mathbf{u}$ .

This *total energy equation* can be dissected into a mechanical and an *internal* part, where former describes the change of kinetic energy of a fluid as the rate of work done on an element by pressure and stress forces. The gas energy part can be formulated as entropy conservation ( $\partial_t(\rho s) + \text{div}(\rho s \mathbf{u}) = 0$ ) and hence implies, that the flow is adiabatic.

## 2.2 Radiation

The fundamentals of radiative transfer and its moments can be found in several appropriate text books (see e.g. Mihalas and Mihalas [32]), therefore we will concentrate on some noteworthy highlights in this section as well. In the previous paragraph we treated the physics of fluids which we now want to extend to radiating fluids *in a nutshell*.

Radiation contributes to the total energy, momentum, stress and pressure in the fluid. In succession we will work out means of coupling among these physical quantities in the material. When we concerned ourselves with the fundamental mathematics of conservation laws, we denoted that also the fundamental dynamics of radiation will appear as hyperbolic conservation laws. In fact, the crucial equation to describe radiation is the radiation transfer equation (RTE), which basically expresses conservation of energy. However, we shall begin to define the fundamental dynamical properties of the radiation field.

### 2.2.1 The Radiation Field and its Momenta

The macroscopic quantities of the radiation field are based on statistical physics of a microscopic description of ultra-relativistic massless particles, i.e. photons. To establish the nexus to the continuum view which we will pursue, we define the scalar non-negative photon distribution function  $f_\gamma(\mathbf{x}, t; \mathbf{n}, \nu) : \mathbb{R}^{3+1} \times \mathbb{R}^3 \times \mathbb{R} \rightarrow \mathbb{R}^+$  which can be interpreted as photon density in the corresponding phase space<sup>4</sup>. The central physical quantity for the upcoming description of the radiation field is the spectral intensity  $I_\gamma(\mathbf{x}, t; \mathbf{n}, \nu)$  defined by

$$I_\gamma = \frac{h^4 \nu^3}{c^2} f_\gamma. \quad (2.6)$$

That implicitly describes a radiative energy transport in the following sense

$$d\mathcal{E}_\gamma = I_\gamma d\mathbf{S} \cdot \mathbf{n} d\omega d\nu dt. \quad (2.7)$$

The spectral intensity  $I_\gamma$  at position  $(\mathbf{x}, t)$ , traveling in direction  $\mathbf{n}$  with frequency  $\nu$  is defined to account for the energy  $\mathcal{E}_\gamma$  transported by radiation of frequencies  $d\nu$  across a

---

<sup>4</sup>The momentum of a photon, traveling in direction  $\mathbf{n}$  is given by  $\mathbf{p}_\gamma = \frac{h\nu}{c} \mathbf{n}$ .  $\nu$  is the frequency,  $c$  the speed of light and  $h$  the Planck constant.  $f_\gamma$  is invariant under Lorentz transformations. The subset  $\gamma$  is chosen to discern mere radiation (here photonic) variables.

surface element  $d\mathbf{S}$  in time  $dt$  into a solid angle  $d\omega$  around  $\mathbf{n}$ . Further useful properties are the angular moments of the radiation field, that is the mean intensity  $J_\gamma$  (zeroth moment), the radiation flux  $\mathbf{F}_\gamma$  (first moment) and the evidently symmetric radiation pressure tensor  $\mathbf{P}_\gamma$  (second moment). The velocity of our particles will simply be given by the speed of light and their direction of motion  $\mathbf{u} = c\mathbf{n}$ , which also illustrates the link to the procedure we carried out for deriving the equations of hydrodynamics.

$$\begin{aligned} J_\gamma(\mathbf{x}, t; \nu) &= \frac{1}{4\pi} \int I_\gamma d\omega \\ \mathbf{F}_\gamma(\mathbf{x}, t; \nu) &= \int I_\gamma \mathbf{n} d\omega \\ \mathbf{P}_\gamma(\mathbf{x}, t; \nu) &= \frac{1}{c} \int I_\gamma \mathbf{n}\mathbf{n} d\omega \end{aligned} \quad (2.8)$$

Analogously to our fundamental equations of hydrodynamics, we can derive dynamic equations for the radiation field by considering the conservation of *density*  $J_\gamma$  and *momentum*  $\mathbf{F}_\gamma$ .

$$\begin{aligned} \int_{V(t)} \left( \partial_t J_\gamma + \operatorname{div} (c\mathbf{F}_\gamma) \right) dV &= 0 \\ \int_{V(t)} \left( \partial_t \mathbf{F}_\gamma + \operatorname{div} (c^2 \mathbf{P}_\gamma) \right) dV &= \mathbf{0} \end{aligned} \quad (2.9)$$

From the viewpoint we pursued in section 1.1 discussing hyperbolic conservation laws we define a density function  $\mathbf{d}(\mathbf{x}, t; \nu) = (J_\gamma, \mathbf{F}_\gamma)$  and a flux  $\mathbf{f}(\mathbf{d}) = c(\mathbf{F}_\gamma, c\mathbf{P}_\gamma)$ . Equations (2.9) can hence be interpreted as homogeneous outlook to the moments of the radiation transfer equation with collision terms (2.12) in the forthcoming section.

## 2.2.2 Interaction with Matter

For the treatment of radiation hydrodynamics it will be necessary to describe the interaction of the radiation field with the fluid. Again the macroscopic approach chosen here to describe this interaction can be understood canonically with concepts from statistical physics and quantum mechanics. Moreover, it will be required to process the variables of the radiation field into the fluid frame of the material correctly via Lorentz transformation and account for the frequency change with respect to the lab frame that comes with Doppler shift.

When radiation passes through material, energy generally will be removed depended on a material property, the opacity or extinction coefficient  $\chi_\gamma$ . On the other hand, the material releases radiation in terms of an emission coefficient  $\eta_\gamma$  which will be isotropic in its rest frame. Both properties are defined as non-negative scalar functions of posi-

## 2 Fundamental Physics of RHD

tion, time, radiation direction and frequency  $(\chi_\gamma, \eta_\gamma)(\mathbf{x}, t; \mathbf{n}, \nu) : \mathbb{R}^{3+1} \times \mathbb{R}^3 \times \mathbb{R} \rightarrow \mathbb{R}^+$ . Both processes, extinction and emission, can be further divided in thermal and scattering events. Thermal extinction and emission converts radiation energy to thermal and vice versa, whereas scattering in principle changes direction and frequency of traveling photons. The amount of energy removed along a material element of length  $dl$  is

$$d\mathcal{E}_\gamma = (\chi_\gamma^{\text{therm}} + \chi_\gamma^{\text{scat}}) I_\gamma dS dl d\omega d\nu dt \quad (2.10)$$

and the amount of radiation energy released by emission is

$$d\mathcal{E}_\gamma = (\eta_\gamma^{\text{therm}} + \eta_\gamma^{\text{scat}}) dS dl d\omega d\nu dt. \quad (2.11)$$

The conservation of spectral intensity (2.9) considering emission and extinction yields

$$\int_{V(t)} \left( \frac{1}{c} \partial_t I_\gamma + \text{div}(I_\gamma \mathbf{n}) - \eta_\gamma + \chi_\gamma I_\gamma \right) dV = 0 \quad (2.12)$$

and is called *radiation transfer equation* in the laboratory frame. In practice of RHD, upper equation and its momenta have yet to be transformed into the fluid frame as mentioned and simplified in several ways.

Firstly the monochromatic quantities  $I_\gamma, \chi_\gamma, \dots$  will solely be considered with their *collective* effects by integrating them over all frequencies<sup>5</sup>.

$$\begin{aligned} \bar{J}_\gamma(\mathbf{x}, t) &= \frac{c}{4\pi} \bar{E}_\gamma = \frac{1}{4\pi} \int I_\gamma d\omega d\nu \\ \bar{\mathbf{F}}_\gamma(\mathbf{x}, t) &= 4\pi \bar{\mathbf{H}}_\gamma(\mathbf{x}, t) = \int I_\gamma \mathbf{n} d\omega d\nu \\ \bar{\mathbf{P}}_\gamma(\mathbf{x}, t) &= \frac{4\pi}{c} \bar{\mathbf{K}}_\gamma(\mathbf{x}, t) = \frac{1}{c} \int I_\gamma \mathbf{nn}^T d\omega d\nu \end{aligned} \quad (2.13)$$

Another commonly used simplification to determine the proportion of extinction and emissivity by a source function  $\bar{S}_\gamma$  is to impose local thermal equilibrium (LTE) where the radiation field is characterized by one single variable, the temperature  $T$  (black body radiation). In this case, the specific intensity depends only on the gas temperature and is given by Planck's law

$$I_{\gamma, \text{LTE}}(\mathbf{x}, t; \nu) = \frac{2h\nu^3}{c^2} \frac{1}{\frac{h\nu}{e k T} - 1} \quad (2.14)$$

and the collective, frequency integrated form yields the source function  $\bar{S}_\gamma(\mathbf{x}, t) : \mathbb{R}^{3+1} \rightarrow$

---

<sup>5</sup>Many authors use a notation, where the frequency  $\nu$  is written as subset, instead of in the list of arguments  $I_\nu(\mathbf{x}, t; \mathbf{n})$  and the frequency integrated variables lack of that subset  $I, \chi, \dots$

$\mathbb{R}^+$ 

$$\bar{S}_\gamma = \frac{4\pi\bar{\eta}_\gamma}{\bar{\chi}_{\gamma,P}} = \int_0^\infty I_{\gamma,\text{LTE}} d\nu = \frac{8\pi^5 k^4}{15c^3 h^3} T^4. \quad (2.15)$$

With  $\bar{\chi}_{\gamma,P}$  we introduce a Planck mean opacity  $\bar{\chi}_{\gamma,P}$  respectively the Planck mean opacity per mass  $\bar{\kappa}_{\gamma,P}$

$$\bar{\kappa}_{\gamma,P}\rho = \bar{\chi}_{\gamma,P} = \frac{\int_0^\infty \chi_\gamma I_{\gamma,\text{LTE}} d\nu}{\int_0^\infty I_{\gamma,\text{LTE}} d\nu} \quad (2.16)$$

and with  $\bar{\chi}_{\gamma,R}$  a Rosseland mean which will emerge in the radiation energy equation.

$$\frac{1}{\bar{\kappa}_{\gamma,R}\rho} = \bar{\chi}_{\gamma,R} = \frac{\int_0^\infty \frac{1}{\chi_\gamma} \frac{\partial I_{\gamma,\text{LTE}}}{\partial T} d\nu}{\int_0^\infty \frac{\partial I_{\gamma,\text{LTE}}}{\partial T} d\nu} \quad (2.17)$$

At this point we have defined all necessary variables and motivated a list of simplifications for our system of radiation hydrodynamics equations. However, two important steps are to be provided yet. First, one has to deal with the problem that in particular equations (2.9) but respectively all  $n$  moment equations contain in each case  $n + 1$  momenta of the radiation field which is known as *closure problem*. The last step to the full set of equations of RHD will be the Lorentz transformation into the fluid frame.

### 2.2.3 Radiation Closure Relation

In section 1.1 it was mentioned, that imposing hyperbolicity on the conservation law can help to narrow possible solutions in some way. A conservation law is called hyperbolic if the Jacobian matrix associated with the fluxes  $\nabla_{\mathbf{d}} \mathbf{f}$  has real eigenvalues and there exists a complete set of corresponding eigenvectors. As we have seen, interaction with matter adds source terms to our radiation conservation laws, we abbreviate them from now on with  $S_\gamma^0$  and  $\mathbf{S}_\gamma^1$ .

$$\begin{aligned} \partial_t J_\gamma + \text{div}(c\mathbf{F}_\gamma) &= \underbrace{\int (\eta_\gamma - \chi_\gamma I_\gamma) d\omega}_{S_\gamma^0} \\ \partial_t \mathbf{F}_\gamma + \text{div}(c^2 \mathbf{P}_\gamma) &= \underbrace{\int (\eta_\gamma - \chi_\gamma I_\gamma) \mathbf{n} d\omega}_{\mathbf{S}_\gamma^1} \end{aligned} \quad (2.18)$$

However, these terms do not influence if the system is hyperbolic or not since they appear without derivatives. We define the two *Eddington factors* (actually they are non-negative

## 2 Fundamental Physics of RHD

tensors)

$$\mathcal{F} = \frac{\mathbf{F}_\gamma}{J_\gamma}, \quad \mathcal{P} = \frac{\mathbf{P}_\gamma}{J_\gamma} \quad (2.19)$$

which can be interpreted as normalized flux and pressure and therefore are a *measure of the geometry* of the radiative field. It is reasonable to assume that  $\mathcal{P}$  is only a function of  $\mathcal{F}$  and henceforth we write  $d\mathcal{P}/d\mathcal{F} = \mathcal{P}'$ . Likewise we define the norms of the Eddington factors  $f = |\mathcal{F}|$  and  $p = |\mathcal{P} \cdot \mathcal{F}/f|$ . Now we express the density function and the flux of the conservation law by means of the Eddington factors which represents our choice of dependent and independent variables for the Jacobian.

$$\mathbf{d}_\gamma = (J_\gamma, c\mathcal{F}J_\gamma), \quad \mathbf{f}_\gamma = (c\mathcal{F}J_\gamma, c^2\mathcal{P}J_\gamma) \quad (2.20)$$

The Jacobian of the radiative conservation law yields<sup>6</sup>

$$\nabla_{\mathbf{d}_\gamma} \mathbf{f}_\gamma = \frac{\partial f^i}{\partial d^j} = \begin{pmatrix} 0 & 1 \\ c^2(\mathcal{P} - \mathcal{F}\mathcal{P}') & c\mathcal{P}' \end{pmatrix}. \quad (2.21)$$

For upper Jacobian we obtain the following characteristic equation

$$\lambda = \frac{1}{2} \left( c\mathcal{P}' \pm \sqrt{c^2(4p + \mathcal{P}'(-4f + \mathcal{P}'))} \right)$$

and system (2.20) is hyperbolic if the discriminant is not negative i.e.  $(\mathcal{P}' - 2f)^2 + 4(p - f^2) \geq 0$  respectively as long as the constraint  $f^2 \leq p$  holds. Moreover,  $f$  and  $p$  as normalized moments obey  $(p, f) \leq 1$  and we derive the important conclusion

$$f^2 \leq p \leq 1. \quad (2.22)$$

Equation (2.22) can be interpreted as flux limiter, which ensures causal values for the flux function, namely that it can not get greater than the energy density  $J_\gamma$  times the speed of light  $c$ . Physically it is clear that  $f$  and  $p$  take the value 1 for transparency which is often called the free-streaming limit. In this case, radiation propagates freely and the total amount of intensity is transported by the flux function. The characteristic speeds in this regime evidently yield  $\lambda = \pm c$ .

On the other end of the opacity scale, the optically thick regime, photons have very small mean free paths  $l_\gamma$  and underlie random-walk processes through the material. In this case, the radiation field is totally isotropic, the net flux vanishes  $\mathbf{F}_\gamma = 0$  and the radiation stress tensor  $\mathbf{P}_\gamma = \frac{1}{3}\mathbf{1}J_\gamma$  gets diagonal (for arguments see Appendix 6.1.3). Consequently the eigenvalues of the Jacobian yield  $\lambda = \pm c\sqrt{1/3}$  which are the characteristic propagation speeds in this case.

---

<sup>6</sup>Using  $\left. \frac{\partial c\mathcal{F}J_\gamma}{\partial J_\gamma} \right|_{(\mathcal{F}, J_\gamma)} = 0$  and  $\partial \frac{1}{\mathcal{F}} = -\frac{1}{\mathcal{F}^2} \partial \mathcal{F}$ .



When we will discuss numerical high resolution methods for such nonlinear conservation laws in section 3.1.4 we will encounter the concept of flux limiting again. To learn more about possible closure relations associated with the hyperbolicity approach, see Pons, Ibanez, Miralles (2000) [35].

### 2.2.4 Fluid Frame

In order to account for the local radiation properties of a fluid, we need to consider the interaction of matter and radiation in a common frame, ideally the comoving frame of the fluid flow. The transformation however not only has to describe advection effects (i.e. change in photon number density), but also impacts on momentum, energy and directions due to the Doppler shift of the photons. For the purpose of simplicity we will ignore pure scattering terms and assume local thermal equilibrium (LTE) again.

An adequate procedure, especially with possibly relativistic fluid flows allowed is to apply Lorentz transformations. Introductions to Minkowski geometry and Lorentz transformation can be found in several appropriate text books like Ray d’Inverno [10]. At this point we just note that the relation between a four-vector  $\mathbf{x} = (ct, \mathbf{r})$  in the lab frame and the moving frame  $\mathbf{x} \rightarrow \mathbf{x}_0$  is given via

$$\begin{pmatrix} ct_0 \\ \mathbf{r}_0 \end{pmatrix} = \underbrace{\begin{pmatrix} \gamma & -\frac{\gamma}{c}\mathbf{u} \\ -\frac{\gamma}{c}\mathbf{u} & \mathbf{1} + (\gamma - 1)\frac{\mathbf{u}\mathbf{u}}{u^2} \end{pmatrix}}_{\mathbf{L}} \begin{pmatrix} ct \\ \mathbf{r} \end{pmatrix} \quad (2.23)$$

respectively  $x^\alpha_0 = L^\alpha_\beta x^\beta$  with  $(\alpha, \beta) = 0, 1, 2, 3$ . The subset 0 denotes variables in the comoving frame, the gamma factor is defined by  $\gamma^{-1} = \sqrt{1 - |\mathbf{u}|^2/c^2}$  where  $\mathbf{u}$  is the fluid relative velocity. When we apply these rules to the photon four-momentum  $p^\alpha_\gamma = \frac{h\nu}{c}(1, n^\alpha)$ , we obtain the required relations for the photon propagation in the fluid frame.

$$\begin{aligned} \nu_0 &= \gamma\nu \left(1 - \frac{\mathbf{n} \cdot \mathbf{u}}{c}\right) \\ \mathbf{n}_0 &= \frac{\nu}{\nu_0} \left(\mathbf{n} - \gamma\frac{\mathbf{u}}{c} \left(1 - \frac{\gamma\mathbf{n} \cdot \mathbf{u}}{\gamma + 1}\right)\right) \end{aligned} \quad (2.24)$$

These formulae for redshift (respectively blueshift) and aberration often are yet simplified for practical astrophysical applications, arguing that terms  $\mathcal{O}(\frac{u}{c})^2$  can be neglected since fluid velocities are at least one magnitude smaller than the speed of light. This reduction also implies that the outstanding transformation is mere spatial as with  $\gamma = \frac{\partial t}{\partial t_0} = 1$  follows  $t = t_0$ .

When we intend to transform the radiative quantities like the spectral intensity and its derived variables we need to occupy ourselves with relativistic kinetics respectively with

## 2 Fundamental Physics of RHD

a relativistic form of the Boltzmann transport equation. To wit, the spectral intensity itself is not Lorentz invariant but the photon distribution function  $f_\gamma$  defined earlier. These considerations date back to Thomas (1930) [42] respectively Lindquist (1966) [29], who drafted a general relativistic formulation.

The connection between the spectral intensity, emissivity and absorption in the lab frame and in the comoving frame accordingly yield

$$I_\gamma = \left(\frac{\nu}{\nu_0}\right)^3 I_{\gamma 0}, \quad \eta_\gamma = \left(\frac{\nu}{\nu_0}\right)^2 \eta_{\gamma 0}, \quad \chi_\gamma = \frac{\nu}{\nu_0} \chi_{\gamma 0}. \quad (2.25)$$

The frequency integrated moments of the radiation field occur as elements of the radiation energy-stress tensor which is defined by

$$T_\gamma^{\alpha\beta} = c^2 \int \frac{d\mathbf{p}}{\epsilon_\gamma} p^\alpha p^\beta f_\gamma \quad (2.26)$$

and can easily be rewritten to a more familiar form<sup>7</sup>.

$$\mathbf{T}_\gamma = \frac{1}{c} \int \int \begin{pmatrix} 1 & \mathbf{n} \\ \mathbf{n} & \mathbf{nn} \end{pmatrix} I_\gamma d\nu d\Omega = \begin{pmatrix} \bar{E}_\gamma & \bar{\mathbf{F}}_\gamma/c \\ \bar{\mathbf{F}}_\gamma/c & \bar{\mathbf{P}}_\gamma \end{pmatrix} \quad (2.27)$$

The conservation law associated with radiation transfer gains its most elegant form in this notation, namely  $\nabla \cdot \mathbf{T}_\gamma = \mathbf{S}_\gamma$  with source terms  $\mathbf{S}_\gamma = (S_\gamma^0, \mathbf{S}_\gamma^1)$  as defined before. The Lorentz transformation of  $\mathbf{T}_\gamma$  yields  $\mathbf{T}_{\gamma 0} = \mathbf{L}\mathbf{T}_\gamma\mathbf{L}$  as the operator is unitary and thus  $\mathbf{L} = \mathbf{L}^T$ .s When we confine ourselves to small velocities again and discard terms higher  $\mathcal{O}(\frac{u}{c})^2$ , we would receive the applicable approximation formulae.

What is left to do, is to mark the moments of the transport equation in this classical limit. For forcible deduction we refer to Buchler (1979) [6] and (1983) [7] who elaborated a fluid frame description in arbitrary geometry inclusive of terms  $\mathcal{O}(\frac{u}{c})$ . The frequency integrated radiation energy equation and the radiation flux equation in the comoving frame accordingly yield

$$\begin{aligned} \partial_t \bar{J}_{\gamma 0} + \text{div}(\mathbf{u} \bar{J}_{\gamma 0}) + c \text{div} \bar{\mathbf{H}}_{\gamma 0} + \bar{\mathbf{K}}_{\gamma 0} : \text{grad} \mathbf{u} - c \bar{\chi}_{\gamma, P0} (\bar{J}_{\gamma 0} - \bar{S}_{\gamma 0}) &= 0 \\ \partial_t \bar{\mathbf{H}}_{\gamma 0} + \text{div}(\mathbf{u} \bar{\mathbf{H}}_{\gamma 0}^T) + c \text{div} \bar{\mathbf{K}}_{\gamma 0} + \bar{\mathbf{H}}_{\gamma 0} \cdot \text{grad} \mathbf{u} + c \bar{\chi}_{\gamma, R0} \bar{\mathbf{H}}_{\gamma 0} &= 0. \end{aligned} \quad (2.28)$$

Notation: from now on, the neat radiation variables ( $J, \mathbf{H}, \dots$ ) shall be read as photonic, frequency integrated functions in the comoving frame ( $\bar{J}_{\gamma 0}, \bar{\mathbf{H}}_{\gamma 0}, \dots$ ).

---

<sup>7</sup>Using  $p_\gamma^\alpha = \frac{h\nu}{c}(1, n^\alpha)$  and  $\epsilon_\gamma = h\nu$ .

## 2.3 Gravitation

In section 1.2 we highlighted some mathematical basics for the Laplace and the Poisson equation in context of elliptical partial differential equations. The Poisson equation for the gravitational potential, a scalar function  $\Phi_{\text{grav}}(\mathbf{x}, t) : \mathbb{R}^{n+1} \rightarrow \mathbb{R}$  yields

$$\Delta \Phi_{\text{grav}} = 4\pi G \rho_m \quad (2.29)$$

where  $\rho_m(\mathbf{x}, t) : \mathbb{R}^{n+1} \rightarrow \mathbb{R}^+$  is the time dependend mass density again in  $n = 1, 2, 3$  spatial dimensions.

However, most applications of radiation hydrodynamics with gravitation avoid solving the Poisson equation for the gravitational potential per se, especially in spherical symmetric applications<sup>8</sup>. The main challenge associated with self gravitation in 2D and 3D is that it requires the numerical solution of the Poisson equation in each time step which is computationally expensive. Moreover, it is not trivial to find appropriate boundary conditions for this elliptical problem in astrophysical context since most objects are not bounded naturally but artificially respectively numerically.

### 2.3.1 Self-Gravitation in 2D and 3D

There have been efforts in finding and applying solution methods for self-gravitating flows in multiple dimensions since decades. Differential algorithms solve the Poisson equation in the form (2.29) whereas integral methods rather consider the theory of Greens functions as briefly mentioned in section 1.2 where the formal solution in 3D yields

$$\Phi_{\text{grav}} = -G \int \frac{\rho(\mathbf{x})}{|\mathbf{x} - \mathbf{x}'|} d\mathbf{x}.$$

With latter family of algorithms the grids boundary causes no problems and the integration could principally be conducted with standard methods. However, the number of grid cells to be summed ( $\sim N^2$ ) and therewith the computational cost get huge in multiple dimensions. Several authors thus suggest to expand the integrand e.g. in spherical harmonics in order to reduce operations to an order  $\sim N$ . Müller and Steinmetz (1995) [34] developed an efficient Poisson solver based on such a separation ansatz. Cosmological hydrodynamic simulations have affiliated these ideas and implemented them in a number of cosmological codes.

Spingel (2009) [39] suggests an interesting method to realize self gravitation in a conservative way by reformulating the total energy equation. He adds a *gravitational source*

---

<sup>8</sup>With radial symmetry, the gravitational acceleration  $\mathbf{G}(r)$  is simply determined by the integrated mass  $m(r) = \int_0^r 4\pi \rho_m(r') dr'$  via the well known relation  $\mathbf{G}(r) = -\partial_r \Phi_{\text{grav}} = -\frac{Gm(r)}{r^2}$ , an integrated form of the Poisson equation.

term on the right hand side of equation (2.5) whereby it gains the form of a conservation law that ensures the total energy to remain constant. The total energy of the system consequently yields the sum over all integrated cell energies. In stars however this modification is rather inapplicable since the contribution by potential energy exceeds all other energy terms by far and this term would numerically dominate the energy equation which is unfit in practice. Hence we stick with the formulation where changes in potential energy directly contribute to the momentum equation (see the full set of equations 2.4). Alternatively we suggest a *non-static* equation for the gravitational force in multiple dimensions.

### 2.3.2 Non-Static Gravitation Equation

The gravitational potential  $\Phi_{\text{grav}}$  is not needed explicitly at any point of the computation since coupling is accomplished via the gravitational force respectively the gradient of the potential i.e.  $\text{grad } \Phi_{\text{grav}}$ .

We define the gravitational force vector  $\mathbf{G}(\mathbf{x}, t) : \mathbb{R}^{n+1} \rightarrow \mathbb{R}^{n+1}$  in the familiar way

$$\mathbf{G} = -\text{grad } \Phi_{\text{grav}} \quad (2.30)$$

hence the Poisson equation can be written  $\text{div } \mathbf{G} = -4\pi G\rho$ . We differentiate with respect to  $t$  and use the continuity equation (2.2) to obtain

$$\begin{aligned} \partial_t \text{div } \mathbf{G} &= -4\pi G \partial_t \rho \\ &= 4\pi G \text{div } (\rho \mathbf{u}). \end{aligned}$$

Since  $\Phi_{\text{grav}}$  is  $\mathcal{C}^\infty$  it is reasonable to assume that the derivatives with respect to  $t$  exists and is continuous as well, the operations can be interchanged. We consider the conservative, integral form of these equations again and use the divergence theorem.

$$\begin{aligned} \int_{V(t)} \text{div } \partial_t \mathbf{G} dV &= \int_{V(t)} 4\pi G \text{div } (\rho \mathbf{u}) dV \\ \int_{\partial V(t)} \partial_t \mathbf{G} \cdot d\mathbf{S} &= 4\pi G \int_{\partial V(t)} (\rho \mathbf{u}) \cdot d\mathbf{S} \end{aligned} \quad (2.31)$$

We obtain an equation for the gravitational force in form of a pure initial value problem.

$$\partial_t \mathbf{G} = 4\pi G \rho \mathbf{u} \quad (2.32)$$

This way we avoid solving the Poisson equation in multiple dimensions by solely considering its gradient, the gravitational force. Equation (2.32) describes gravitation non-statically by understanding temporal changes of gravitational forces as mass transport.

If, respectively in what extent, this formulation is numerically preferable will have to be studied in future computations.

Self-gravitation expressed via (2.32) would not have to be solved at any time of the evolution but only initially contrary to Poisson equation implementations. Hence it is supposedly especially suited for explicit and parallelized methods.

## 2.4 Full Set of RHD Equations with Self-Gravitation

The system of equations of radiation hydrodynamics with gravitation is now presented in its for our purposes somewhat simplified formulation. The following system has been basis for a number of implicit RHD computations like Dorfi (1999) [13] and Stökl (2006) [40]. In latter PhD thesis physical assumptions and simplifications are illustrated and their consequences executed more detailed than in this paper.

### Continuity Equation

$$\partial_t \rho + \operatorname{div}(\mathbf{u}\rho) = 0 \quad (2.33)$$

### Equation of motion

$$\partial_t(\rho\mathbf{u}) + \operatorname{div}(\rho\mathbf{u}\mathbf{u} + \mathbf{P} - \sigma) - \rho\mathbf{G} - \frac{4\pi}{c}\chi_R\mathbf{H} = 0 \quad (2.34)$$

### Equation of Internal Energy

$$\partial_t(\rho\epsilon) + \operatorname{div}(\rho\epsilon\mathbf{u} + (\mathbf{P} - \sigma) \cdot \mathbf{u}) - 4\pi\chi_P(J - S) = 0 \quad (2.35)$$

### Equation of Radiation Energy

$$\partial_t J + \operatorname{div}(\mathbf{u}J) + c \operatorname{div} \mathbf{H} + \mathbf{K} : \operatorname{grad} \mathbf{u} - c\chi_P(J - S) = 0 \quad (2.36)$$

### Radiation Flux Equation

$$\partial_t \mathbf{H} + \operatorname{div}(\mathbf{u}\mathbf{H}) + c \operatorname{div} \mathbf{K} + \mathbf{H} \cdot \operatorname{grad} \mathbf{u} + c\chi_R\mathbf{H} = 0 \quad (2.37)$$

### Poisson Equation

$$\Delta\phi = 4\pi G\rho \quad (2.38)$$

respectively

### Non-Static Gravitation Equation

$$\partial_t \mathbf{G} = 4\pi G \rho \mathbf{u} \quad (2.39)$$

Basically we collected equations (2.2), (2.4), (2.5) plus (2.28) and added gravitation. The viscosity  $\sigma$  will be replaced by an artificial viscous pressure  $-\mathbf{Q}$  which we establish in section 3.1.4. In section 3.3 we present this system of equations in strong conservation form for non-steady curvilinear coordinates.

## 3 Conservative Numerics

In this chapter we want to develop some numerical methods for conservation laws after having motivated and anticipated relevant mathematical concepts in the previous sections. Concepts for error functions, convergence and stability for linear and nonlinear equations will be studied in form of an overview. A particular focus will lie on conservative methods for nonlinear problems in general curvilinear coordinates which will require some tensor analysis and differential geometry.

In sections 3.2 and 3.3 we will present the mathematical framework for strong conservative numerics in non-steady curvilinear coordinates and exemplarily sketch the system of RHD in spherical and polar coordinates. An articulate introduction and motivation to computational methods in astrophysical context can be found in LeVeque, Mihalas, Dorfi, Müller [25].

### 3.1 Numerical Methods for Conservation Laws

Standard numerical methods for partial differential equations are established under the assumption of (classical) differentiability. Routine finite difference schemes of first order usually smear or *smoothen* the solution in the vicinity of discontinuities, since they come with intrinsic numerical viscosity. Standard second order methods show something to the effect of the Gibbs phenomenon, where we see oscillations around shocks. In the past decades so called *high resolution methods* have been developed in order to achieve proper accuracy and resolution for nonlinear, discontinuous problems as they appear also in radiation hydrodynamics. In the following sections we will introduce some basic technical terms in discrete numerical methods for conservation laws and present some important concepts for nonlinear problems.

#### 3.1.1 Introduction to Discretization Methods

The basic idea of discretization methods for PDEs is to represent functions by a finite amount of data and to approximate differential operators by difference operators. To simplify matters, we confine ourselves to 1 + 1 dimensional problems and constant increments in the upcoming introductory sections. Our toy model for analysis shall be the time-dependent Cauchy problem (1.5), namely  $\partial_t \mathbf{d} + \operatorname{div} \mathbf{f}(\mathbf{d}) = \mathbf{0}$  but in linear form

### 3 Conservative Numerics

and one space dimension<sup>1</sup>  $\partial_t \mathbf{d} + A \partial_x \mathbf{d} = 0$  with constant  $A$ . Concerning structure and nomenclature we basically follow LeVeque [26] in the following sections.

For the spatial part we introduce a mesh width  $h = \Delta x$  and a time step  $k = \Delta t$  for the temporal discretization. Any point in this computational domain can be attained by multiple steps in  $t$  and  $x$ , that is  $(x_j, t_n) = (jh, nk)$ , where  $j \in \mathbb{Z}$  and  $n \in \mathbb{N}$  with starting point or initial condition  $\mathbf{d}(x_j, t_0)$ . What we want to obtain is the approximate solution of the exact  $\mathbf{d}(x, t)$  at discrete grid points  $\mathbf{d}(x_j, t_n)$  and we characterize these approximation as  $\mathbf{D}_j^n$ .

The difference scheme is somewhat arbitrary and its design depends on the concrete problem to be approximated. The essential requirement is that in the limit of  $(j, n) \rightarrow 0$  the difference operator reproduces the differential operator. The method is called explicit when the function at the new time step is calculated directly via function values at prior time steps. We introduce a special notation for such operators with  $\mathcal{H}(\mathbf{D}^n; j) = \mathbf{D}_j^{n+1}$  which reproduces the vector of approximations at the new time step  $\mathbf{D}_j^{n+1}$ . Some well known explicit schemes for our toy model are for example the so called *Upwind*, *Lax-Friedrichs*, *Leapfrog* and *Lax-Wendroff* method.

$$\begin{aligned}
 \mathcal{H}(\mathbf{D}^n; j) &= \mathbf{D}_j^n - \frac{k}{h} A (\mathbf{D}_j^n - \mathbf{D}_{j-1}^n) \\
 &= \frac{1}{2} (\mathbf{D}_{j-1}^n + \mathbf{D}_{j+1}^n) - \frac{k}{2h} A (\mathbf{D}_{j+1}^n - \mathbf{D}_{j-1}^n) \\
 &= \mathbf{D}_j^{n-1} - \frac{k}{h} A (\mathbf{D}_{j+1}^n - \mathbf{D}_{j-1}^n) \\
 &= \mathbf{D}_j^n - \frac{k}{2h} A (\mathbf{D}_{j+1}^n - \mathbf{D}_{j-1}^n) + \frac{k^2}{2h^2} A^2 (\mathbf{D}_{j+1}^n - 2\mathbf{D}_j^n + \mathbf{D}_{j-1}^n)
 \end{aligned} \tag{3.1}$$

#### 3.1.2 Error and Stability in the Linear Case

There is a number of criteria that reveal the quality of a numerical method, however the most obvious is to define an error function which states the difference between the exact and the numerical approximate solution. In this sense the pointwise error is defined by

$$\mathbf{E}_j^n = \mathbf{D}_j^n - \mathbf{d}_j^n. \tag{3.2}$$

---

<sup>1</sup>We maintain the *tensor notation* in boldface  $\mathbf{d}$  for densities and fluxes for distinction purposes als in 1+1 dimensions.



### 3.1 Numerical Methods for Conservation Laws

In conjunction with conservation laws the numerical solution is often seen as an approximation to a cell average of  $\mathbf{d}(x_j, t_n)$ , defined by

$$\bar{\mathbf{d}}_j^n = \frac{2}{x_{j+1} - x_{j-1}} \int_{x_{j-1/2}}^{x_{j+1/2}} \mathbf{d}(x', t_n) dx', \quad (3.3)$$

where the half step is simply  $x_{j+1/2} = x_j + h/2$  and the pointwise error in terms of cell averages yields

$$\bar{\mathbf{E}}_j^n = \bar{\mathbf{D}}_j^n - \bar{\mathbf{d}}_j^n. \quad (3.4)$$

Let be  $\mathbf{D}_k(x, t) = \mathbf{D}_j^n$  for  $(x, t) \in [x_{j-1/2}, x_{j+1/2}] \times [t_n, t_{n+1})$ , then the *error function* in terms of piecewise constant functions is defined by

$$\mathbf{E}_k(x, t) = \mathbf{U}_k(x, t) - \mathbf{u}(x, t). \quad (3.5)$$

We have already mentioned that the difference operator has to approximate the differential operator properly. Regarding the temporal iteration we want that smaller time steps cause smaller errors. We call the numerical method *convergent* (in a norm<sup>2</sup>), if for arbitrary initial condition  $\mathbf{d}_0$ ,  $\forall t > 0$

$$\lim_{k \rightarrow 0} \|\mathbf{E}_k(\cdot, t)\| = 0. \quad (3.6)$$

Assuming smooth solution we always can expand the exact solution into a Taylor series and compare the leading terms to the numerical scheme. By that means we get a measure of how well the difference equation reproduces the difference equation locally. The *local truncation error* is therefore defined by

$$\mathbf{L}_k(x, t) = \frac{1}{k} \left( \mathbf{d}(x, t+k) - \mathcal{H}(\mathbf{d}(\cdot, t); x) \right) \quad (3.7)$$

and we call the numerical method *consistent*, if

$$\lim_{k \rightarrow 0} \|\mathbf{L}_k(\cdot, t)\| = 0. \quad (3.8)$$

The method is of *order*  $p$ , if for all sufficiently smooth initial data with compact support, there is some constant  $C_L$ , such that

$$\|\mathbf{L}_k(\cdot, t)\| \leq C_L k^p, \quad (3.9)$$

---

<sup>2</sup>For conservation laws the a practicable norm is the 1-norm  $\|\dots\| = \int_{-\infty}^{\infty} |\dots| dx$ , since more rigorous demands come into conflict with approximation of discontinuities;  $\|\mathbf{D}_k(\cdot, t_n)\|_1 = h \sum_j |\mathbf{D}_j^n|$ .

### 3 Conservative Numerics

for all  $k < k_0$  and  $t < T$ . The restriction to a local  $T$  falls for stable methods, where the order remains the same for any  $t$  or  $k$ .

There is a profound stability theory for linear methods; its details can be found in several relevant text books (e.g. Richtmeyer, Morton [36]). Nevertheless, at this point we shall mention the *Lax-Richtmeyer stability* which states that a method is stable if for each time  $T$  there is a constant  $C_S$  and a value  $k_0 > 0$  such that

$$\|\mathcal{H}_k^n\| \leq C_S \tag{3.10}$$

for all  $nk \leq T$ , where  $k < k_0$ . The important *Lax equivalence theorem* claims that for consistent linear methods stability is necessary and sufficient for convergence.

In this context we also should mention the *Courant, Friedrichs, Lewy (CFL) condition*, which seizes the fact that hyperbolic equations stand out due to a bounded *domain of dependence*. The solution at a point  $\mathbf{d}(x, t)$  is determined by initial data within some finite distance to this point. This range of influence is related to the fact, that hyperbolic equations always have finite propagation speed, as briefly mentioned in the introduction to section 1.1. When Courant, Friedrichs and Lewy studied convergence of numerical schemes for hyperbolic conservation laws, they observed that one necessary condition for convergence is that the domain of dependence of the finite difference scheme includes the domain of dependence of the PDE. In other words, data from one time point must not propagate faster than the characteristic speed of the original equation. Mathematically worded, the domain of dependence  $\mathcal{D}(\bar{x}, \bar{t})$  is a set of points  $(x, t)$  with the property that a disturbance of  $\mathbf{d}(x, t)$  influences the solution at  $(\bar{x}, \bar{t})$ . The numerical domain of influence  $\mathcal{D}_k(\bar{x}, \bar{t})$  is analogously defined. For the stability of an (explicit) method it is necessary that for  $h, k \rightarrow 0$  the numerical domain of dependence  $\Omega_k(\bar{x}, \bar{t})$  contains asymptotically the domain of dependence the corresponding initial value problem. Practically, an inevitable (but not sufficient) stability condition for such methods is represented by a limited ratio of time step to mesh size. For a scalar advection equation with propagation speed  $a$ , the CFL condition yields  $0 \geq \frac{ak}{h} \geq 1$  as an example.

#### 3.1.3 Conservative Methods and Lax Wendroff Theorem

In the linear case, the Lax equivalence theorem states that a consistent and stable discretization scheme automatically converges to the weak solution of the conservation law. For nonlinear equations, consistent methods do not necessarily converge to the weak solution of the conservation law<sup>3</sup>. We have already mentioned that nonlinear conservation laws can have several weak solutions but we are only interested in those, that also

---

<sup>3</sup>E.g. the CIR method, a nonlinear generalization of the Upwind scheme, is not applicable for discontinuous solutions, since it is not conservative.

satisfy the entropy condition. So it is not surprising that it is required to make sure, the numerical scheme satisfies some discrete analogon of the entropy condition (1.14).

The proper postulation to the numerical scheme that prevents convergence to non-solutions is that the difference method has *conservation form*, i.e.

$$\mathbf{D}_j^{n+1} = \mathbf{D}_j^n - \frac{k}{h} \left( \mathbf{F}(\mathbf{D}_{j-p}^n, \dots, \mathbf{D}_{j+q}^n) - \mathbf{F}(\mathbf{D}_{j-p-1}^n, \dots, \mathbf{D}_{j+q-1}^n) \right) \quad (3.11)$$

for a *numerical flux function*  $\mathbf{F}$  of  $p + q + 1$  arguments. This numerical flux can be interpreted as averaged flux through  $x_{j+1/2}$  and  $[t_n, t_{n+1}]$  in the sense that  $\mathbf{F} \cong \frac{1}{k} \int_{t_n}^{t_{n+1}} \mathbf{f}(\mathbf{d}(x_{j+1/2}, t)) dt$ . In section 3.2 we will turn our intensive attention to this numerical quantity when we concern ourselves with conservative methods in general coordinates.

We also reformulate the concept of *consistency for conservative schemes*. The conservative method is consistent with the original conservation law, if the numerical flux function  $\mathbf{F}$  reproduces the true flux  $\mathbf{f}$  in the case of constant flow  $\bar{\mathbf{d}}$  so that

$$\mathbf{F}(\bar{\mathbf{d}}, \dots, \bar{\mathbf{d}}) = \mathbf{f}(\bar{\mathbf{d}}). \quad (3.12)$$

Moreover, we require as the arguments of  $\mathbf{F}$  approach a common value  $\bar{\mathbf{d}}$ , that the value of  $\mathbf{F}$  meets  $\mathbf{f}(\bar{\mathbf{d}})$  smoothly<sup>4</sup>. So for each  $\bar{\mathbf{d}}$  there may exist some constant  $K > 0$  so that

$$\left\| \mathbf{F}(\mathbf{D}_{j-p}, \dots, \mathbf{D}_{j+q}) - \mathbf{f}(\bar{\mathbf{d}}) \right\| \leq K \max_{-p \leq l \leq q} \left\| \mathbf{D}_{j+l} - \bar{\mathbf{d}} \right\|. \quad (3.13)$$

Before we can establish a nonlinear convergence theorem we first have to define a *total variation* of an arbitrary  $\mathcal{L}^\infty$  function  $\mathbf{v}$ .

$$\text{TV}(\mathbf{v}) = \limsup_{\varepsilon \rightarrow 0} \frac{1}{\varepsilon} \int_{-\infty}^{\infty} \|\mathbf{v}(x) - \mathbf{v}(x - \varepsilon)\| dx \quad (3.14)$$

which reduces to a more familiar look for differentiable  $\mathbf{v}$  respectively appropriate distribution derivatives, namely  $\text{TV}(\mathbf{v}) = \int_{-\infty}^{\infty} \|\mathbf{v}'\| dx$ . We call a sequence of solutions  $\mathbf{D}_i$  *convergent* to a solution  $\mathbf{d}$ , if for every bounded set  $[a, b] \times [0, T]$

$$\int_0^T \int_a^b \|\mathbf{D}_i(x, t) - \mathbf{d}(x, t)\| dx dt \rightarrow 0 \quad \text{for } i \rightarrow \infty \quad (3.15)$$

---

<sup>4</sup>The requirement is Lipschitz continuity which is exigently given for any smooth and consequently differentiable flux function  $\mathbf{f}$ .

### 3 Conservative Numerics

and there exists an upper bound  $R$  for the total variation such that

$$\mathrm{TV}(\mathbf{D}_i(\cdot, t)) < R \quad (3.16)$$

for  $0 \leq t \leq T$  and  $i \in \mathbb{N}$ .

This leads us to the essential *Lax-Wendroff theorem* which averts the following. Let  $\{\mathbf{D}_i(x, t)\}$  be a sequence of solutions of a conservative and consistent difference method for the one dimensional conservation law, where the mesh parameters  $(k, h) \rightarrow 0$  for  $i \rightarrow \infty$ . Suppose the numerical approximation at the  $i$ -th grid  $\{\mathbf{D}_i(x, t)\}$  converges to a function  $\mathbf{d}(x, t)$  in the sense made precise before; then  $\mathbf{d}(x, t)$  is a weak solution of the conservation law.

Still, the consistent conservative scheme can converge to a weak solution that does not satisfy the entropy condition (1.14). We add a comparable condition for the numerical method in form of the *Lax-Wendroff corollary*. Let  $\sigma$  entropy function and  $\phi$  entropy flux and let be  $\Phi$  the consistent (in the above defined sense) corresponding numerical flux function. Given the Lax-Wendroff theorem is satisfied and

$$\sigma(\mathbf{D}_j^{n+1}) \leq \sigma(\mathbf{D}_j^n) - \frac{k}{h} (\Phi(\mathbf{D}^n, j) - \Phi(\mathbf{D}^n, j-1)) \quad (3.17)$$

holds, then  $\mathbf{d}(x, t)$  satisfies entropy condition (1.19).

As in the linear case, the picture is not drawn completely until we clarify stability of the numerical method. All we know now is, that if a sequence of approximation converges, the limit is a weak solution. However, we require intrinsic stability of the method in order to ensure convergence of the difference scheme. Without going into details, *total variation stability* is the suitable concept for nonlinear methods, for which the Lax equivalence theorem is not applicable. It can be shown that TV-stability, consistency and conservativeness guarantee nonoscillatory convergence of the advection scheme.

As a further remark to the topic of methods for nonlinear conservation laws, we want to present an important class of methods that ensure TV-stability. The idea goes back to Harten (1983) [18], who was studying high resolution methods for hyperbolic conservation laws and proposed so called *total variation diminishing (TVD)* (originally *non-increasing*) methods. We call a numerical scheme  $\mathcal{H}(\mathbf{D}^n; j)$  total variation diminishing if

$$\mathrm{TV}(\mathbf{D}^{n+1}) \leq \mathrm{TV}(\mathbf{D}^n) \quad (3.18)$$

for all grid functions  $\mathbf{D}^n$  at all time steps  $n$ . Of course, the true solution of the conservation law must be compatible with this postulation and indeed it can be shown, that any weak solution  $\mathbf{d}(x, t)$  satisfies  $\mathrm{TV}(\mathbf{d}(\cdot, t_{n+1})) \leq \mathrm{TV}(\mathbf{d}(\cdot, t_n))$  for any  $n > 0$ .

In the upcoming two subsections we want to present some sophisticated high resolution numerical methods incorporating these techniques for nonlinear conservation laws. The

emphasis will lie on concepts and techniques relevant for our RHD problem as they have been implemented in applications like Dorfi (1999) [13] respectively Dorfi et al. (2004) [12]

### 3.1.4 Artificial Viscosity

The TVD approach is not the only one to find entropy-satisfying weak solutions with numerical schemes. One of the simplest techniques are monotone methods<sup>5</sup>, however the have one main disadvantage. Monotone methods are at most first order accurate. In the past decades major efforts were made in developing numerical methods for nonlinear hyperbolic conservation laws that are at least second order.

One patent attempt to finding such a high resolution method is to adapt a well known high order method like Lax-Wendroff for nonlinear problems. As we have contemplated in section 1.1.3 we can add an *artificial viscosity* term to the conservation law in a way that the entropy condition is satisfied. Numerically we are keen to design this viscosity in a manner that it affects discontinuities but vanishes sufficiently elsewhere so that the order of accuracy can be maintained those regimes where the solution is smooth. Interestingly this idea was inspired by physical dissipation mechanisms and dates back more than half a century to VonNeumann and Richtmeyer (1950) [47] who investigated new methods to treat shocks in hydrodynamic simulations. Bearing in mind that we have to provide conservation form, the numerical flux function gets modified by an artificial viscosity  $\mathbf{q}(\mathbf{D}; j)$  for instance in the following way.

$$\mathbf{F}_{\text{visc}}(\mathbf{D}; j) = \mathbf{F}(\mathbf{D}; j) - h\mathbf{q}(\mathbf{D}; j)(\mathbf{D}_{j+1} - \mathbf{D}_j) \quad (3.19)$$

Since the original design of this additional viscous pressure in the form  $q = c_2\rho(\Delta\mathbf{u})^2$ ,  $c_2 \in \mathbb{R}$ , for one dimensional advection  $\partial_t\mathbf{d} + a\partial_x\mathbf{d} = q\partial_{xx}\mathbf{d}$  it underwent a number of modifications and generalizations. It turned out to be numerically preferable to add a linear term, see Landshoff (1955) [24] in order to control oscillations, generalizations to multi-dimensional flows mostly retained the original analogy to physical dissipation and reformulated the velocity term accordingly, e.g. Wilkins (1980) [49].

In any case artificial viscosity broadens shocks to steep gradients at some characteristic length scale but on the other hand shall not cause unintentional smearing. The concrete composition and implementation of this artificial viscosity coefficient  $\mathbf{q}$  depends on the application. Tscharnuter and Winkler (1979) [44] pointed out that the viscous pressure in 3D radiation hydrodynamics has to unravel normal stress, quantified by the divergence of the velocity field and shear stress, which is expressed by the symmetrized gradient of the velocity field according to the general theory of viscosity. It is designed to *switch on*

---

<sup>5</sup>The more general concept is called  $l_1$ -contracting methods, see e.g. Harten et al. (1976) [19].

### 3 Conservative Numerics

only in case of compression ( $\text{div } \mathbf{u} < 0$ ) yielding

$$\mathbf{Q} = -q_2^2 l_{\text{visc}}^2 \rho \max(-\text{div } \mathbf{u}, 0) \left( \left[ \nabla \mathbf{u} \right]_s - \frac{1}{3} \mathbf{e} \text{div } \mathbf{u} \right), \quad (3.20)$$

and is set zero otherwise. In section 3.2.4 we will elaborate, why we have to modify this definition for general geometries by replacing the unit tensor  $\mathbf{e}$  by a metric tensor  $\mathbf{g}$ . In section 3.3 we will specify co- and contravariant components of the artificial viscosity tensor in spherical coordinates.

#### 3.1.5 Flux Limiters

When we discussed the radiation closure relation in section 2.2.3, the approach was analytical respectively physical. Hyperbolicity of a conservation law implies real eigenvalues of the corresponding Jacobian  $\nabla_{\mathbf{d}} \mathbf{f}$  which leads to characteristic propagation speeds which in case of radiation are connected with the speed of light. Pons, Ibanez, Miralles (2000) [35] studied flux limiting in context of Gudonov-methods based on these constraints on propagation speeds, Levermore (1984) [27] studied flux limiters and Ed-dington factors in anisotropic cases.

Flux limiters (or slope limiters) basically restrain solution gradients near shocks and thereby avoid oscillation in high resolutions methods (such as second order TVD). With flux limiting, the advection scheme gets split up in high order fluxes in smooth regions and lower order schemes (like Upwind) in the vicinity of discontinuities. With a limiter function  $\Phi(\mathbf{D}; j)$  the flux yields  $\mathbf{F} = \mathbf{F}_{\text{low}} + \Phi(\mathbf{F}_{\text{high}} - \mathbf{F}_{\text{low}})$  respectively in a more practical formulation

$$\mathbf{F}(\mathbf{D}; j) = \mathbf{F}_{\text{high}}(\mathbf{D}; j) - (1 - \Phi(\mathbf{D}; j))(\mathbf{F}_{\text{high}}(\mathbf{D}; j) - \mathbf{F}_{\text{low}}(\mathbf{D}; j)). \quad (3.21)$$

There is a number of different ways in implementing such a flux limiter albeit they are typically functions of the steepness of the gradient. One ambiguity lies in this *measure of smoothness* in discrete terms, in this context commonly denominated  $\theta_j$ . One passable way is the ratio of consecutive gradients

$$\theta_j = \frac{\mathbf{D}_j - \mathbf{D}_{j-1}}{\mathbf{D}_{j+1} - \mathbf{D}_j} \quad (3.22)$$

and is obviously near 1 for smooth data. Several flux limiter methods, i.e. different functions  $\Phi(\theta_j)$  have been suggested and tested extensively (e.g. Van Leer (1979) [45]). In implicit RHD computations like Dorfi et al. (2004) [12] and previous papers implement

### 3.2 Conservative Methods in General Curvilinear Coordinates

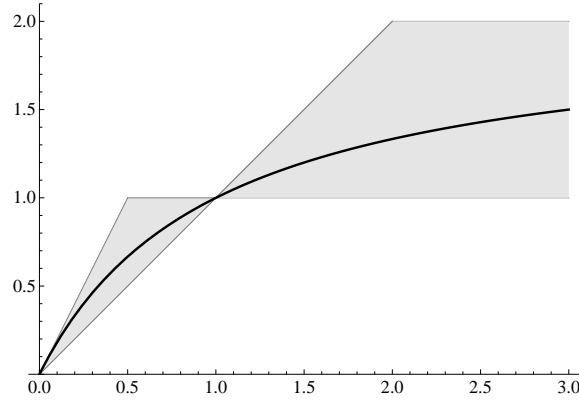


Figure 3.1: Van Leer Limiter

the Van Leer limiter which is constructed in the following way.

$$\Phi(\theta_j) = \begin{cases} \frac{2\theta}{1+\theta} & \text{if } \theta \geq 0 \\ 0 & \text{otherwise} \end{cases} \quad (3.23)$$

The Van Leer limiter describes a smooth function, a somewhat distinct characteristic in comparison to other feasible methods. In figure 3.1 the gray region denotes TVD; for details we refer to LeVeque [26] once again.

## 3.2 Conservative Methods in General Curvilinear Coordinates

In the previous section we presented necessary premises for conservative difference schemes, particularly the conservation form for a numerical method (3.11). The numerical flux function  $\mathbf{F}$  we defined can be interpreted as flux averaged over a cell (3.3) and a time interval  $\mathbf{F} \cong \frac{1}{k} \int_{t_n}^{t_{n+1}} \mathbf{f}(\mathbf{d}(x_{j+1/2}, t)) dt$ . Descriptively written, the conservation form ensures that whatever fraction of the density gets transported from one to another cell, arrives there. In other words, if supposedly all density of one cell gets advected to another, we need to find the same *physical* amount in there afterwards. However, if the cell volumes differ and the flux is a cell integrated quantity it is required to assess the cell volume itself properly. Hence in order to conserve a certain density function  $\mathbf{d}(\mathbf{x}, t)$  in general coordinates where non non-steady, nonlinear volume elements occur, we need to investigate the numerical flux more thoroughly in terms of differential and integral calculus.

Mathematically the fluxes that occur in hyperbolic conservation laws are generated via spatial differential operators which are obtained by applying the divergence theorem to a differential volume, bounded by a surface (1.4). In the upcoming subsections we want

### 3 Conservative Numerics

to elaborate how differential geometric considerations lead to a reformulation of these differential operators, Gradient and Divergence in a *geometrically conservative* form.

#### 3.2.1 Tensor Calculus and Elementary Differential Geometry

To begin with, we want to recapitulate some relations from tensor analysis and elementary differential geometry and define linear and nonlinear coordinate systems, coordinate transformations, base vectors and co- and contravariant vector components. In the following section we will use Einstein summation convention, indices in braces do not designate components but coordinate systems. Consequent argumentations and proofs can be found in Lichnerowicz [28], Schutz [37] and Liseikin [31].

Let  $\mathcal{M}$  be an affine space with corresponding vector space  $\mathcal{V}$  and  $\Sigma_{(\alpha)}$  a *linear coordinate system*. The coordinate system maps points  $\mathbf{x} \in \mathcal{M}$  (linear, bijective) to a  $d$ -tuple of numbers  $x^i$ .  $\Sigma_{(\alpha)} : \mathcal{M} \rightarrow \mathbb{R}^d$ ,  $\mathbf{x} \mapsto (x_{(\alpha)}^i)$ . Coordinate lines of a linear coordinate system are straight lines on the affine space. Two linear coordinate systems  $\Sigma_{(\alpha)}$  and  $\Sigma_{(\beta)}$  are connected via a *coordinate transformation*

$$x_{(\alpha)}^i = \Lambda_{(\alpha\beta)}^i x_{(\beta)}^j + \lambda_{(\alpha\beta)}^i. \quad (3.24)$$

Such affine transformations imply translation ( $\lambda_{(\alpha\beta)}^i$ ) as well as rotation and shearing ( $\Lambda_{(\alpha\beta)}^i$ ) of coordinate lines. The natural *base vectors* of any coordinate system are tangential vectors to the coordinate lines and thus constant in the linear case.

$$\mathbf{e}_{(\alpha)i} = \frac{\partial \mathbf{x}}{\partial x_{(\alpha)}^i} \quad (3.25)$$

The index  $i$  in this case denotes the  $i$ -th base vector. The dual base is implicitly defined via the inner product  $\mathbf{e}_{(\alpha)}^i \cdot \mathbf{e}_{(\alpha)j} = \delta^i_j$ ; the dual base  $\mathbf{e}_{(\alpha)}^i \in \mathcal{V}^*$  is a linear map  $\mathcal{V}^* \rightarrow \mathbb{R}$ , which maps the base vectors  $\mathbf{e}_{(\alpha)j} \in \mathcal{V}$  to zero or one. The natural and the dual base vectors transform unequally to a new coordinate system  $\Sigma_{(\beta)}$ .

$$\begin{aligned} \mathbf{e}_{(\beta)i} &= \Lambda_{(\alpha\beta)}^j_i \mathbf{e}_{(\alpha)j} = \frac{\partial x_{(\alpha)}^j}{\partial x_{(\beta)}^i} \mathbf{e}_{(\alpha)j} \\ \mathbf{e}_{(\beta)}^i &= \Lambda_{(\alpha\beta)}^i_j \mathbf{e}_{(\alpha)}^j = \frac{\partial x_{(\alpha)}^i}{\partial x_{(\beta)}^j} \mathbf{e}_{(\alpha)}^j \end{aligned} \quad (3.26)$$

The matrix  $\Lambda_{(\alpha\beta)}$  is referred to as *Jacobian* of the coordinate transformation.

A transformation to a *curvilinear coordinate system* is no longer necessarily linear nor bijective. With nonlinear coordinate systems, the base vectors are not constant but



### 3.2 Conservative Methods in General Curvilinear Coordinates

functions of position.

$$\mathbf{e}_{(\alpha)i}(\mathbf{x}) = \frac{\partial \mathbf{x}}{\partial x_{(\alpha)}^i} \quad (3.27)$$

Of course, the entries of the Jacobian  $\Lambda_{(\alpha\beta)}$  are now functions too

$$\Lambda_{(\alpha\beta)_j}^i(\mathbf{x}) = \frac{\partial x_{(\alpha)}^i}{\partial x_{(\beta)}^j} \quad (3.28)$$

and  $\mathbf{e}_{(\alpha)}^i(\mathbf{x}) \cdot \mathbf{e}_{(\alpha)j}(\mathbf{x}) = \delta^i_j$  is valid pointwise. All vectorial and tensorial quantities  $T_{\dots}$  in this domain are defined via their components with respect to the local base in the following sense.

$$T_{(\alpha)\rho\dots\sigma}^{i\dots j}(\mathbf{x}) = T(\mathbf{e}_{(\alpha)}^i(\mathbf{x}), \dots, \mathbf{e}_{(\alpha)}^j(\mathbf{x}), \mathbf{e}_{(\alpha)\rho}(\mathbf{x}), \dots, \mathbf{e}_{(\alpha)\sigma}(\mathbf{x})) \quad (3.29)$$

We define the *covariant components of the metric tensor*  $\mathbf{g}$  as local measure of distances in the coordinate system

$$\mathbf{e}_i(\mathbf{x}) \cdot \mathbf{e}_j(\mathbf{x}) = g_{ij}(\mathbf{x}). \quad (3.30)$$

The metric tensor is obviously symmetrical due to commutativity of the scalar product and implicates a symmetrical bilinear form  $\mathbf{x} \cdot \mathbf{y} = g_{ij}x^i y^j$  on the Euclidean vector space  $\mathcal{V}$ . From now on lower indices designate *covariant* and upper indices *contravariant* components. Together with the contravariant metric tensor  $\mathbf{e}^i(\mathbf{x}) \cdot \mathbf{e}^j(\mathbf{x}) = g^{ij}(\mathbf{x})$  we gain the following transformation rules between co- and contravariant components of a tensor.

$$v_i = g_{ij}v^j, \quad v^i = g^{ij}v_j \quad (3.31)$$

Raising and lowering indices in linear coordinates just means to transpose respectively to interchange rows and columns of higher rank tensors. With curvilinear coordinate systems the dual space is also *metrically* different.

Next we want to liaise the recently defined geometrical items with differential calculus. Vectorial and tensorial quantities feature a *native* construction in differential geometric terms. Vector components that are generated via a Gradient of a scalar are covariant by definition, e.g.  $\partial_i \phi = p_i$  whereas coordinates  $x^i$  are contravariant. Higher rank tensors are constructed by differentiation or tensorial products, e.g.  $\mathbf{t} = \mathbf{p}\mathbf{q}$ <sup>6</sup>, and its native depiction in components is  $t_i^j = p_i q^j$ . The explicit form of such a tensor  $\mathbf{t}$  in coordinates  $x^l$  is

$$\mathbf{t}(\mathbf{x}) = t_i^j(\mathbf{x}) \mathbf{e}^i(\mathbf{x}) \mathbf{e}_j(\mathbf{x}). \quad (3.32)$$

For this reason, the tensorial physical quantities in the equations of radiation hydrodynamics will have to be considered firstly in their native form as well. When performing

---

<sup>6</sup>We generally omit explicit tensor products  $\mathbf{p}\mathbf{q} = \mathbf{p} \otimes \mathbf{q}$  respectively  $\mathbf{e}^i \mathbf{e}^j = \mathbf{e}^i \otimes \mathbf{e}^j$ .

### 3 Conservative Numerics

operations at and between them it will be necessary to consider a consistent denotation (e.g. contravariant components) and raising and lowering indices according to (3.31) will be required.

Evidently when differentiating a tensor we have to consider not only its components as functions but also the generally non constant base vectors in the coordinate system  $\Sigma_{(\alpha)}$ . Without forceful motivation we define a *covariant derivative* of a vector field  $\nabla_{(\alpha)}\mathbf{v}$  and the *Christoffel symbols*  $\Gamma_{(\alpha)}$  in the following way. Let  $\nabla$  be a map that transforms a tensor of rank  $(m, n)$  to a tensor of rank  $(m, n + 1)$ , satisfying  $\nabla\phi = \partial\phi$  for any scalar  $\phi$ . Let it furthermore satisfy all congenital demands on a derivative like the Leibnitz rule, additivity, commutativity and torsion-freeness and it shall be associated with the partial derivative via

$$\nabla_i v^j = \partial_i v^j + \Gamma^j_{ik} v^k \quad (3.33)$$

where the Christoffel symbols compensate for the locality of the base vectors.

$$\Gamma^j_{ik}(\mathbf{x})\mathbf{e}_j(\mathbf{x}) = \partial_i \mathbf{e}_k(\mathbf{x}) \quad (3.34)$$

We postulate that this covariant derivative provides the proper *affine connection* and implicitly defines the correct transformations between general coordinate systems and can be expanded to tensors of higher rank and arbitrary composition of co- and contravariant components.

$$\begin{aligned} \nabla_i v^i &= \partial_i v^i + \Gamma^i_{ik} v^k = \text{div } \mathbf{v} \\ \nabla_i v_j &= \partial_i v_j - \Gamma^k_{ij} v_k \\ \nabla_i t_j^k &= \partial_i t_j^k + \Gamma^k_{it} t_j^l - \Gamma^l_{ji} t_l^k \\ \dots &= \dots \end{aligned} \quad (3.35)$$

For linear coordinate systems the Christoffel symbols vanish trivially and the covariant derivative is identical to the partial derivative. Moreover, the covariant derivative can be called *metrical* in terms of compatibility with the metric tensor  $\mathbf{g}$ . The *Ricci Lemma* for the fundamental tensor states that the covariant derivative of the covariant components of  $\mathbf{g}$  vanish, which can be checked quickly.

$$\nabla_i g_{jk} = \partial_i g_{jk} - \Gamma^l_{ij} g_{lk} - \Gamma^l_{ik} g_{jl} = 0 \quad (3.36)$$

When we contract upper equation with  $g^{jk}$  we obtain  $g^{jk}\partial_i g_{jk} - \Gamma^j_{ij} - \Gamma^k_{ik} = 0$  and gain an interesting formula

$$\Gamma^j_{jk} = \frac{1}{2} g^{jk} \partial_i g_{jk} \quad (3.37)$$

which reminds of the derivative of the determinant of the metric tensor  $\det \mathbf{g} = g$  which

### 3.2 Conservative Methods in General Curvilinear Coordinates

is

$$\partial_i g = g g^{jk} \partial_i g_{jk}. \quad (3.38)$$

This yields to the following important relation between the Christoffel symbols and the metric.

$$\Gamma^k_{ki} = \frac{1}{2} \frac{\partial_i g}{g} = \frac{\partial_i \sqrt{|\mathbf{g}|}}{\sqrt{|\mathbf{g}|}} \quad (3.39)$$

We recognize the left hand side as a geometrical term in the divergence of a vector field (3.35) which leads to a meaningful reformulation of this derivative.

$$\operatorname{div} \mathbf{v} = \frac{1}{\sqrt{|\mathbf{g}|}} \partial_i \left[ \sqrt{|\mathbf{g}|} v^i \right] \quad (3.40)$$

Immediately we see the connection to the divergence theorem from integral calculus when we remember that the Jacobian determinant defines the volume element  $dV_{(\alpha)} = |\Lambda_{(\alpha)}| dx^i$  and we know that  $|\Lambda_{(\alpha)}| = \sqrt{|\mathbf{g}_{(\alpha)}|}$ .

$$\begin{aligned} \int \operatorname{div} \mathbf{v} dV &= \int \frac{1}{\sqrt{|\mathbf{g}|}} \partial_i \left[ \sqrt{|\mathbf{g}|} v^i \right] \sqrt{|\mathbf{g}|} dx^1 \dots dx^n \\ &= \int \partial_i \left[ \sqrt{|\mathbf{g}|} v^i \right] dx^1 \dots dx^n \end{aligned} \quad (3.41)$$

Latter expression equals the flux of the vector field  $\mathbf{v}$  over the borders of the volume, a factor which shall be crucial for our geometrically conservative formulation of the equations of RHD. Unfortunately the clue (3.41) is confined to scalar equations which is expressed in *Vinokur's theorem* published by Vinokur (1974) [46] and proven elegantly by Bridges (2008) [5]. It states, how *strong conservation form* (i.e. geometrically conservative in our diction) can be maintained regardless of what coordinate system used also for vectorial conservation laws.

#### 3.2.2 Strong Conservation Form

The numerical flux function we introduced in (3.11) as *integral* quantity has to be understood not solely as a function at nodes but as a function of cells and their geometries, that is to say

$$\mathbf{F} = \mathbf{F}(\mathbf{D}, \sqrt{|\mathbf{g}|}, \mathbf{e}^i). \quad (3.42)$$

Before we postulate how we obtain geometrically conservative fluxes or in other word, how we need to rephrase the covariant derivative (3.35) generally, we gain insight to another eclectic concept in differential geometry. The theory of *differential forms* is an approach to differential calculus in more dimensions that is independent of coordinates. Again we have to refer to relevant literature like Bishop and Goldberg [17] for stringent

### 3 Conservative Numerics

motivation and definitions. For us, differential forms shall just be *objects that emerge under integrals*, like  $w dx, \mathbf{f} d\mathbf{S}, \phi dV, \dots$  and in that manner we have seen them consistently. We are going to like them because our (numerical) fluxes are objects that emerge under integrals as well. Moreover, we accept that there is a peculiar generalized concept of differentiating such differential forms which basically simplifies to the covariant derivatives when we settle for particular coordinates.

We introduce a new notation, the *wedge product* of two vectors  $\mathbf{p}$  and  $\mathbf{q}$  as the following antisymmetric tensor<sup>7</sup>

$$\mathbf{p} \wedge \mathbf{q} = \mathbf{p}\mathbf{q} - \mathbf{q}\mathbf{p}. \quad (3.43)$$

Tensor analytically this wedge product is motivated from the observation that any antisymmetric tensor  $\mathbf{t}$  can be decomposed to linear combinations  $\mathbf{t} = t^{ij}(\mathbf{e}_i\mathbf{e}_j - \mathbf{e}_j\mathbf{e}_i)$ , ( $i < j$ ) respectively in terms of the wedge product  $\mathbf{t} = t^{ij}\mathbf{e}_i \wedge \mathbf{e}_j$ .

We define a *p-form* (i.e. a differential form of degree  $p$ ) by

$$\omega = w_{i_1\dots i_p} dx^{i_1} \wedge dx^{i_2} \wedge \dots \wedge dx^{i_p} \quad (3.44)$$

which is obviously totally antisymmetric in its indices. The *exterior derivative*  $d\omega$  of a  $p$ -form  $\omega = w_{i_1\dots i_p} dx^{i_1} \wedge \dots \wedge dx^{i_p}$  is

$$d\omega = \partial_j w_{i_1\dots i_p} dx^j \wedge dx^{i_1} \wedge \dots \wedge dx^{i_p} \quad (3.45)$$

which yields a  $(p+1)$ -form. As an example, the exterior derivative of a 1-form  $\omega = w_i dx^i$  yields  $d\omega = \partial_i w_j dx^i dx^j$ . The general *Stokes theorem* shows the connection of the exterior derivative on differential forms to integration theory, namely

$$\int_{\Omega} d\omega = \int_{\partial\Omega} \omega. \quad (3.46)$$

The generalized concept of the *covariant derivative* maps a  $p$ -form to a  $(p-1)$ -form and is defined by

$$\delta\omega = (-1)^{p+1} * d * \omega \quad (3.47)$$

where  $*$  is the *Hodge star operator* which could be understood as generalization of the Levi-Civita tensor  $\varepsilon$  with metrical weight.

$$* (dx^{i_1} \wedge \dots \wedge dx^{i_p}) = dx^{i_{p+1}} \wedge dx^{i_{p+2}} \wedge \dots \wedge dx^{i_n} \quad (3.48)$$

The Hodge operator is the source for the volume form  $\omega_{\text{Vol}} = *1 = \sqrt{|\mathbf{g}|} dx^1 \wedge \dots \wedge dx^n$  which we already encountered in the divergence theorem (3.41).

The benefit of dealing with differential forms shows when we associate them with well

---

<sup>7</sup>Of course we imply tensor products  $\mathbf{p}\mathbf{q} = \mathbf{p} \otimes \mathbf{q}$  again.

## 3.2 Conservative Methods in General Curvilinear Coordinates

known concepts of tensor calculus. The exterior derivative of an 1-form  $\omega$  in  $\mathbb{R}^3$  yields the Curl, to wit  $d(w d\mathbf{x}) = \text{curl } w d\mathbf{S}$  which in component notation is often expressed by  $d(w d\mathbf{x}) = \partial_i w^j \varepsilon_{ijk} dS^k$ . Moreover, as pointer to the nativeness of dealing with differential forms we mention that we mathematically defined the Curl of a vector field via a closed line integral (in a plane orthogonal to a normal vector  $\mathbf{n}$ ) in the limit of vanishing path, i.e.  $(\text{curl } \omega) \cdot \mathbf{n} = \lim_{A \rightarrow 0} \frac{1}{A} \oint \omega \cdot d\mathbf{r}$ <sup>8</sup>. The main difference to tensorial concepts is, that with operations on differential forms we map *something that emerges under an integral* to *something that emerges under an integral*. Without further excursions we claim that we now have the munition to design geometrically conservative differential operators for general coordinates.

The first elaborate insight to geometrically conservative differential operators can be found in Thompson, Warsi, Mastin [43], although they completely exclude differential forms and play extensively with tensor analysis what makes the book a little delicate to comprehend. However, differential form theory perfectly endorses their conclusions and also Bridges' proof (2008) [5] of Vinokur's theorem resorts to differential forms as virtually inherent description for conservation laws. We conclude the connection between covariant derivatives in terms of (3.35) and differential forms. The covariant derivative on a 1-form  $\omega = w_i dx^i$  yields explicitly

$$\begin{aligned}
 \delta\omega &= *d*\omega \\
 &= *d\left(\frac{1}{(3-1)!} \omega_i g^{ij} \varepsilon_{jkl} \sqrt{|\mathbf{g}|} dx^k dx^l\right) \\
 &= *\left(\frac{1}{2} \varepsilon_{jkl} \partial_m \left[w_i g^{ij} \sqrt{|\mathbf{g}|}\right] dx^m dx^k dx^l\right) \\
 &= \frac{1}{2} \varepsilon_{jkl} \partial_m \left[w_i g^{ij} \sqrt{|\mathbf{g}|}\right] \frac{1}{0!} \underbrace{g^{mr} g^{ks} g^{lt} \varepsilon_{rst}}_{|\mathbf{g}|^{-1} \varepsilon^{mkl}} \sqrt{|\mathbf{g}|} \\
 &= \frac{1}{\sqrt{|\mathbf{g}|}} \partial_m \left[\sqrt{|\mathbf{g}|} w^m\right]
 \end{aligned} \tag{3.49}$$

which we recognize as result (3.40), namely  $\text{div } w$ . For the *strong conservation form* of the equations of radiation hydrodynamics we will basically need the following three operations.

### Gradient of a scalar $\phi$

$$\text{grad } \phi = \nabla_i \phi \mathbf{e}^i = \frac{1}{\sqrt{|\mathbf{g}|}} \partial_i \left[\sqrt{|\mathbf{g}|} \mathbf{e}^i \phi\right] \tag{3.50}$$

---

<sup>8</sup>Let be  $\omega = a dx + b dy + c dz$ , then  $d\omega = (\partial_y a dy + \partial_z a dz) \wedge dx + \dots = (\partial_y c - \partial_z b) dy \wedge dz + (\partial_z a - \partial_x c) dz \wedge dx + (\partial_x b - \partial_y a) dx \wedge dy = \text{rot } \omega$  where  $dy \wedge dz = \mathbf{e}^1$ ,  $dz \wedge dx = \mathbf{e}^2$  etc.

**Divergence of a vector field  $\mathbf{v}$**

$$\operatorname{div} \mathbf{v} = \nabla_i v^i = \frac{1}{\sqrt{|\mathbf{g}|}} \partial_i \left[ \sqrt{|\mathbf{g}|} \mathbf{e}^i \cdot \mathbf{v} \right] \quad (3.51)$$

**Divergence of a second rank tensor  $\mathbf{t}$**

$$\operatorname{div} \mathbf{t} = \nabla_i t^{ij} \mathbf{e}_j = \frac{1}{\sqrt{|\mathbf{g}|}} \partial_i \left[ \sqrt{|\mathbf{g}|} \mathbf{e}^i \cdot \mathbf{t} \right] \quad (3.52)$$

Of course these differential operators can be translated to the well known covariant derivatives (3.35) with tensor analysis as well.

$$\begin{aligned} \frac{1}{\sqrt{|\mathbf{g}|}} \partial_\mu \left[ \sqrt{|\mathbf{g}|} \phi \mathbf{e}^\mu \right] &= \Gamma^\nu_{\nu\mu} \mathbf{e}^\mu \phi + \partial_\mu \mathbf{e}^\mu \phi + \mathbf{e}^\mu \partial_\mu \phi \\ &= \Gamma^\nu_{\nu\mu} \mathbf{e}^\mu \phi + \partial_\mu (g^{\mu\rho} \mathbf{e}_\rho) \phi + \mathbf{e}^\mu \partial_\mu \phi \\ &= \Gamma^\nu_{\nu\mu} \mathbf{e}^\mu \phi - \Gamma^\mu_{\mu\sigma} \mathbf{e}^\sigma \phi + \mathbf{e}^\mu \partial_\mu \phi \\ &= \mathbf{e}^\mu \partial_\mu \phi \end{aligned} \quad (3.53)$$

The canonic shape of tensorial conservation laws  $\int (\partial_t \mathbf{d} + \operatorname{div} \mathbf{f}(\mathbf{d})) dV dt = \mathbf{0}$  in strong conservation form for non-steady coordinates<sup>9</sup> yields

$$\partial_t \left[ \sqrt{|\mathbf{g}|} \mathbf{d} \right] + \partial_i \left[ \sqrt{|\mathbf{g}|} \mathbf{f}(\mathbf{d}) \cdot \mathbf{e}^i \right] = 0 \quad (3.54)$$

where of course  $\mathbf{d}$  and  $\mathbf{f}$  still have to be decomposed according to their native tensorial components.

We substantiate upper proposition by an example of a vector conservation law, the equation of motion (2.4) in  $n$  dimensions. The differential expression

$$\partial_t \left[ \sqrt{|\mathbf{g}|} \rho \mathbf{u} \right] + \partial_i \left[ \sqrt{|\mathbf{g}|} (\rho \mathbf{u} \mathbf{u} + \mathbf{P} + \sigma) \cdot \mathbf{e}^i \right] = 0, \quad i = 1, \dots, n \quad (3.55)$$

implicates the integral form of conservation of momentum which would be considered numerically for non-steady coordinates. The important difference to a component-wise structure is that in this case undifferentiated terms would arise in  $n$  equations (see Vinokur (1974) [46]).

Neither the covariant derivative form for the divergence  $\nabla(\cdot) = \partial(\cdot) + \Gamma(\cdot)$ , nor the  $k$ -th component of the expression  $\partial_i [\sqrt{|\mathbf{g}|} f^{ik}]$  which would even be analytically true only for antisymmetric tensors  $\mathbf{f}$  anyway, satisfies the conservation law adequately. Since the base vectors  $\mathbf{e}^i$  are functions of position for general coordinates, a separation as implied would introduce undifferentiated terms. However, the  $k$  Cartesian components

---

<sup>9</sup>In the following section we will argue, why the volume element  $\sqrt{|\mathbf{g}|}$  also appears in the time derivative.

## 3.2 Conservative Methods in General Curvilinear Coordinates

of equation (3.55) are geometrically conservative which means they satisfy the strong conservation form that we demand<sup>10</sup>.

$$\left\{ \partial_t \left[ \sqrt{|\mathbf{g}|} \rho u^l \mathbf{e}_l \right] + \partial_i \left[ \sqrt{|\mathbf{g}|} \left( \rho u^i u^l + p^{il} + \sigma^{il} \right) \mathbf{e}_l \right] \right\}^k = 0$$

By now we have established a mathematical framework to deal with nonlinear conservation laws in curvilinear coordinates. For practical astrophysical applications though we will have to dissect this framework a little further to time dependent coordinate systems in order to work with adaptive grids as we motivated them for implicit numerical methods.

### 3.2.3 Adaptive Grids

In fluid dynamics we basically distinguish two main reference systems that suit unequally for various applications. The *Eulerian frame* is the fixed reference system of an external observer in which the fluid moves with velocity  $\mathbf{u}$  whereas the *Lagrangian specification* describes the physics in the rest frame of the fluid. The transformation of an advection term for a density  $\mathbf{d}$  between these two systems that obviously move with relative velocity  $\mathbf{u}$  is given via the *material derivative*  $D_t = \partial_t \mathbf{d} + \mathbf{u} \cdot \nabla \mathbf{d}$ . Hence, when we work with comoving frames, the coordinate system respectively the computational grid is time dependent. There is a number of purposes where strict Eulerian or Lagrangian grids are suboptimal and we need to generalize the concept of the comoving frame to ubiquitous grid movements. We will come back to this topic in chapter 4 when we deal with generation of moving grids in multiple dimensions.

For now we want to evolve the strong conservation form for time dependent general coordinate systems. The time derivative of a density  $\mathbf{d}$  in the coordinate system  $\Sigma_{(\beta)}$  relative to a (e.g. static) coordinate system  $\Sigma_{(\alpha)}$  is given by  $\partial_t \mathbf{d}_{(\beta)} = \partial_t \mathbf{d}_{(\alpha)} + \nabla_{(\alpha)} \mathbf{d} \cdot \dot{\mathbf{x}}_{(\beta)}$  and from the view point of system  $\Sigma_{(\alpha)}$ , the time derivative yields

$$\partial_t \mathbf{d}_{(\alpha)} = \partial_t \mathbf{d}_{(\beta)} - \dot{\mathbf{x}} \cdot \nabla_{(\alpha)} \mathbf{d}. \quad (3.56)$$

With  $\dot{\mathbf{x}}$  we introduced the *grid velocity* and the second term on the right side we call *grid advection*, see e.g. Warsi (1981) [48] and Thompson, Warsi, Mastin [43]. Now let us consider an inhomogeneous advective term of a conservation law  $\mathbf{K} = \mathbf{d}_t + \text{div}(\mathbf{ud})$  referring to a fixed coordinate system.

$$\mathbf{K} = \mathbf{d}_t - \dot{\mathbf{x}} \cdot \nabla \mathbf{d} + \text{div}(\mathbf{ud}) \quad (3.57)$$

When we apply transformation rules (3.50), (3.51), (3.52) to the spatial derivatives, we

<sup>10</sup>Here we simply used  $t^{jl} \mathbf{e}_j \mathbf{e}_l \cdot \mathbf{e}^i = t^{jl} \mathbf{e}_j \delta_l^i = t^{ji} \mathbf{e}_j$ .

### 3 Conservative Numerics

gain the following form.

$$\mathbf{K} = \mathbf{d}_t - \dot{\mathbf{x}} \cdot \frac{1}{\sqrt{|\mathbf{g}|}} \partial_i [\sqrt{|\mathbf{g}|} \mathbf{e}^i \mathbf{d}] + \frac{1}{\sqrt{|\mathbf{g}|}} \partial_i [\sqrt{|\mathbf{g}|} \mathbf{u} \cdot \mathbf{e}^i \mathbf{d}]. \quad (3.58)$$

Admittedly this is not yet geometrically conservative, since it is not of an *integral* structure. Following the idea of the Reynolds transport theorem we consider the temporal derivative of the volume respectively the determinant of the time dependent metric tensor  $\sqrt{|\mathbf{g}(\mathbf{x}, \mathbf{t})|}$  in order to study the conservation of a density function in variable volumes and obtain the *strong conservation form for time dependent coordinate systems*<sup>11</sup>.

$$\sqrt{|\mathbf{g}|} \mathbf{K} = \partial_t [\sqrt{|\mathbf{g}|} \mathbf{d}] + \partial_i [\sqrt{|\mathbf{g}|} \mathbf{e}^i \cdot (\mathbf{u} - \dot{\mathbf{x}}) \mathbf{d}] \quad (3.59)$$

If we define the contravariant velocity components relative to the moving grid by  $U^i = \mathbf{e}^i \cdot (\mathbf{u} - \dot{\mathbf{x}})$  the upper equations yields

$$\sqrt{|\mathbf{g}|} \mathbf{K} = \partial_t [\sqrt{|\mathbf{g}|} \mathbf{d}] + \partial_i [\sqrt{|\mathbf{g}|} U^i \mathbf{d}]. \quad (3.60)$$

#### 3.2.4 Artificial Viscosity

We introduced artificial viscosity in form of a three dimensional viscous pressure tensor in section 3.1.4 according to Tscharnuter and Winkler (1979) [44] by equation (3.20) but also mentioned that we will have to adapt it slightly for curvilinear coordinates.

This has to do with one previous comment to the *native* form of tensorial quantities as they are generated in differential geometry. The crucial term in (3.20) is the symmetrized velocity gradient that accounts for shear stresses. The symmetrization rule is defined for lower indices and yields in component formulation  $[\nabla \mathbf{u}]_{sij} = \frac{1}{2}(\nabla_i u_j + \nabla_j u_i)$  which comes into conflict with the demand of vanishing trace  $\text{Tr} \mathbf{Q} = 0$  when the divergence term contains the unit tensor  $\mathbf{e}$ .

**Proposition.** *The correct form of the viscous pressure tensor in general coordinates is*

$$\mathbf{Q} = -q_2^2 t_{visc}^2 \rho \max(-\text{div} \mathbf{u}, 0) \left( [\nabla \mathbf{u}]_s - \frac{1}{3} \mathbf{g} \text{div} \mathbf{u} \right). \quad (3.61)$$

Since this is an important result, we want to deduce this explicitly step by step. The viscous pressure tensor must be symmetrical by definition, i.e.  $Q_{ij} = Q_{ji}$  and as already stated  $\text{Tr} \mathbf{Q} = Q^i_i = 0$  so we first consider its *native* covariant components

$$Q_{ij} = -\mu_2 \max(-\text{div} \mathbf{u}, 0) \left( \frac{1}{2}(\nabla_i u_j + \nabla_j u_i) - \frac{1}{3} g_{ij} \text{div} \mathbf{u} \right) \quad (3.62)$$

<sup>11</sup>A derivation of the strong conservative form for adaptive grids can be found in Appendix 6.1.4



### 3.3 Strong Conservation Form of RHD in Spherical and Polar Coordinates

where we renamed  $q_2^2 l_{\text{visc}}^2 \rho = \mu_2$ . In order to proof that the trace vanishes, we need to raise an index with the metric and use the essential identity  $g^{li} g_{lj} = g^i_j = \delta^i_j$ .

$$Q^i_j = Q_{lj} g^{li} = -\mu_2 \max(-\text{div } \mathbf{u}, 0) \left( \frac{1}{2} g^{li} (\nabla_l u_j + \nabla_j u_l) - \frac{1}{3} \delta^i_j \text{div } \mathbf{u} \right)$$

The Ricci Lemma (3.36) for the fundamental tensor naturally also holds for the contravariant components and we can permute  $g$  into the derivatives  $\nabla_l g^{li} u_j$  and  $\nabla_j g^{li} u_l$  which yields twice the Divergence  $\nabla_i u^i = \text{div } \mathbf{u}$  when we conduct the contraction  $j \rightarrow i$ . In three dimensions the summation  $\delta^i_i = 3$  and we obtain our desired result

$$Q^i_i = \dots \left( \frac{1}{2} (2 \text{div } \mathbf{u}) - \frac{1}{3} 3 \text{div } \mathbf{u} \right) = 0. \quad (3.63)$$

Tscharnutter and Winklers form of  $\mathbf{Q}$  is not compatible with our differential geometric definitions, since the symmetrization is only defined for lower indices whereas the unit element  $\mathbf{e}$  of a metric space is only defined for mixed indices, meaning there is no such thing as  $\delta_{ij}$ . However, they and other authors like Mihalas and Mihalas [32] did not notice that little inconsistency since they considered mixed indices from the start respectively 1D flows at last. Corrections have been suggested by Benson (1993) [3] albeit they do not explicitly concern curvilinear coordinates and were derived based on a TVD approach. The usefulness of our correction might not show until even more general coordinate systems respectively grids are considered. In chapter 4 we will discuss nonorthogonal grids and concern ourselves with the question at what step in the calculation geometric operations like raising or lowering indices should be made ideally.

In the upcoming section we will recapitulate our general results for spherical coordinates without explicitly performing the discretization and marking down numerical fluxes according to (3.11) respectively Dorfi et al. (2004) [12]. It will become comprehensible why we suggest generating these discretized equations with Mathematica as well.

### 3.3 Strong Conservation Form of RHD in Spherical and Polar Coordinates

When we think of problem oriented coordinate systems in astrophysical applications spherical and polar coordinates are a first natural choice. In the following section we present the geometrically conservative form of the equations of radiation hydrodynamics in these cases exemplarily. We consider the transformation  $(x, y, z) \rightarrow (r \in \mathbb{R}^+, \vartheta \in [0, \pi], \varphi \in [0, 2\pi])$  with  $x = r \sin \vartheta \cos \varphi$ ,  $y = r \sin \vartheta \sin \varphi$  and  $z = r \cos \vartheta$  as spherical coordinates. The map  $(x, z) \rightarrow (r \in \mathbb{R}^+, \vartheta \in [0, 2\pi])$  shall be our polar coordinates  $x = r \sin \vartheta$  and  $z = r \cos \vartheta$ . This convention was chosen in favor of somewhat simplified generation of the equations components for which we used the computer algebra system

### 3 Conservative Numerics

Mathematica. Some of the equation generating files as well as some computational tests on consistency like  $Q^i_i = 0$  and  $Q_{ij} = Q_{ji}$  can be found in the Appendix 6.2.

For the sake of completeness we mention some important geometrical attributes of our choice.

**Spherical Coordinates** The covariant components of the metric tensor for these spherical coordinates are  $g_{ij} = \text{diag}(1, r^2, r^2 \sin^2 \vartheta)$  and due to their orthogonality the contravariant components simply yield  $g^{ij} = \text{diag}(1, 1/r^2, 1/(r^2 \sin^2 \vartheta))$  and the volume element  $\sqrt{|\mathbf{g}|} = r^2 \sin \vartheta$ . For the contravariant base vectors we obtain

$$\begin{aligned} \mathbf{e}^r &= (\cos \varphi \sin \vartheta, \sin \varphi \sin \vartheta, \cos \vartheta) \\ \mathbf{e}^\vartheta &= \left( \frac{\cos \varphi \cos \vartheta}{r}, \frac{\cos \vartheta \sin \varphi}{r}, -\frac{\sin \vartheta}{r} \right) \\ \mathbf{e}^\varphi &= \left( -\frac{\csc \vartheta \sin \varphi}{r}, \frac{\cos \varphi \csc \vartheta}{r}, 0 \right) \end{aligned} \quad (3.64)$$

and the non vanishing Christoffel symbols

$$\begin{aligned} \Gamma^r_{\vartheta\vartheta} &= -r, & \Gamma^r_{\varphi\varphi} &= -r \sin^2 \vartheta \\ \Gamma^\vartheta_{r\vartheta} &= \Gamma^\vartheta_{\vartheta r} = \frac{1}{r}, & \Gamma^\vartheta_{\varphi\varphi} &= -\cos \vartheta \sin \vartheta \\ \Gamma^\varphi_{r\varphi} &= \Gamma^\varphi_{\varphi r} = \frac{1}{r}, & \Gamma^\varphi_{\varphi\vartheta} &= \cot \vartheta. \end{aligned} \quad (3.65)$$

**Polar Coordinates** Also polar coordinates are orthogonal and the metric components yield  $g_{ij} = \text{diag}(1, r^2)$  respectively  $g^{ij} = \text{diag}(1, 1/r^2)$ . For the volume element we obtain  $\sqrt{|\mathbf{g}|} = r$ . The contravariant base vectors yield

$$\begin{aligned} \mathbf{e}^r &= (\sin \vartheta, \cos \vartheta) \\ \mathbf{e}^\vartheta &= \left( \frac{\cos \vartheta}{r}, -\frac{\sin \vartheta}{r} \right) \end{aligned} \quad (3.66)$$

and the non vanishing Christoffel symbols are

$$\Gamma^\vartheta_{r\vartheta} = \frac{1}{r}, \quad \Gamma^\vartheta_{\vartheta r} = \frac{1}{r}, \quad \Gamma^r_{\vartheta\vartheta} = -r. \quad (3.67)$$

#### 3.3.1 Continuity Equation

The strong conservation form of the conservation of mass (2.2) in form of the continuity equation

$$\partial_t \rho + \text{div}(\rho \mathbf{u}) = 0 \quad (3.68)$$

### 3.3 Strong Conservation Form of RHD in Spherical and Polar Coordinates

for time dependent coordinates yields

$$\partial_t [\sqrt{|\mathbf{g}|} \rho] + \partial_i [\sqrt{|\mathbf{g}|} \mathbf{e}^i \cdot (\mathbf{u} - \dot{\mathbf{x}}) \rho] = 0. \quad (3.69)$$

Since the conservation of mass is scalar the divergence term may also be written in components  $\partial_t [\sqrt{|\mathbf{g}|} \rho] + \partial_i [\sqrt{|\mathbf{g}|} (u^i - \dot{x}^i) \rho] = 0$ . The explicit form of (3.69) in spherical coordinates yields

$$\begin{aligned} & \partial_t [r^2 \sin \vartheta \rho] + \partial_r [r^2 \sin \vartheta (u^r - \dot{x}^r) \rho] + \\ & + \partial_\vartheta [r^2 \sin \vartheta (u^\vartheta - \dot{x}^\vartheta) \rho] + \partial_\varphi [r^2 \sin \vartheta (u^\varphi - \dot{x}^\varphi) \rho] = 0 \end{aligned} \quad (3.70)$$

which we can rewrite via the transformation  $\cos \vartheta = \mu$  with differential  $d\vartheta = -\sqrt{1 - \mu^2} d\mu$  and divide the equation by  $\sqrt{1 - \mu^2}$  in the case of solely radial adaptivity. Note that even for solely radially adaptive grids the grid velocity  $\dot{\mathbf{x}}$  contains angular dependencies, e.g.  $\dot{x}^r = \dot{r} \sin \vartheta \cos \varphi$  which obviously means  $\dot{x} \neq \dot{r}$ .

$$\begin{aligned} & \partial_t [r^2 \rho] + \partial_r [r^2 (u^r - \dot{x}^r) \rho] - \\ & - r^2 \partial_\mu [\sqrt{1 - \mu^2} (u^\vartheta - \dot{x}^\vartheta) \rho] + r^2 \partial_\varphi [(u^\varphi - \dot{x}^\varphi) \rho] = 0 \end{aligned} \quad (3.71)$$

With the radial grid velocity expanded we obtain the following form of the conservation of mass.

$$\begin{aligned} & \partial_t [r^2 \rho] + \partial_r [r^2 (u^r - \dot{r} \sqrt{1 - \mu^2} \cos \varphi) \rho] - \\ & - r^2 \partial_\mu [\sqrt{1 - \mu^2} (u^\vartheta - \dot{r} \sqrt{1 - \mu^2} \sin \varphi) \rho] + r^2 \partial_\varphi [(u^\varphi - \dot{r} \mu) \rho] = 0 \end{aligned} \quad (3.72)$$

In the case of 2D polar coordinates the continuity equation yields

$$\partial_t [r \rho] + \partial_r [r (u^r - \dot{x}^r) \rho] - r \sqrt{1 - \mu^2} \partial_\mu [(u^\vartheta - \dot{x}^\vartheta) \rho] = 0 \quad (3.73)$$

respectively in case of radially time dependent coordinates

$$\partial_t [r \rho] + \partial_r [r (u^r - \dot{r} \sqrt{1 - \mu^2}) \rho] - r \sqrt{1 - \mu^2} \partial_\mu [(u^\vartheta - \dot{r} \mu) \rho] = 0. \quad (3.74)$$

#### 3.3.2 Equation of Motion

The equation of motion that we consider in radiation hydrodynamics contains the conservation of moment of plain fluid dynamics (2.4) as well as the radiative flux as coupling

### 3 Conservative Numerics

term (2.18), gravitational force as indicated in section 2.3.2 and artificial viscosity (3.61).

$$\partial_t(\rho\mathbf{u}) + \operatorname{div}(\rho\mathbf{u}\mathbf{u} + \mathbf{P} + \mathbf{Q}) + \rho\mathbf{G} - \frac{4\pi}{c}\kappa_{RR}\rho\mathbf{H} = \mathbf{0} \quad (3.75)$$

We investigate the elements of the energy stress tensor a little closer before we designate the consistent strong conservation form. We define an *effective tensor of gaseous momentum*  $\mathbf{R}$  that accounts for the motion of the coordinates

$$\mathbf{R} = r^{ij}\mathbf{e}_i\mathbf{e}_j = \rho(\mathbf{u} - \dot{\mathbf{x}})\mathbf{u} \quad (3.76)$$

with components  $r^{ij} = \rho(u^i - \dot{x}^i)u^j$ . The *isotropic gas pressure tensor*  $\mathbf{P}$  as anticipated is defined by the scalar pressure and the metric tensor

$$\mathbf{P} = p\mathbf{g} \quad (3.77)$$

with obvious decomposition  $P^{ij} = pg^{ij}$ . The *viscous pressure tensor*  $\mathbf{Q}$  needs some special attention. We emanate from the following definition

$$\mathbf{Q} = - \left( \underbrace{q_1 l_{\text{visc}} \rho c_S}_{\mu_1} + \underbrace{q_2^2 l_{\text{visc}}^2 \rho}_{\mu_2} \max(-\operatorname{div} \mathbf{u}, 0) \right) \left( \left[ \nabla \mathbf{u} \right]_s - \mathbf{g} \frac{1}{3} \nabla \cdot \mathbf{u} \right), \quad (3.78)$$

and remember that in order to get its contravariant components we need to raise them with our metric.

$$\begin{aligned} Q_{ij} &= (\mu_1 + \mu_2 \max(-\operatorname{div} \mathbf{u}, 0)) \left( (\nabla_i u_j + \nabla_j u_i) - g_{ij} \frac{1}{3} \operatorname{div} \mathbf{u} \right) \\ Q^i_j = Q_{lj} g^{li} &= \dots \left( g^{li} (\nabla_l u_j + \nabla_j u_l) - \delta^i_j \frac{1}{3} \operatorname{div} \mathbf{u} \right) \\ Q^{ij} = Q_{lm} g^{li} g^{mj} &= \dots \left( g^{li} g^{mj} (\nabla_l u_m + \nabla_j u_m) - g^{ij} \frac{1}{3} \operatorname{div} \mathbf{u} \right) \end{aligned} \quad (3.79)$$

We also promised to particularly calculate the trace of  $\mathbf{Q}$  in spherical coordinates in order to confirm consistency. To do so, we need the mixed components which are listed on the following page.

### 3.3 Strong Conservation Form of RHD in Spherical and Polar Coordinates

$$\begin{aligned}
Q^r_r &= Q_{rr}g^{rr} + Q_{\vartheta r}g^{\vartheta r} + Q_{\varphi r}g^{\varphi r} = Q_{rr} \\
&= -\frac{1}{3}\operatorname{div} \mathbf{u} + \partial_r u_r \\
Q^r_{\vartheta} &= Q_{r\vartheta}g^{rr} + Q_{\vartheta\vartheta}g^{\vartheta r} + Q_{\varphi\vartheta}g^{\varphi r} = Q_{\vartheta r} \\
&= -\frac{1}{r}u_{\vartheta} + \frac{1}{2}\partial_r u_{\vartheta} + \frac{1}{2}\partial_{\vartheta} u_r \\
Q^r_{\varphi} &= Q_{r\varphi}g^{rr} + Q_{\vartheta\varphi}g^{\vartheta r} + Q_{\varphi\varphi}g^{\varphi r} = Q_{r\varphi} \\
&= -\frac{1}{r}u_{\varphi} + \frac{1}{2}\partial_r u_{\varphi} + \frac{1}{2}\partial_{\varphi} u_r \\
Q^{\vartheta}_r &= Q_{rr}g^{r\vartheta} + Q_{\vartheta r}g^{\vartheta\vartheta} + Q_{\varphi r}g^{\varphi\vartheta} = \frac{1}{r^2}Q_{\vartheta r} \\
&= \frac{1}{r^2} \left( -\frac{1}{r}u_{\vartheta} + \frac{1}{2}\partial_r u_{\vartheta} + \frac{1}{2}\partial_{\vartheta} u_r \right) \\
Q^{\vartheta}_{\vartheta} &= Q_{r\vartheta}g^{r\vartheta} + Q_{\vartheta\vartheta}g^{\vartheta\vartheta} + Q_{\varphi\vartheta}g^{\varphi\vartheta} = \frac{1}{r^2}Q_{\vartheta\vartheta} \\
&= -\frac{1}{3}\operatorname{div} \mathbf{u} + \frac{1}{r}u_r + \frac{1}{r^2}\partial_{\vartheta} u_{\vartheta} \\
Q^{\vartheta}_{\varphi} &= Q_{r\varphi}g^{r\vartheta} + Q_{\vartheta\varphi}g^{\vartheta\vartheta} + Q_{\varphi\varphi}g^{\varphi\vartheta} = \frac{1}{r^2}Q_{\vartheta\varphi} \\
&= \frac{1}{r^2} \left( -\cot \vartheta u_{\varphi} + \frac{1}{2}\partial_{\varphi} u_{\vartheta} + \frac{1}{2}\partial_{\vartheta} u_{\varphi} \right) \\
Q^{\varphi}_r &= Q_{rr}g^{r\varphi} + Q_{\vartheta r}g^{\vartheta\varphi} + Q_{\varphi r}g^{\varphi\varphi} = \frac{1}{r^2 \sin^2 \vartheta} Q_{\varphi r} \\
&= \frac{1}{r^2 \sin^2 \vartheta} \left( -\frac{1}{r}u_{\varphi} + \frac{1}{2}\partial_{\varphi} u_r + \frac{1}{2}\partial_r u_{\vartheta} \right) \\
Q^{\varphi}_{\vartheta} &= Q_{r\vartheta}g^{r\varphi} + Q_{\vartheta\vartheta}g^{\vartheta\varphi} + Q_{\varphi\vartheta}g^{\varphi\varphi} = \frac{1}{r^2 \sin^2 \vartheta} Q_{\varphi\vartheta} \\
&= \frac{1}{r^2 \sin^2 \vartheta} \left( -\cot \vartheta u_{\varphi} + \frac{1}{2}\partial_{\varphi} u_{\vartheta} + \frac{1}{2}\partial_{\vartheta} u_{\varphi} \right) \\
Q^{\varphi}_{\varphi} &= Q_{r\varphi}g^{r\varphi} + Q_{\vartheta\varphi}g^{\vartheta\varphi} + Q_{\varphi\varphi}g^{\varphi\varphi} = \frac{1}{r^2 \sin^2 \vartheta} Q_{\varphi\varphi} \\
&= -\frac{1}{3}\operatorname{div} \mathbf{u} + \frac{1}{r}u_r + \frac{1}{r^2} \cot \vartheta u_{\vartheta} + \frac{1}{r^2 \sin^2 \vartheta} \partial_{\varphi} u_{\varphi}
\end{aligned}$$

### 3 Conservative Numerics

$$\begin{aligned}
\text{Tr}\mathbf{Q} = Q^i_i &= -\frac{1}{3}\text{div}\mathbf{u} + \partial_r u_r - \frac{1}{3}\text{div}\mathbf{u} + \frac{1}{r}u_r + \frac{1}{r^2}\partial_\vartheta u_\vartheta - \frac{1}{3}\text{div}\mathbf{u} + \frac{1}{r}u_r + \\
&\quad + \frac{1}{r^2}\cot\vartheta u_\vartheta + \frac{1}{r^2\sin^2\vartheta}\partial_\varphi u_\varphi \\
&= -\text{div}\mathbf{u} + \frac{2}{r} + \frac{1}{r^2}\cot\vartheta u_\vartheta + \partial_r u_r + \frac{1}{r^2}\partial_\vartheta u_\vartheta + \frac{1}{r^2\sin^2\vartheta}\partial_\varphi u_\varphi \\
&= -\text{div}\mathbf{u} + \underbrace{\frac{2}{r} + \cot\vartheta u^\vartheta + \partial_r u^r + \partial_\vartheta u^\vartheta + \partial_\varphi u^\varphi}_{\text{div}\mathbf{u}} = 0
\end{aligned}$$

So in fact the viscous pressure tensors trace vanishes in spherical coordinates explicitly<sup>12</sup>.

The native decompositions of our tensors  $\mathbf{R}$  and  $\mathbf{P}$  are contravariant hence we will consider also  $\mathbf{Q}$ 's contravariant components for the sake of coherency. In the following array we list  $Q^{ij}$  for spherical coordiantes.

$$\begin{aligned}
Q^{rr} &= -\frac{1}{3}\text{div}\mathbf{u} + \partial_r u_r \\
Q^{r\vartheta} &= \frac{1}{r^2}\left(-\frac{1}{r}u_\vartheta + \frac{1}{2}\partial_r u_\vartheta + \frac{1}{2}\partial_\vartheta u_r\right) \\
Q^{r\varphi} &= \frac{1}{r^2\sin^2\vartheta}\left(-\frac{1}{r}u_\varphi + \frac{1}{2}\partial_\varphi u_r + \frac{1}{2}\partial_r u_\varphi\right) \\
Q^{\vartheta r} &= \frac{1}{r^2}\left(-\frac{1}{r}u_\vartheta + \frac{1}{2}\partial_r u_\vartheta + \frac{1}{2}\partial_\vartheta u_r\right) \\
Q^{\vartheta\vartheta} &= \frac{1}{r^2}\left(-\frac{1}{3}\text{div}\mathbf{u} + \frac{1}{r}u_r + \frac{1}{r^2}\partial_\vartheta u_\vartheta\right) \\
Q^{\vartheta\varphi} &= \frac{1}{r^4\sin^2\vartheta}\left(-\cot\vartheta u_\varphi + \frac{1}{2}\partial_\varphi u_\vartheta + \frac{1}{2}\partial_\vartheta u_\varphi\right) \\
Q^{\varphi r} &= \frac{1}{r^2\sin^2\vartheta}\left(-\frac{1}{r}u_\varphi + \frac{1}{2}\partial_\varphi u_r + \frac{1}{2}\partial_r u_\varphi\right) \\
Q^{\varphi\vartheta} &= \frac{1}{r^4\sin^2\vartheta}\left(-\cot\vartheta u_\varphi + \frac{1}{2}\partial_\varphi u_\vartheta + \frac{1}{2}\partial_\vartheta u_\varphi\right) \\
Q^{\varphi\varphi} &= \frac{1}{r^2\sin^2\vartheta}\left(-\frac{1}{3}\text{div}\mathbf{u} + \frac{1}{r}u_r + \frac{1}{r^2}\cot\vartheta u_\vartheta + \frac{1}{r^2\sin^2\vartheta}\partial_\varphi u_\varphi\right)
\end{aligned}$$

We will investigate the following strong conservation form of the equation of motion

$$\begin{aligned}
\partial_t\left[\sqrt{|\mathbf{g}|}\rho\mathbf{u}\right] + \partial_i\left[\sqrt{|\mathbf{g}|}(\mathbf{R} + \mathbf{P} + \mathbf{Q}) \cdot \mathbf{e}^i\right] + \\
+ \rho\partial_i\left[\sqrt{|\mathbf{g}|}\Phi\mathbf{e}^i\right] - \frac{4\pi}{c}\kappa_R\sqrt{|\mathbf{g}|}\rho\mathbf{H} = \mathbf{0}.
\end{aligned} \tag{3.80}$$

The  $k$ -th component of the strong conservation equation of motion is given by the  $k$ -th cartesic component of our unit vector, e.g.  $\mathbf{e}^r = \cos\varphi\sin\vartheta\mathbf{e}^x + \sin\varphi\sin\vartheta\mathbf{e}^y + \cos\vartheta\mathbf{e}^z$  and

<sup>12</sup>The geometrical terms  $2/r$  and  $\cot\vartheta$  are Christoffel symbols of the spherical coordinates (3.65) from  $\nabla_i u^i = \partial_i u^i + \Gamma^i_{ik}u^k$ .

### 3.3 Strong Conservation Form of RHD in Spherical and Polar Coordinates

its derivatives. The projection of each physical tensor on the contravariant coordinate lines can be simplified by its contravariant components with respect to its covariant basis without losing strong conservation form, i.e.  $\mathbf{f} \cdot \mathbf{e}^i = f^{in} \mathbf{e}_n$ . We prefer this form with contravariant components since it meets the native design of the stress tensor (2.3).

$$\left\{ \partial_t \left[ \sqrt{|\mathbf{g}|} \rho u^n \mathbf{e}_n \right] + \partial_i \left[ \sqrt{|\mathbf{g}|} \left( r^{in} + p^{in} + Q^{in} \right) \mathbf{e}_n \right] + \rho \partial_n \left[ \sqrt{|\mathbf{g}|} \Phi \mathbf{e}^n \right] - \frac{4\pi}{c} \kappa_R \sqrt{|\mathbf{g}|} \rho H^n \mathbf{e}_n \right\}^k = 0 \quad (3.81)$$

The three components of upper equation in spherical coordinates are listed in the following arrays.

$$\begin{aligned} & \partial_t \left[ \rho r^2 \sqrt{1-\mu^2} \cos \varphi u^r + \rho r^3 \mu \rho \cos \varphi u^\vartheta - \rho r^3 \sqrt{1-\mu^2} \sin \varphi u^\varphi \right] + \\ & + \partial_r \left[ r^2 \sqrt{1-\mu^2} \cos \varphi \left( \rho u^r (u^r - \dot{x}^r) + p + Q^{rr} \right) + r^3 \mu \cos \varphi \left( \rho u^\vartheta (u^r - \dot{x}^r) + Q^{r\vartheta} \right) - \right. \\ & \left. - r^3 \sqrt{1-\mu^2} \sin \varphi \left( \rho u^\varphi (u^r - \dot{x}^r) + Q^{r\varphi} \right) \right] - \partial_\mu \left[ r^2 (1-\mu^2) \cos \varphi \left( \rho u^r (u^\vartheta - \dot{x}^\vartheta) + Q^{\vartheta r} \right) + \right. \\ & \left. + r^3 \mu \sqrt{1-\mu^2} \cos \varphi \left( \rho u^\vartheta (u^\vartheta - \dot{x}^\vartheta) + \frac{1}{r^2} p + Q^{\vartheta\vartheta} \right) - r^3 (1-\mu^2) \sin \varphi \left( \rho u^\varphi (u^\vartheta - \dot{x}^\vartheta) + Q^{\vartheta\varphi} \right) \right] + \\ & + \partial_\varphi \left[ r^2 \sqrt{1-\mu^2} \cos \varphi \left( \rho u^r (u^\varphi - \dot{x}^\varphi) + Q^{\varphi r} \right) + r^3 \mu \cos \varphi \left( \rho u^\vartheta (u^\varphi - \dot{x}^\varphi) + Q^{\varphi\vartheta} \right) - \right. \\ & \left. - r^3 \sqrt{1-\mu^2} \sin \varphi \left( \rho u^\varphi (u^\varphi - \dot{x}^\varphi) + \frac{1}{r^2 (1-\mu^2)} p + Q^{\varphi\varphi} \right) \right] + \\ & + \rho \left( \partial_r \left[ r^2 \sqrt{1-\mu^2} \cos \varphi \Phi \right] - \partial_\mu \left[ \mu r \sqrt{1-\mu^2} \cos \varphi \Phi \right] + \frac{1}{\sqrt{1-\mu^2}} \partial_\varphi \left[ -r \sin \varphi \Phi \right] \right) - \\ & - \frac{4\pi}{c} r^2 \left( \sqrt{1-\mu^2} \cos \varphi H^r + \mu r \cos \varphi H^\vartheta - \sqrt{1-\mu^2} r \sin \varphi H^\varphi \right) = 0. \end{aligned} \quad (3.82)$$

$$\begin{aligned} & \partial_t \left[ r^2 \sqrt{1-\mu^2} \rho \sin \varphi u^r + r^3 \mu \rho \sin \varphi u^\vartheta + r^3 \sqrt{1-\mu^2} \rho \cos \varphi u^\varphi \right] + \\ & + \partial_r \left[ r^2 \sqrt{1-\mu^2} \sin \varphi \left( \rho u^r (u^r - \dot{x}^r) + p + Q^{rr} \right) + r^3 \mu \sin \varphi \left( \rho u^\vartheta (u^r - \dot{x}^r) + Q^{r\vartheta} \right) + \right. \\ & \left. + r^3 \sqrt{1-\mu^2} \cos \varphi \left( \rho u^\varphi (u^r - \dot{x}^r) + Q^{r\varphi} \right) \right] - \partial_\mu \left[ r^2 (1-\mu^2) \sin \varphi \left( \rho u^r (u^\vartheta - \dot{x}^\vartheta) + Q^{\vartheta r} \right) + \right. \\ & \left. + r^3 \mu \sqrt{1-\mu^2} \sin \varphi \left( \rho u^\vartheta (u^\vartheta - \dot{x}^\vartheta) + \frac{p}{r^2} + Q^{\vartheta\vartheta} \right) + r^3 (1-\mu^2) \cos \varphi \left( \rho u^\varphi (u^\vartheta - \dot{x}^\vartheta) + Q^{\vartheta\varphi} \right) \right] + \\ & + \partial_\varphi \left[ r^2 \sqrt{1-\mu^2} \sin \varphi \left( \rho u^r (u^\varphi - \dot{x}^\varphi) + Q^{\varphi r} \right) + r^3 \mu \sin \varphi \left( \rho u^\vartheta (u^\varphi - \dot{x}^\varphi) + Q^{\varphi\vartheta} \right) + \right. \\ & \left. + r^3 \sqrt{1-\mu^2} \cos \varphi \left( \rho u^\varphi (u^\varphi - \dot{x}^\varphi) + \frac{p}{r^2 (1-\mu^2)} + Q^{\varphi\varphi} \right) \right] + \\ & + \rho \left( \partial_r \left[ r^2 \sqrt{1-\mu^2} \sin \varphi \Phi \right] - \partial_\mu \left[ \mu r \sqrt{1-\mu^2} \sin \varphi \Phi \right] + \frac{1}{\sqrt{1-\mu^2}} \partial_\varphi \left[ r \cos \varphi \Phi \right] \right) - \\ & - \frac{4\pi}{c} r^2 \left( \sqrt{1-\mu^2} \sin \varphi H^r + \mu r \sin \varphi H^\vartheta + \sqrt{1-\mu^2} r \cos \varphi H^\varphi \right) = 0. \end{aligned} \quad (3.83)$$

### 3 Conservative Numerics

$$\begin{aligned}
& \partial_t \left[ r^2 \mu \rho u^r - r^3 \sqrt{1 - \mu^2} \rho u^\vartheta \right] + \\
& + \partial_r \left[ r^2 \mu \left( \rho u^r (u^r - \dot{x}^r) + p + Q^{rr} \right) - r^3 \sqrt{1 - \mu^2} \left( \rho u^\vartheta (u^r - \dot{x}^r) + Q^{r\vartheta} \right) \right] - \\
& - \partial_\mu \left[ r^2 \mu \sqrt{1 - \mu^2} \left( \rho u^r (u^\vartheta - \dot{x}^\vartheta) + Q^{\vartheta r} \right) - r^3 (1 - \mu^2) \left( \rho u^\vartheta (u^\vartheta - \dot{x}^\vartheta) + \frac{p}{r^2} + Q^{\vartheta\vartheta} \right) \right] + \\
& + \partial_\varphi \left[ \mu r^2 \left( \rho u^r (u^\varphi - \dot{x}^\varphi) + Q^{\varphi r} \right) - r^3 \sqrt{1 - \mu^2} \left( \rho u^\vartheta (u^\varphi - \dot{x}^\varphi) + Q^{\varphi\vartheta} \right) \right] + \\
& + \partial_r \left[ r^2 \mu \Phi \right] + \partial_\mu \left[ r (1 - \mu^2) \Phi \right] - \frac{4\pi}{c} r^2 \left( \mu H^r - r \sqrt{1 - \mu^2} H^\vartheta \right) = 0.
\end{aligned} \tag{3.84}$$

When we paste the contravariant components of the artificial viscosity explicitly, the 1-component yields as an example

$$\begin{aligned}
& \partial_t \left[ \rho r^2 (1 - \mu^2) \cos \varphi u^r + \rho r^3 \mu \sqrt{1 - \mu^2} \rho \cos \varphi u^\vartheta - \rho r^3 (1 - \mu^2) \sin \varphi u^\varphi \right] + \\
& + \partial_r \left[ r^2 (1 - \mu^2) \cos \varphi \left( \rho u^r (u^r - \dot{x}^r) + p - \frac{1}{3} \operatorname{div} \mathbf{u} + \partial_r u_r \right) + \right. \\
& \left. r^3 \mu \sqrt{1 - \mu^2} \cos \varphi \left( \rho u^\vartheta (u^r - \dot{x}^r) + \frac{1}{r^2} \left( -\frac{1}{r} u_\vartheta + \frac{1}{2} \partial_r u_\vartheta + \frac{1}{2} \partial_\vartheta u_r \right) \right) - \right. \\
& \left. - r^3 (1 - \mu^2) \sin \varphi \left( \rho u^\varphi (u^r - \dot{x}^r) + \frac{1}{r^2 (1 - \mu^2)} \left( -\frac{1}{r} u_\varphi + \frac{1}{2} \partial_r u_\varphi + \frac{1}{2} \partial_\vartheta u_r \right) \right) \right] - \\
& - \sqrt{1 - \mu^2} \partial_\mu \left[ r^2 (1 - \mu^2) \cos \varphi \left( \rho u^r (u^\vartheta - \dot{x}^\vartheta) + \frac{1}{r^2} \left( -\frac{1}{r} u_\vartheta + \frac{1}{2} \partial_r u_\vartheta + \frac{1}{2} \partial_\vartheta u_r \right) \right) + \right. \\
& \left. + r^3 \mu \sqrt{1 - \mu^2} \cos \varphi \left( \rho u^\vartheta (u^\vartheta - \dot{x}^\vartheta) + \frac{1}{r^2} p + \frac{1}{r^2} \left( -\frac{1}{3} \operatorname{div} \mathbf{u} + \frac{1}{r} u_r + \frac{1}{r^2} \partial_\vartheta u_\vartheta \right) \right) - \right. \\
& \left. - r^3 (1 - \mu^2) \sin \varphi \left( \rho u^\varphi (u^\vartheta - \dot{x}^\vartheta) + \frac{1}{r^4 (1 - \mu^2)} \left( -\frac{\mu}{\sqrt{1 - \mu^2}} u_\varphi + \frac{1}{2} \partial_\varphi u_\vartheta + \frac{1}{2} \partial_\vartheta u_\varphi \right) \right) \right] + \\
& + \partial_\varphi \left[ r^2 (1 - \mu^2) \cos \varphi \left( \rho u^r (u^\varphi - \dot{x}^\varphi) + \frac{1}{r^2 (1 - \mu^2)} \left( -\frac{1}{r} u_\varphi + \frac{1}{2} \partial_\varphi u_r + \frac{1}{2} \partial_r u_\vartheta \right) \right) + \right. \\
& \left. + r^3 \mu \sqrt{1 - \mu^2} \cos \varphi \left( \rho u^\vartheta (u^\varphi - \dot{x}^\varphi) + \frac{1}{r^4 (1 - \mu^2)} \left( -\frac{\mu}{\sqrt{1 - \mu^2}} u_\varphi + \frac{1}{2} \partial_\varphi u_\vartheta + \frac{1}{2} \partial_\vartheta u_\varphi \right) \right) - \right. \\
& \left. - r^3 (1 - \mu^2) \sin \varphi \left( \rho u^\varphi (u^\varphi - \dot{x}^\varphi) + \frac{1}{r^2 (1 - \mu^2)} p + \right. \right. \\
& \left. \left. + \frac{1}{r^2 (1 - \mu^2)} \left( -\frac{1}{3} \operatorname{div} \mathbf{u} + \frac{1}{r} u_r + \frac{1}{r^2} \frac{\mu}{\sqrt{1 - \mu^2}} u_\vartheta + \frac{1}{r^2 (1 - \mu^2)} \partial_\varphi u_\varphi \right) \right) \right] + \\
& + \rho \left( \partial_r \left[ r^2 (1 - \mu^2) \cos \varphi \Phi \right] - \sqrt{1 - \mu^2} \partial_\mu \left[ \mu r \sqrt{1 - \mu^2} \cos \varphi \Phi \right] + \partial_\varphi \left[ -r \sin \varphi \Phi \right] \right) - \\
& - \frac{4\pi}{c} r^2 \sqrt{1 - \mu^2} \left( \sqrt{1 - \mu^2} \cos \varphi H^r + \mu r \cos \varphi H^\vartheta - \sqrt{1 - \mu^2} r \sin \varphi H^\varphi \right) = 0.
\end{aligned} \tag{3.85}$$

The two components of the equation of motion in polar coordinates yield



### 3.3 Strong Conservation Form of RHD in Spherical and Polar Coordinates

$$\begin{aligned}
& \partial_t \left[ r \sqrt{1 - \mu^2} \rho u^r + r^2 \mu \rho u^\vartheta \right] + \\
& + \partial_r \left[ r \sqrt{1 - \mu^2} \left( \rho u^r (u^r - \dot{x}^r) + p + Q^{rr} \right) + r^2 \mu \left( \rho u^\vartheta (u^r - \dot{x}^r) + Q^{r\vartheta} \right) \right] - \\
& - \sqrt{1 - \mu^2} \partial_\mu \left[ r \sqrt{1 - \mu^2} \left( \rho u^r (u^\vartheta - \dot{x}^\vartheta) + Q^{\vartheta r} \right) + r^2 \mu \left( \rho u^\vartheta (u^\vartheta - \dot{x}^\vartheta) + \frac{p}{r^2} + Q^{\vartheta\vartheta} \right) \right] + \\
& + \rho \left( \sqrt{1 - \mu^2} \partial_r [r\Phi] - \sqrt{1 - \mu^2} \partial_\mu [\mu\Phi] \right) - \frac{4\pi}{c} r \left( \sqrt{1 - \mu^2} H^r + r \mu H^\vartheta \right) = 0.
\end{aligned} \tag{3.86}$$

$$\begin{aligned}
& \partial_t \left[ r \mu \rho u^r - r^2 \sqrt{1 - \mu^2} \rho u^\vartheta \right] + \\
& + \partial_r \left[ r \mu \left( \rho u^r (u^r - \dot{x}^r) + p + Q^{rr} \right) - r^2 \sqrt{1 - \mu^2} \left( \rho u^\vartheta (u^r - \dot{x}^r) + Q^{r\vartheta} \right) \right] - \\
& - \sqrt{1 - \mu^2} \partial_\mu \left[ r \mu \left( \rho u^r (u^\vartheta - \dot{x}^\vartheta) + Q^{\vartheta r} \right) - r^2 \sqrt{1 - \mu^2} \left( \rho u^\vartheta (u^\vartheta - \dot{x}^\vartheta) + \frac{p}{r^2} + Q^{\vartheta\vartheta} \right) \right] + \\
& + \rho \left( \mu \partial_r [r\Phi] + \sqrt{1 - \mu^2} \partial_\mu [\sqrt{1 - \mu^2} \Phi] \right) - \frac{4\pi}{c} r \left( \mu H^r - r \sqrt{1 - \mu^2} H^\vartheta \right) = 0.
\end{aligned} \tag{3.87}$$

#### 3.3.3 Equation of Internal Energy

The energy equation we are going to impose contains the thermodynamics of the fluid (2.5) as well as the energy exchange with the radiation field (2.18) and viscous energy dissipation, expressed by the contraction of the viscosity with the velocity gradient  $\mathbf{Q} : \nabla \mathbf{u}$ .

$$\partial_t(\rho\epsilon) + \text{div}(\mathbf{u}\rho\epsilon) + \mathbf{P} : \nabla \mathbf{u} - 4\pi\kappa_P\rho(J - S) + \mathbf{Q} : \nabla \mathbf{u} = 0 \tag{3.88}$$

Since we assume isotropic gas pressure  $\mathbf{P} = p\mathbf{g}$  we can reformulate its contribution via the Ricci Lemma (3.36) and obtain a very simple scalar expression.

$$\begin{aligned}
\mathbf{P} : \nabla \mathbf{u} &= g^{ij} p \nabla_i u_j \\
&= p \nabla_i u^i = p \text{div} \mathbf{u}
\end{aligned} \tag{3.89}$$

The *viscous energy dissipation* is a little more work to do, since both matrices contain a priori no zeros. However, for this contraction we do not need to appeal to strong

### 3 Conservative Numerics

conservation differentiation since this term does not have its seeds in a conservation law.

$$\begin{aligned}
\mathbf{Q} : \nabla \mathbf{u} &= Q^{ij} \nabla_i u_j \\
&= Q^{ij} \left( \partial_i u_j - \Gamma^k_{ij} u_k \right) \\
&= Q^{rr} \partial_r u_r + Q^{r\vartheta} \left( \partial_r u_\vartheta - \frac{1}{r} u_\vartheta \right) + Q^{r\varphi} \left( \partial_r u_\varphi - \frac{1}{r} u_\varphi \right) + \dots \\
&= \mathbf{E}_{\text{diss}}
\end{aligned} \tag{3.90}$$

Of course also this quantity from now on denominated  $\mathbf{E}_{\text{diss}}$  is calculated with the aid of Mathematica.

The strong conservative form of the energy equation yields

$$\begin{aligned}
\partial_t \left[ \sqrt{|\mathbf{g}|} \rho \epsilon \right] + \partial_i \left[ \sqrt{|\mathbf{g}|} \rho \epsilon \mathbf{e}^i \cdot (\mathbf{u} - \dot{\mathbf{x}}) \right] + \sqrt{|\mathbf{g}|} p \operatorname{div} \mathbf{u} - \\
- 4\pi \sqrt{|\mathbf{g}|} \kappa_P \rho (J - S) + \sqrt{|\mathbf{g}|} \mathbf{E}_{\text{diss}} = 0.
\end{aligned} \tag{3.91}$$

We project the velocities on the covariant base, multiply with  $\sqrt{|\mathbf{g}|}$  and divide by  $\sqrt{1 - \mu^2}$  to obtain the energy equation in spherical

$$\begin{aligned}
\partial_t \left[ r^2 \rho \epsilon \right] + \partial_r \left[ r^2 \rho \epsilon (u^r - \dot{x}^r) \right] - r^2 \partial_\mu \left[ \sqrt{1 - \mu^2} \rho \epsilon (u^\vartheta - \dot{x}^\vartheta) \right] + \\
+ r^2 \partial_\varphi \left[ \rho \epsilon (u^\varphi - \dot{x}^\varphi) \right] + r^2 p \operatorname{div} \mathbf{u} - 4\pi r^2 \kappa_P \rho (J - S) + r^2 \mathbf{E}_{\text{diss}} = 0
\end{aligned} \tag{3.92}$$

and polar coordinates.

$$\begin{aligned}
\partial_t \left[ r \rho \epsilon \right] + \partial_r \left[ r \rho \epsilon (u^r - \dot{x}^r) \right] - r \sqrt{1 - \mu^2} \partial_\mu \left[ \rho \epsilon (u^\vartheta - \dot{x}^\vartheta) \right] + \\
+ r p \operatorname{div} \mathbf{u} - 4\pi r \kappa_P \rho (J - S) + r \mathbf{E}_{\text{diss}} = 0
\end{aligned} \tag{3.93}$$

#### 3.3.4 Equation of Radiation Energy

The simplified frequency integrated radiation energy equation in the comoving frame was defined in equation (2.28).

$$\partial_t J + \operatorname{div} (\mathbf{u} J) + c \operatorname{div} \mathbf{H} + \mathbf{K} : \nabla \mathbf{u} + c \chi_P (J - S) = 0 \tag{3.94}$$

### 3.3 Strong Conservation Form of RHD in Spherical and Polar Coordinates

For the scalar energy input of radiative pressure into the material we analogously define a new coupling variable

$$\begin{aligned}
\mathbf{K} : \nabla \mathbf{u} &= K^{ij} \nabla_i u_j \\
&= K^{rr} \partial_r u_r + K^{r\vartheta} \left( \partial_r u_\vartheta - \frac{1}{r} u_\vartheta \right) + K^{r\varphi} \left( \partial_r u_\varphi - \frac{1}{r} u_\varphi \right) + \dots \\
&= \mathbf{P}_{\text{coup}}
\end{aligned} \tag{3.95}$$

In strong conservation form it yields

$$\begin{aligned}
\partial_t \left[ \sqrt{|\mathbf{g}|} J \right] + \partial_i \left[ \sqrt{|\mathbf{g}|} \mathbf{e}^i \cdot (J(\mathbf{u} - \dot{\mathbf{x}}) + c\mathbf{H}) \right] + \\
+ \sqrt{|\mathbf{g}|} \mathbf{P}_{\text{coup}} + \sqrt{|\mathbf{g}|} c\chi_P (J - S) = 0.
\end{aligned} \tag{3.96}$$

In spherical coordinates with fixed  $\vartheta$  we obtain

$$\begin{aligned}
\partial_t \left[ r^2 J \right] + \partial_r \left[ r^2 (J(u^r - \dot{x}^r) + cH^r) \right] - \\
r^2 \partial_\mu \left[ \sqrt{1 - \mu^2} (J(u^\vartheta - \dot{x}^\vartheta) + cH^\vartheta) \right] + \\
+ r^2 \partial_\varphi \left[ (J(u^\varphi - \dot{x}^\varphi) + cH^\varphi) \right] + r^2 \mathbf{P}_{\text{coup}} + r^2 c\chi_P (J - S) = 0.
\end{aligned} \tag{3.97}$$

and the radiation energy equation in polar coordinates yields

$$\begin{aligned}
\partial_t \left[ rJ \right] + \partial_r \left[ r (J(u^r - \dot{x}^r) + cH^r) \right] - \\
\sqrt{1 - \mu^2} r \partial_\mu \left[ (J(u^\vartheta - \dot{x}^\vartheta) + cH^\vartheta) \right] + r \mathbf{P}_{\text{coup}} + r c\chi_P (J - S) = 0.
\end{aligned} \tag{3.98}$$

#### 3.3.5 Radiative Flux Equation

The radiative flux equation, another vectorial conservation law remains to be sketched in strong conservation form for general non-steady coordinates. We emanate from equation (2.28).

$$\partial_t \mathbf{H} + \text{div}(\mathbf{u}\mathbf{H}) + c \text{div} \mathbf{K} + \mathbf{H} \cdot \nabla \mathbf{u} + c\chi_R \mathbf{H} = 0 \tag{3.99}$$

and for a start define an *effective radiative flux tensor*  $\mathbf{L}$  analogously to the effective tensor of gaseous momentum.

$$\begin{aligned}
(\mathbf{u} - \dot{\mathbf{x}})\mathbf{H} &= \mathbf{L} = l^{ij} \mathbf{e}_i \mathbf{e}_j \\
l^{ij} &= (u^i - \dot{x}^i) H^j
\end{aligned} \tag{3.100}$$

### 3 Conservative Numerics

The contribution of radiative momentum to the material  $\mathbf{H} \cdot \nabla \mathbf{u}$  will be abbreviated via another new coupling variable with components

$$F_{\text{coup}}^j = H^i \nabla_i u^j.$$

The geometrically conservative form in non-steady coordinates of upper equation will be considered in the following shape.

$$\begin{aligned} \partial_t [\sqrt{|\mathbf{g}|} \mathbf{H}] + \partial_i [\sqrt{|\mathbf{g}|} \mathbf{e}^i \cdot (\mathbf{L} + c\mathbf{K})] + \\ + \sqrt{|\mathbf{g}|} F_{\text{coup}} + \sqrt{|\mathbf{g}|} \kappa_R \rho \mathbf{H} = 0. \end{aligned} \quad (3.101)$$

The three components of the radiative flux equation in spherical coordinates yields

### 3.3 Strong Conservation Form of RHD in Spherical and Polar Coordinates

$$\begin{aligned}
& \partial_t \left[ r^2 \sqrt{1-\mu^2} \cos \varphi H^r + r^3 \mu \cos \varphi H^\vartheta - r^3 \sqrt{1-\mu^2} \sin \varphi H^\varphi \right] + \\
& + \partial_r \left[ r^2 \sqrt{1-\mu^2} \cos \varphi \left( H^r(u^r - \dot{x}^r) + cK^{rr} \right) + r^3 \mu \cos \varphi \left( H^\vartheta(x^r - \dot{x}^r) + cK^{r\vartheta} \right) - \right. \\
& \left. - r^3 \sqrt{1-\mu^2} \sin \varphi \left( H^\varphi(x^r - \dot{x}^r) \right) \right] - \partial_\mu \left[ r^2(1-\mu^2) \cos \varphi \left( H^r(u^\vartheta - \dot{x}^\vartheta) + cK^{\vartheta r} \right) + \right. \\
& + r^3 \mu \sqrt{1-\mu^2} \cos \varphi \left( H^\vartheta(u^\vartheta - \dot{x}^\vartheta) + cK^{\vartheta\vartheta} \right) - r^3(1-\mu^2) \sin \varphi \left( H^\varphi(x^\vartheta - \dot{x}^\vartheta) + cK^{\vartheta\varphi} \right) \left. \right] + \\
& \partial_\varphi \left[ r^2 \sqrt{1-\mu^2} \cos \varphi \left( H^r(u^\varphi - \dot{x}^\varphi) + cK^{\varphi r} \right) + r^3 \mu \cos \varphi \left( H^\vartheta(u^\varphi - \dot{x}^\varphi) + cK^{\varphi\vartheta} \right) - \right. \\
& \left. - r^3 \sqrt{1-\mu^2} \sin \varphi \left( H^\varphi(u^\varphi - \dot{x}^\varphi) + cK^{\varphi\varphi} \right) \right] + \\
& + r^2 \left( \sqrt{1-\mu^2} \cos \varphi \mathbf{F}_{\text{coup}}^r + r\mu \cos \varphi \mathbf{F}_{\text{coup}}^\vartheta - r\sqrt{1-\mu^2} \sin \varphi \mathbf{F}_{\text{coup}}^\varphi \right) + \\
& + \text{constr}^2 \left( \sqrt{1-\mu^2} \cos \varphi H^r + r\mu \cos \varphi H^\vartheta - r\sqrt{1-\mu^2} \sin \varphi H^\varphi \right) = 0.
\end{aligned} \tag{3.102}$$

$$\begin{aligned}
& \partial_t \left[ r^2 \sqrt{1-\mu^2} \sin \varphi H^r + r^3 \mu \sin \varphi H^\vartheta + r^3 \sqrt{1-\mu^2} \cos \varphi H^\varphi \right] + \\
& + \partial_r \left[ r^2 \sqrt{1-\mu^2} \sin \varphi \left( H^r(u^r - \dot{x}^r) + cK^{rr} \right) + r^3 \mu \sin \varphi \left( H^\vartheta(u^r - \dot{x}^r) + cK^{r\vartheta} \right) + \right. \\
& + r^3 \sqrt{1-\mu^2} \cos \varphi \left( H^\varphi(x^r - \dot{x}^r) + cK^{r\varphi} \right) \left. \right] - \partial_\mu \left[ r^2(1-\mu^2) \sin \varphi \left( H^r(u^\vartheta - \dot{x}^\vartheta) + cK^{\vartheta r} \right) + \right. \\
& + r^3 \mu \sqrt{1-\mu^2} \sin \varphi \left( H^\vartheta(u^\vartheta - \dot{x}^\vartheta) + cK^{\vartheta\vartheta} \right) + r^3(1-\mu^2) \cos \varphi \left( H^\varphi(u^\vartheta - \dot{x}^\vartheta) + cK^{\vartheta\varphi} \right) \left. \right] + \\
& \partial_\varphi \left[ r^2 \sqrt{1-\mu^2} \sin \varphi \left( H^r(u^\varphi - \dot{x}^\varphi) + cK^{\varphi r} \right) + r^3 \mu \sin \varphi \left( H^\vartheta(u^\varphi - \dot{x}^\varphi) + cK^{\varphi\vartheta} \right) + \right. \\
& \left. + r^3 \sqrt{1-\mu^2} \cos \varphi \left( H^\varphi(u^\varphi - \dot{x}^\varphi) + cK^{\varphi\varphi} \right) \right] + \\
& + r^2 \left( \sqrt{1-\mu^2} \sin \varphi \mathbf{F}_{\text{coup}}^r + \mu r \sin \varphi \mathbf{F}_{\text{coup}}^\vartheta + r\sqrt{1-\mu^2} \cos \varphi \mathbf{F}_{\text{coup}}^\varphi \right) + \\
& + \text{constr}^2 \left( \sqrt{1-\mu^2} \sin \varphi H^r + \sqrt{1-\mu^2} \cos \varphi H^\varphi + r\mu \sin \varphi H^\vartheta \right) = 0.
\end{aligned} \tag{3.103}$$

$$\begin{aligned}
& \partial_t \left[ r^2 \mu H^r - r^3 \sqrt{1-\mu^2} H^\vartheta \right] + \\
& + \partial_r \left[ r^2 \mu \left( H^r(u^r - \dot{x}^r) + cK^{rr} \right) - r^3 \sqrt{1-\mu^2} \left( H^\vartheta(x^r - \dot{x}^r) + cK^{r\vartheta} \right) \right] - \\
& - \partial_\mu \left[ r^2 \mu \sqrt{1-\mu^2} \left( H^r(u^\vartheta - \dot{x}^\vartheta) + cK^{\vartheta r} \right) - r^3(1-\mu^2) \left( H^\vartheta(u^\vartheta - \dot{x}^\vartheta) + cK^{\vartheta\vartheta} \right) \right] + \\
& \partial_\varphi \left[ r^2 \mu \left( H^r(u^\varphi - \dot{x}^\varphi) + cK^{\varphi r} \right) - r^3 \sqrt{1-\mu^2} \left( H^\vartheta(u^\varphi - \dot{x}^\varphi) + cK^{\varphi\vartheta} \right) \right] + \\
& + r^2 \left( \mu \mathbf{F}_{\text{coup}}^r - r\sqrt{1-\mu^2} \mathbf{F}_{\text{coup}}^\vartheta \right) + \text{constr}^2 \left( \mu H^r - r\sqrt{1-\mu^2} H^\vartheta \right) = 0.
\end{aligned} \tag{3.104}$$

### 3 Conservative Numerics

The two components in polar coordinates can be found in the following arrays.

$$\begin{aligned}
& \partial_t \left[ r\sqrt{1-\mu^2}H^r + r^2\mu H^\vartheta \right] + \\
& + \partial_r \left[ r\sqrt{1-\mu^2} \left( H^r(u^r - \dot{x}^r) + cK^{rr} \right) + r^2\mu \left( H^\vartheta(u^r - \dot{x}^r) + cK^{r\vartheta} \right) \right] - \\
& - \sqrt{1-\mu^2}\partial_\mu \left[ r\sqrt{1-\mu^2} \left( H^r(u^\vartheta - \dot{x}^\vartheta) + cK^{\vartheta r} \right) + r^2\mu \left( H^\vartheta(u^\vartheta - \dot{x}^\vartheta) + cK^{\vartheta\vartheta} \right) \right] + \\
& + r \left( \sqrt{1-\mu^2}HradU^r + r\mu\mathbf{F}_{\text{coup}}^\vartheta \right) + constr \left( \sqrt{1-\mu^2}H^r + r\mu H^\vartheta \right) = 0. \quad (3.105)
\end{aligned}$$

$$\begin{aligned}
& \partial_t \left[ r^2\mu H^r - r^2\sqrt{1-\mu^2}H^\vartheta \right] + \\
& + \partial_r \left[ r\mu \left( H^r(u^r - \dot{x}^r) + cK^{rr} \right) - r^2\sqrt{1-\mu^2} \left( H^\vartheta(u^r - \dot{x}^r) + cK^{r\vartheta} \right) \right] - \\
& - \sqrt{1-\mu^2}\partial_\mu \left[ r\mu \left( H^r(u^\vartheta - \dot{x}^\vartheta) + cK^{\vartheta r} \right) - r^2\sqrt{1-\mu^2} \left( H^\vartheta(u^\vartheta - \dot{x}^\vartheta) + cK^{\vartheta\vartheta} \right) \right] + \\
& + r \left( \mu\mathbf{F}_{\text{coup}}^r - r\sqrt{1-\mu^2}H^\vartheta \right) + constr \left( \mu H^r - r\sqrt{1-\mu^2}H^\vartheta \right) = 0. \quad (3.106)
\end{aligned}$$

## 4 Orthogonal and Nonorthogonal Adaptive Grids

In the forthcoming sections we want to motivate and discuss the necessity for multi-dimensionally adaptive grids for astrophysical applications with radiation hydrodynamics in 2D and 3D and thereby justify our excessive mathematics hitherto. At first we will give a brief introduction to fundamental concepts in grid generation and then phrase three crucial postulations for suitable adaptive grids in implicit RHD numerics. We will discover that not all three postulation can be fulfilled and therefore occupy ourselves with possible compromises and prospective continuation of our ideas and approaches.

### 4.1 Basic Principles of Grid Generation

Finite difference and finite element methods for numerical solutions of partial differential equations require a grid which represents the physical domain in discrete terms, often referred to as the *logical space*. Generally the grid is a set of points, lines, (hyper)surfaces and (hyper)volumes that arise from an appropriate transformation between these two domains. In many applications the points, also called *nodes* and volumes or *cells* are to be chosen in a way that the underlying problem gets simplified; for instance a transformation to a rectangular, an orthogonal or a merely smooth domain. Such *structured meshes* can be obtained via coordinate transformations, algebraic methods like polynomial interpolation or differential methods respectively hybrid variants (a textbook giving a profound overview is e.g. Knupp and Steinberg [22]). In chapter 3 we anticipated generating a structured mesh by discretization of coordinates we obtained from a well known coordinate transformation even though we never explicitly conducted this transition from  $(r, \vartheta, \varphi)$  to  $(r_i, \vartheta_j, \varphi_k)$  and differential to difference operators.

*Unstructured grids* cover the computational domain with cells of arbitrary shape and do rather appear with complex geometrical domains. Practical problems of unstructured meshes arise from numbering and ordering the cells and edges which puts high computational demands even if boundaries do not move. Clearly also the numerical solution of a partial differential equation on such an unstructured is more expensive than on a structured mesh. However, one advantage of unstructured grids is a quite handy local mesh refinement by dividing grid cells appropriately (Liseikin [30]).

Grid generation itself must be understood as an essential step of finding suitable methods for solving PDEs numerically<sup>1</sup>. In the following sections we want to point out some possible approaches to grid generation in 2 and 3 dimensions. However, for the sake of clearness 2D grids will be favored.

Time dependent problems with steep gradients as they appear in hydrodynamics state special challenges for numerical techniques, likewise for numerical grid generation. Basically one can distinguish between three main approaches to handle non static finite differences or finite elements; the Eulerian, the Lagrangian and methods that allow generally adaptive grids. As pointed out in section 3.2.3, Eulerian grids remain static throughout the computation and all physical quantities and fluxes are calculated with respect to steady nodes and cells whereas Lagrangian grids move with the very velocity of one particular physically interesting component, in most cases the gas. Analysis reveals (Furzeland et al. (1990) [15]) that *generally adaptive grids* are definitely privileged. Connecting the grid with physical quantities respectively some measure of their computational error and adjusting its profile iteratively provides the best results whenever the number of nodes is fixed (i.e. no mesh refinement).

Fundamental ideas of dynamically adaptive grids in RHD were developed by Winkler (1977) [50], Winkler, Norman and Mihalas (1984) [51] and [33] respectively a sophisticated method for grid control in 1D was found by Dorfi and Drury (1987) [11]. In the following paragraphs we shall investigate some potential amplifications to multi-dimensionally adaptive grids.

### 4.2 The Grid We Are Looking For

First and foremost we are looking for a grid that geometrically operates radiation hydrodynamics in problem-oriented domains. Since we know that all stars rotate and therefore are rather geoids than spheres, polar and spherical coordinates do not match optimally. In latter geometries, shock waves would not propagate alongside coordinate lines respectively within coordinate surfaces but skew to them. Immense fluxes in multiple directions would be the consequence which is numerically troublesome. Hence, an adaptive grid that satisfies our demands ideally would have to allow adaptiveness in more than one dimension but remain orthogonal all along.

**Postulation.** *The grid should be adaptive in more than one dimension but remain orthogonal throughout the computation.*

In the case of strong conservation finite volume methods in complex geometries the orthogonality of the coordinate lines would ensure that the metric tensor (as we have

---

<sup>1</sup>There are popular numerical methods working without meshes like the family of spectral methods or smoothed-particle hydrodynamics but as the chapter title suggests we concern ourselves with grid-based techniques exclusively.



seen a function of space and time) remains diagonal. With more general metrics, not only the volume element  $|\mathbf{g}|$  becomes rather elaborate as it is calculated by the determinant of the metric. All projections and summations of our physical tensors require far more arithmetic operations. For instance, each of the nine contravariant component of the viscous pressure  $\mathbf{Q}$  requires nine arithmetic operations. In discrete terms this implicates to execute these  $27 \times 2$  operations at each node and time step at worst.

$$Q^{ij} = Q_{lm} g^{li} g^{mj} = \dots \left( g^{li} g^{mj} (\nabla_l u_m + \nabla_j u_m) - g^{ij} \frac{1}{3} \text{div } \mathbf{u} \right)$$

With orthogonal grids, all off diagonal components of the metric are zero  $g^{ij} = 0 \forall i \neq j$  and in this case 54 operations reduce to effective six. After all this objection is not that relevant practically, since in implicit radiation hydrodynamics most CPU time is consumed by the matrix inversion (Dorfi (1999) [13]).

Even if orthogonality can not be maintained (which indeed will be one of our conclusions), the adaptive grids by any means needs some kind of mollifying property that avoids excessively twisted, acute-angled or one another overtaking cells.

**Postulation.** *Grid cells should basically maintain their local geometries.*

Moreover, the one dimensional special case of simple radial geometry shall be inherent in more dimensional grid generation so that one can easily compare calculations, e.g. with previous works in implicit RHD numerics like Dorfi (1999) [13] respectively Dorfi et al. (2004) [12].

**Postulation.** *The more dimensional grid should contain the one dimensional special case of radial geometry.*

In the upcoming section we will discuss several approaches to grid generation in the face of problem oriented geometries and suggest feasible approaches to multi-dimensionally adaptive grids in 2D and 3D radiation hydrodynamics.

### 4.3 Remarks on Grid Generation Methods

In this section we present some possible approaches to grid generation for implicit adaptive mesh techniques and discuss their compatibility with our three postulations. A common premise is an a priori fixed number of grid points that is redistributed during the temporal evolution. Again our perspective emphasizes on methods for neither fully Eulerian nor fully Lagrangian grid but a hybrid where gas velocity and grid velocity are associated but not equal as introduced in section 3.2.3.

Before we glance at adaptive grid techniques we present some fundamental *static* grid generation methods that could be adapted for time dependent problems.

### 4.3.1 Differential Methods

Grid generation using differential equation techniques are very popular for structured meshes, especially with complex geometries. The idea is to set up a system of partial differential equations whose solution defines a coordinate transformation. Well known properties of special differential equations can be used to control coordinates to some extent and on the other hand help to find suitable solution methods. These and a lot of other methods are well described in several text books, e.g. Castillo [8] or Liseikin [30].

Grid generation methods based on solving partial differential equations are naturally classified elliptic, hyperbolic and parabolic. Hyperbolic equations are preferred for meshes around bodies but prove inappropriate for internal and closed domains which means they naturally disqualify for astrophysical applications. Moreover, inherent singularities propagate and grid oscillation and overlapping of volumes is encountered frequently. Parabolic techniques combine some positive aspects of hyperbolic properties like being able to formulate an initial value problem on the one hand and elliptical properties like diffusion effects smoothing out singularities on the other hand. Numerous references to hyperbolic and parabolic as well as combined techniques can also be found in [30], p191 ff. Mathematical fundamentals as well as research activities in the field of differential grid generation are presented in Knupp and Steinberg [22].

Exemplary we want to sketch some basic properties of *elliptic systems* using Laplace or Poisson equations. Elliptic equations have one important characteristic as they ensure smooth solutions in the total interior of the domain even if the boundaries are non-smooth. For smooth boundaries continuous derivatives of the resulting coordinates are also granted on the boundaries. Elliptic equations that obey the extremum principle like the Laplace Equation are also known to have very small tendency for folding of grid cells (see e.g. Spekreijse (1995) [38], Zhang et al. (2006) [53]). However, we should mention that elliptic systems are numerically costly and Laplace-type equations allow practically no control of the geometric properties of the grid. In anticipation of more sophisticated methods the Laplace system is presented briefly.

### 4.3.2 Laplace Systems

Many of the commonly used techniques to generate grids via differential equations are derivations of a method proposed by Winslow (1966) [52] where the nonlinear two dimensional Poisson equation is solved. In these approaches the constructed meshes can be understood as equipotential surfaces.

We shall study an archetype of such an elliptical grid generation method and consider a computational domain  $\Xi^d$ , a physical domain  $X^d$  and a coordinate system  $\Sigma_{(\alpha)}$ .

$$\Sigma_{(\alpha)} : \Xi^d \rightarrow X^d, \quad \mathbf{x}(\xi) \mapsto (x_{(\alpha)}^i(\xi)), \quad i = 1, \dots, d \quad (4.1)$$

The most obvious elliptic system is the *Laplace system* that can be formulated in the physical

$$\Delta x^i = \frac{\partial^2}{\partial \xi^j \partial \xi^j} x^i = 0 \quad (4.2)$$

or computational domain (interchange  $x$  and  $\xi$ ) which is equivalent with  $g^{lm} \partial_l \partial_m x^i = 0$ , a coupled quasilinear system of partial differential equations in  $\Xi$ . In most cases the transformation  $\mathbf{x}(\xi)$  will be considered since this formulation in the physical space allows direct control of grid spacing and orthogonality.

One main requirement for the transformation is that the Jacobian of the transformation  $\mathbf{x}(\xi) : \Xi^n \rightarrow X^n$  is nonzero, i.e. the two domains are diffeomorphic which is confirmed by the theorem of Rado for harmonic functions. This leads us to the first discrepancies with our postulations made before. There is no diffeomorphism between Cartesian and polar respectively spherical coordinates that includes  $r = 0$ . Moreover, even if we cut out the origin, polar and spherical coordinates do not even satisfy the Laplace nor a Poisson equation.

Nevertheless we briefly discuss one application and consider the transformation  $\mathbf{x}(\xi, \eta)$  in a two dimensional simply connected bounded domain  $X^2$  and let  $\Xi^2$  be a unit square as commonly imposed. In section 3.2.1 when we introduced basic differential geometric relations, we also mentioned that the metric tensor  $\mathbf{g}$  is symmetric which leads to the following boundary value problem<sup>2</sup>.

$$(g^{\xi\xi} \partial_\xi^2 + 2g^{\xi\eta} \partial_\xi \partial_\eta + g^{\eta\eta} \partial_\eta^2) x^i = 0 \quad (4.3)$$

Computations as well as differential geometric deliberations reveal that grid lines obtained by (4.3) are attracted to concave boundaries and repelled in the vicinity of convex boundaries. In stellar astrophysics this would implicate that the mesh gets tighter towards the center of the star automatically. The bottom line is that such elliptical systems as pure boundary value problems disqualify for grid adaptiveness with respect to *inner* domain dynamics.

### 4.3.3 Conformal Mapping

When thinking about our first postulation of more dimensional adaptivity and orthogonality one might consider conformal maps since they are angle-preserving. Conformal transformations would remain orthogonal throughout the evolution of the grid which is represented by a diagonal metric  $g_{ij} = \text{diag}(g_{ii})$ . Unfortunately coordinate caustics and overlapping problems are not the only challenges one would have to face. Both domains,

---

<sup>2</sup>For our orthogonal reference, the polar coordinates we obtain a contradiction  $(\partial_r^2 + \frac{1}{r} \partial_\vartheta^2)(r \cos \vartheta, r \sin \vartheta) \neq 0$ .

## 4 Orthogonal and Nonorthogonal Adaptive Grids

$\Xi^n$  and  $X^n$  have to be *conformally equivalent* which is expressed by the fact that the metric tensor is a multiple of the unit matrix.

$$g_{ij} = g(\xi)\delta^i_j \quad (4.4)$$

Again we come into conflict with our postulations given that our reference systems, polar and spherical coordinates are not conformally equivalent to Cartesian ones<sup>3</sup>.

### 4.3.4 Algebraic Methods

*Algebraic grid generation methods* rely on coordinate transformations constructed by interpolation techniques. According to concrete requirements to the solutions, different interpolation functions respectively polynomials are evaluated and transformations are governed by the coefficients of these polynomials.

These schemes prove computationally efficient but lack some convenient intrinsic properties we presented in context of differential methods. Algebraic grid generation requires significant control techniques to obtain practicable meshes otherwise skewness of cells and grid point spacing can get messy. There are several ideas to regulate the grid such as adding differential calculus elements in order to inhibit that coordinate surfaces come too close or even overlap respectively degenerate. Other approaches directly influence the interpolation coefficients.

In the following section we present an idea of a hybrid method that combines concepts of algebraic methods with equidistribution techniques.

### 4.3.5 Equidistribution

The idea of *equidistribution methods* is to place the grid nodes in a way that the numerical error is distributed uniformly throughout the computational domain. In practice that means to adjust the mesh size locally according to the local numerical derivatives - the steeper the gradients the higher the spatial resolution required in order to get uniform resolution. In one dimension a given physical quantity gets equidistributed along an arc (see e.g. Thompson, Warsi, Mastin [43], Dorfi and Drury (1987) [11]) and the grid is determined uniquely by imposing a proper grid equation.

The approach presented in [11] is to construct a grid equation distributing the nodes  $n_i$  proportionally to a desired resolution  $R$  which is defined in terms of the arc-length along the graph of an approximated function  $\mathbf{f}$ ,  $R = \sqrt{1 + (d\mathbf{f}/dx)^2}$  which originates from the definition of the line element  $ds^2 = g_{ij}dx^i dx^j$ . The choice of function  $\mathbf{f}$  depends on what regime in the calculation shall be the focus of resolution, e.g. pressure or temperature.

---

<sup>3</sup>In polar coordinates the metric yields  $g_{ij} = \text{diag}(1, r) \neq g(r, \vartheta)\delta^i_j$ .

A *smoothing* respectively variation limiting control of the grid is obtained by imposing constraints on grid spacing and the resolution function.

Generalizations to more dimensions follow different strategies. Several attempts have been made to generalize one-dimensional equidistribution directly to two and more dimensions by applying a series of 1D equidistributions along coordinate arcs. The concept of arc equidistribution however can only be satisfied locally but not globally in the domain as pointed out by Anderson (1987) [2] as well as Hunag and Sloan (1995) [20]. Moreover, successive arc equidistributions along *fixed* coordinates fails to adapt the geometries of the cells which was one of our postulations. Hence such a straight approach is rather comparable to adaptive mesh refinement methods.

As motivated in previous chapters, it is reasonable to perceive physical quantities and their numerical pendants in strong conservation form in a volume integrated framework respectively even in terms of differential forms. So it would seem natural to investigate methods that equidistribute a quantity with respect to surfaces and volumes, studied e.g. in Delzanno et al. (2008) [9] or Sulman, Williams and Russell (2009) [41].

One of our first attempts to obtain a multi-dimensionally adaptive grid that remains orthogonal during temporal evolution was to combine one dimensional equidistribution techniques and algebraic methods.

## 4.4 Equidistribution and Interpolation Attempt

The intention is to generate a 2D grid that allows certain deformations from a polar coordinate system but remain orthogonal globally<sup>4</sup>. One family of curves shall represent the angular coordinate and a family of normal curves would define the radial one. Optimally we would start with a polar grid and according to an equidistribution principle, e.g. the angular curves would deform and intrinsically define the family of orthogonal radial coordinates.

### 4.4.1 Toy Model

Let us consider a transformation  $\xi(x, y, t), \eta(x, y, t)$  where the coordinates  $(\xi, \eta)$  are represented as *angular* and a *radial* family of curves. In favor of simplification we assume azimuthal symmetry and confine our analysis on a quadrant of the real plane. The most obvious deformation we would want to be considered is oblateness by rotation which means in 2D the deformation from a circle to an elliptical shape. As naive toy model we

---

<sup>4</sup>For the time being we shall blind out that this undertaking is futile altogether and refer to posterior findings.

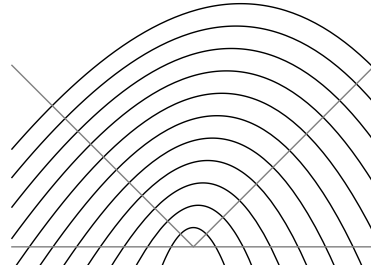


Figure 4.1: Angular coordinate lines of toy model

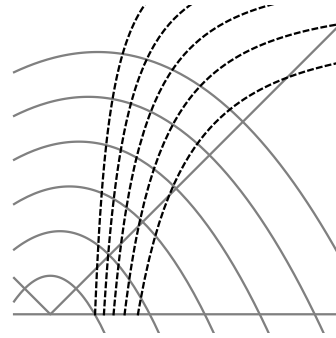


Figure 4.2: Coverage and Caustic

let  $\eta : \mathbb{R} \times \mathbb{R} \times \mathbb{R}^+ \rightarrow \mathbb{R}$  be a polynomial with a family of time dependent coefficients<sup>5</sup>.

$$\eta(x, \tau, t) = \sum_{i < i_{\max}} a_i(\tau, t)x^i \quad (4.5)$$

The coefficients  $a_i$  are partially determined by boundary conditions as we demand normal tangents of  $\eta$  at  $y = 0$  and  $x = 0$  in order to guarantee smooth transitions to the other quadrants of the real plane. The  $\xi$  curve at a point  $x_0$  is expectedly determined by

$$\xi(x, \tau, t) = \eta(x_0, \tau, t) - \frac{1}{\eta'(x_0, \tau, t)}(x - x_0). \quad (4.6)$$

For principal analysis we set  $i_{\max} = 3$  and studied this system in **Mathematica**. This choice determines the angular curves with noted boundary conditions uniquely, each further term would bring ambiguousness into the grid that could be used to include physics respectively grid control mechanisms.

---

<sup>5</sup>Evidently with this ansatz our reference frame, the polar coordinates are not included which we also blind out for the present.

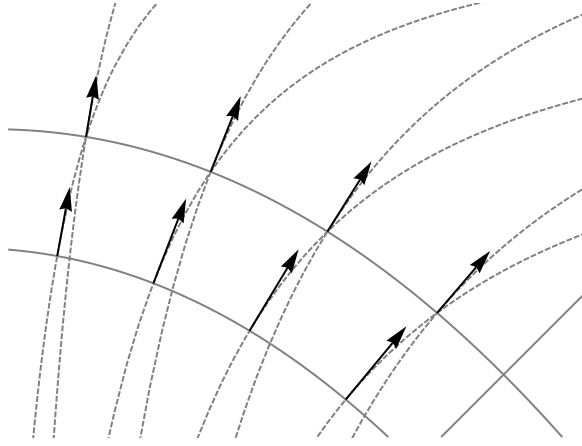


Figure 4.3: Normal vectors

#### 4.4.2 Analysis

We define differently equidistributed points at the  $x$ - and the  $y$ -axis. Since the boundary condition for the  $\eta$  curves at  $y = 0$  would imply infinite slope, we rotated the whole setting by  $\alpha = \pi/4$ . What we get is a set of curves that increases in *ellipticity* with the radius which describes the physical situation of a rotating configuration, drafted in figure 4.1. As already mentioned both the angular coordinate lines and their normal curves are determined a priori. With determination of one orthogonal curve at a point  $x_0$ , it necessarily would have to be normal at all intersections if there existed such a family of curves. The most obvious observation we make in figure 4.2 is that the radial curves do not intersect with the natural point of origin nor reproduce the (45 degree rotated)  $x$ -axis and cause coordinate caustics. Of course with growing order of the polynomials further boundary conditions can be imposed.

However, this leads to the second quite evident observation that the orthogonal curves to the outermost polynomial are not normal at all other intersections with inner polynomials. If we wanted to impose orthogonality at  $n$  intersections, the order of polynomial in this ansatz would at least have to match the number of radial nodes  $i_{\max} \geq n$  which is rather pointless when we consider e.g. 500 radii.

This graphical analysis already discloses the limitation of grid generation in two dimensions considering our postulations. Any deviation from polar coordinates reproduces either nonorthogonal grids or fails to reproduce the domains boundaries; hence postulation one will have to be renounced in its original form. The only kind of orthogonal adaptiveness in a polar grid is dislocation of nodes alongside the original coordinate lines which corresponds to adaptive mesh refinement methods. In the following section we want to substantiate our conclusions analytically.

## 4.5 On the Peculiarity of Orthogonal Coordinates

In section 3.2.1 we studied differential geometry of coordinate transformations such as the definition of base vectors (3.27) and the metric tensor (3.30). We noticed that orthogonal coordinates imply diagonal metrics, a factor that can be used to study this family of coordinate transformations. Since one feature of coordinate lines is that all other coordinates are constant alongside the coordinate, transformations have to factorize and the following product ansatz is justified<sup>6</sup>.

$$x(\xi, \eta) = a(\xi)\alpha(\eta), \quad y(\xi, \eta) = b(\xi)\beta(\eta) \quad (4.7)$$

With aforesaid definitions we obtain the base vectors  $\mathbf{e}_\xi = (\alpha a', \beta b')$ ,  $\mathbf{e}_\eta = (a\alpha' b\beta')$  and following covariant metric components.

$$\begin{aligned} g_{\xi\xi} &= \alpha^2 a'^2 + \beta^2 b'^2 \\ g_{\eta\eta} &= a^2 \alpha'^2 + b^2 \beta'^2 \\ g_{\xi\eta} = g_{\eta\xi} &= a\alpha a' \alpha' + b\beta b' \beta' \end{aligned} \quad (4.8)$$

In order to obtain a PDE we can study and solve analytically, the off diagonal entries  $g_{\xi\eta}$  are set zero and functions of  $\xi$  are separated from functions of  $\eta$  which yields

$$\frac{aa'}{bb'} = -\frac{\beta\beta'}{\alpha\alpha'} = \lambda \quad (4.9)$$

where  $\lambda \in \mathbb{R}$ . With the substitution  $A = a^2$  and  $B = b^2$  we obtain  $A'/B' = \lambda$  respectively  $a^2 = \lambda b^2 + c$  with  $c \in \mathbb{R}$  is an arbitrary constant. Our boundary conditions come from the postulation that the coordinate system shall in principle contain the special case of polar coordinates hence we set the point of origin for the radial coordinate to zero  $a(0) = 0$ ,  $b(0) = 0$  and obtain

$$a = \sqrt{\lambda}b \quad (4.10)$$

which means that the  $a$  and  $b$  differ just by an arbitrary factor. When we replace  $\alpha^2 = \bar{A}$ ,  $\beta^2 = \bar{B}$  we obtain  $\bar{B} = -\lambda\bar{A} + k$  and determine the constant  $k$  with the boundary conditions that the angular coordinate reproduces the  $x$ -axis at  $\eta = 0$  and the  $y$ -axis at  $\eta = 1$  to  $k = \lambda$  yielding

$$\beta = \sqrt{\lambda}\sqrt{1 - \alpha^2}. \quad (4.11)$$

---

<sup>6</sup>We confine the analysis on 2D but reasoning and results are equivalent in 3D of course.



A general orthogonal coordinate transformation which contains the reference frame of polar coordinates hence necessarily has to satisfy

$$x(\xi, \eta) = \sqrt{\lambda}b(\xi)\alpha(\eta), \quad y(\xi, \eta) = \sqrt{\lambda}b(\xi)\sqrt{1 - \alpha(\eta)^2}. \quad (4.12)$$

The scaling factor  $\sqrt{\lambda}$  can evidently be set to  $\sqrt{\lambda} = 1$  without loss of generality which leads to our result

$$a = b, \quad \alpha^2 + \beta^2 = 1. \quad (4.13)$$

The postulation for orthogonality inevitably leads to radial symmetry and the grid can never gain an elliptic or even more deformed shape.

## 4.6 Quasi-Polar Coordinates Attempt

Evidently it is necessary to adapt our postulations for a multi-dimensionally adaptive grid in the light of our previous results. Since orthogonality can not be sustained we renounce that strong demand and concentrate on producing adaptive grids that include our reference frame. The following ansatz includes algebraic elements as well as some differential boundary conditions that control the grid properly.

### 4.6.1 Toy Model

Again we consider a transformation  $\xi(x, y, t), \eta(x, y, t)$  with radial and angular coordinates  $(\xi, \eta)$  and azimuthal symmetry. The product ansatz we suggest is

$$\begin{aligned} a(\xi, t) &= \sum_{i=1}^{i_{\max}} a_i(t)\xi^i, & b(\xi, t) &= \sum_{i=1}^{i_{\max}} b_i(t)\xi^i \\ \alpha(\eta, t) &= \left(1 + \sum_{j=1}^{j_{\max}} \alpha_j(t)\eta^j\right) \sin \eta, & \beta(\eta, t) &= \left(1 + \sum_{j=1}^{j_{\max}} \beta_j(t)\eta^j\right) \cos \eta \end{aligned} \quad (4.14)$$

where  $(a_i, b_i, \alpha_j, \beta_j)$  are time dependent coefficients that govern the adaptivity of the grid. One main feature of this approach is that it allows to *turn off* all deviations from radial symmetry by setting  $(a_1, b_1) = 1$  and  $(a_i, b_i) = 0 \forall i \geq 2$  plus  $(\alpha_j, \beta_j) = 0$  which yields polar coordinates. Basically the unknown coefficients are determined via appropriate boundary conditions and whatever coupling with physics would be implemented (e.g. equidistribution along coordinate arcs or with respect to cell volumes).

In order to discuss basic characteristics of this proposal, we set  $i_{\max} = 2$  and  $j_{\max} = 3$  and dissect the system in **Mathematica**.

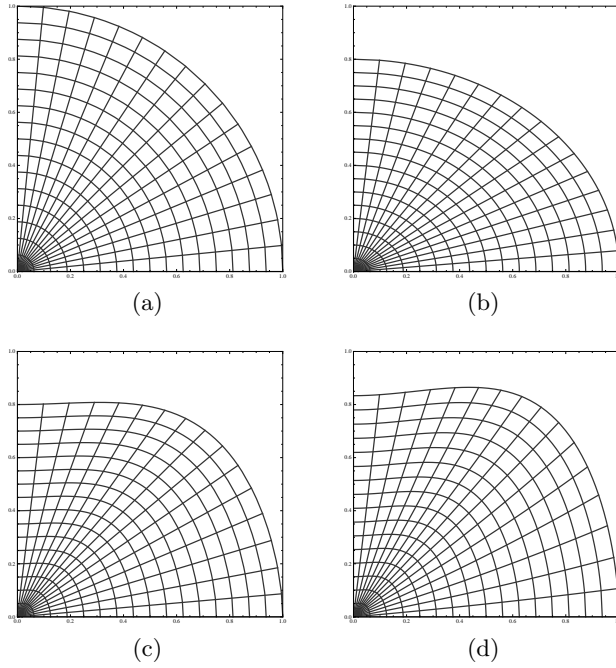


Figure 4.4: Toy Model Grids

### 4.6.2 Analysis

For feasible analysis of course we need to constrain the degrees of freedom of our toy model but leave some undetermined parameters to be manipulated. With boundary conditions that on the one hand assure smooth transitions to other quadrants (normal derivatives at  $x$ - and  $y$ -axis) and on the other hand are consistent with the reference frame we effectively solve a system of algebraic equations in eight unknowns and gain three *free* parameters. The **Mathematica** Notebook we used for solving and plotting these functions can be found in Appendix 6.2.

One example of a coordinate transformation that in principle satisfies all postulations from 4.2 besides orthogonality yields

$$\begin{aligned}
 x &= \xi \cos \eta \\
 y &= (b_1 \xi + b_2 \xi^2) \left( 1 + \frac{(\beta_3 \pi^3 - 16b_2 \xi + b_2 \beta_3 \pi^3 \xi)}{4\pi(1 + b_2 \xi)} \eta + \right. \\
 &\quad \left. + \frac{(-\beta_3 \pi^3 + 4b_2 \xi - b_2 \beta_3 \pi^3 \xi)}{\pi^2(1 + b_2 \xi)} \eta^2 + \beta_3 \eta^3 \right) \sin \eta
 \end{aligned} \tag{4.15}$$

where  $b_1, b_2$  and  $\beta_3 \in \mathbb{R}$  are free parameters. Certainly they are not totally free but need to be confined to certain bounds that ensure unique covering of the domain. Further

Table 4.1: Maxima of geometrical parameters for toy model

	$b_1$	$b_2$	$\beta_3$	$\max  g_{12}(\xi, \eta)/\xi $	$\max \sqrt{\mathbf{g}_{\text{rel}}}(\xi, \eta)$
(a)	1	0	0	0	1
(b)	0.8	0	0	0.18 at (0.85, 0.73)	0.64 at (0.9, 0.71)
(c)	0.8	0	0.5	0.13 at (0.89, 0.79)	1.19 at (0.86, 0.33)
(d)	0.8	0.2	0.5	0.25 at (1, 0.43)	1.62 at (1, 0.29)

constraints emerge from differential geometric requirements to the grid like a maximal skewness of cells.

In figure 4.4 we visualize grids with varying parameters that are listed in table 4.1 along with some characteristics of the grid. The off-diagonal metric elements  $g_{12} = g_{21} \neq 0$  quantify the skewness of the grid and  $\sqrt{\mathbf{g}_{\text{rel}}}$  designates the local cell volume in relation to polar coordinates. Both characteristics were numerically maximized in *Mathematica* in the ranges  $\xi \in (0, 1]$  and  $\eta \in [0, \pi/2]$  since the functional expressions get rather bulky. For the simplest quasi-polar model (b) however the coordinate transformation is  $x = \xi \cos \eta, y = 0.8 \xi \sin \eta$  and the grid characteristics yield explicitly  $g_{12,(b)} = -0.36 \xi \cos \eta \sin \eta$  and  $\sqrt{\mathbf{g}_{\text{rel,(b)}}} = 0.64$ . Due to our boundary conditions the minima are mostly to be found at the origin respectively at the axes, for details see section 6.2.

## 4.7 Strong Conservation Form in Nonorthogonal Coordinates

In section 3.3 the equations of RHD were explicitly formulated in polar and spherical coordinates and we noticed that even with orthogonal coordinates the expressions get rather cumbersome. From the view point of tensor calculus, the number of operations like raising and lowering of indices with non-diagonal metrics increases with the square of the spatial dimension considered. Strong conservation form radiation hydrodynamics in general curvilinear coordinates hence can be expected to arouse extensive equations.

In fact, if we take the full ansatz (4.14) into our *Mathematica* files that generate the equations of radiation hydrodynamics in strong conservation form the computing time for just generating the equations gets sizable and the outputs become huge. The question arises at what point of such calculations the geometric relations and terms are to be determined respectively computed ideally. A profound answer will have to be given in future investigations. However, without a doubt the actual solution of the RHD system which is a matrix inversion problem in implicit numerics as described e.g. in Dorfi et al. (2004) [12] will remain the most time consuming part even or especially in multiple dimensions.



## 5 Conclusions and Prospective

We present versatile conceptual and methodical fundamentals for strong conservation numerics in general non-steady curvilinear coordinates in 2D and 3D. The first chapters 1, 2 and 3 emphasize on mathematical rigorousness and consistency which led to the important finding (3.61) where we reformulated the artificial viscosity for curvilinear coordinates. The relevance of this finding does not come clear until general curvilinear coordinates are used that is why previous calculations were not necessarily affected by this inconsistency.

As *lateral* result we suggest a dynamic equation for the self-gravitation in multiple dimensions by considering the specific gravitational force and the continuity equation (2.32). We avoid pursuing the Laplace equation in 2D and 3D where its unique nature as elliptical PDE in our otherwise hyperbolic problem evokes difficulties in posing adequate boundary conditions. Our non-static gravitation equation will have to be studied in future calculations whereat its imaginable applications range from stellar physics to galactic and cosmological computations where self-gravitation plays a role.

We derive the equations of RHD in strong conservation form an exemplarily sketch them in polar and spherical coordinates in chapter 3.3. They might be understood as intermediate step to more applicable implementations in general curvilinear coordinates and play a role as reference frame a after all.

In chapter 4 we study adaptive grid generation for curvilinear coordinates and find that orthogonality of coordinate lines can not be maintained for multi-dimensionally adaptive grids that contain the reference frames of polar and spherical coordinates. In this sense the polar and polar spherical take an exceptional position as orthogonal grids in 2D and 3D. However, we propose an interesting ansatz that satisfies our main postulations for an astrophysically applicable grid and study possible adoptions. For practical implementation one has to develop means of controlling the skewness of the grid respectively the off-diagonal elements of the metric tensor adequately. A stringent design of such a technique would have exceeded the extent of this thesis and will have to be deferred to future investigations. Moreover one will have to contemplate feasible methods of generating and handling the enormous equations that emerge with non-orthogonal coordinates considered. Clearly, one will have to pursue automatized techniques like those presented with *Mathematica*. Concrete implementations shall also indicate at what point in the computations the geometric terms are to be calculated ideally.



## 6 Appendix

### 6.1 Arguments and Details

#### 6.1.1 Symmetry of the Stress Tensor

In section 2.1 we argue that the symmetry of the stress tensor is due to the conservation of angular momentum. If so, the rate of change of the angular momentum of a fluid  $\rho \mathbf{x} \times \mathbf{v}$  must equal the total applied torque. With  $d\mathbf{S}$  oriented with normal  $\mathbf{n}$ , let  $\mathbf{t}$  be the surface force across this element and the  $i$ -th component be defined by  $t^i = T^{ij}n_j$ .

$$\begin{aligned} \int_{V(t)} (\mathbf{x} \times \partial_t(\rho \mathbf{u})) dV + \int_{\partial V(t)} (\mathbf{x} \times \mathbf{t}) \cdot d\mathbf{S} &= 0 \\ \int_{V(t)} \partial_t(\rho \varepsilon_{ijk} x^j u^k) dV + \int_{\partial V(t)} \varepsilon_{ijk} x^j T^{lk} n_l dS &= 0 \\ \int_{V(t)} (\partial_t(\rho \varepsilon_{ijk} x^j u^k) + \nabla_l \varepsilon_{ijk} x^j T^{lk}) dV &= 0 \end{aligned}$$

Since the volume of our conservation law is arbitrary, we can focus on the integrand.

$$\begin{aligned} \underbrace{\partial_t(\rho \varepsilon_{ijk} x^j u^k) + \varepsilon_{ijk} x^j T^{lk}_{,l} + \varepsilon_{ijk} x^j_{,l} T^{lk}}_{=\varepsilon_{ijk} x^j (\partial_t \rho u^k + T^{lk}_{,l})=0} &= 0 \\ \varepsilon_{ijk} \delta^j_l T^{lk} &= 0 \\ \varepsilon_{ijk} T^{jk} &= 0 \end{aligned} \tag{6.1}$$

The left hand side of equation (6.1) is zero, if  $T^{jk} = T^{kj} \quad \forall j, k$ .

#### 6.1.2 Rankine-Hugoniot Conditions

We consider a one-dimensional Riemann-problem for 1.4 with discontinuous initial condition

$$d_0(x) = \begin{cases} d_l, & x < 0 \\ d_r, & x > 0 \end{cases} \tag{6.2}$$

## 6 Appendix

and look for a solution  $d(x, t)$  for the left and the right hand side of the shock

$$d(x, t) = \begin{cases} d_l, & x < u_s t \\ d_r, & x > u_s t \end{cases} \quad (6.3)$$

with positive velocity  $u_s$ . To do so, we split the integrals in (1.9) cleverly at the discontinuity and get for the first term

$$\begin{aligned} \int_0^\infty \int_{-\infty}^\infty d \partial_t \gamma \, dx dt &= \int_{-\infty}^0 \int_0^\infty d \partial_t \gamma \, dx dt + \int_0^\infty \int_0^{x/u_s} d \partial_t \gamma \, dx dt + \\ &\quad + \int_0^\infty \int_{u_s/x}^\infty d \partial_t \gamma \, dx dt \\ &= -d_l \int_{-\infty}^0 \gamma(x, 0) \, dx - d_r \int_0^\infty \gamma(x, 0) \, dx + \\ &\quad + \int_0^\infty \gamma(x, x/u_s) (d_r - d_l) \, dx \\ &= - \int_{-\infty}^\infty \gamma(x, 0) d_0(x) \, dx - \int_0^\infty \gamma(x, x/u_s) (d_l - d_r) \, dx. \end{aligned} \quad (6.4)$$

For the flux term on the right hand side we proceed analogously and rewrite the integral over  $dx$  with  $t = x/u_s$ .

$$\begin{aligned} \int_0^\infty \int_{-\infty}^\infty f(d) \partial_x \gamma \, dx dt &= \int_0^\infty \left( \int_{-\infty}^{u_s t} \gamma \partial_x f(d) \, dx + \int_{u_s t}^\infty \partial_x f(d) \, dx \right) dt \\ &= \int_0^\infty \gamma(u_s t, t) (f(d_l) - f(d_r)) \, dt \\ &= \frac{1}{u_s} \int_0^\infty \gamma(x, x/u_s) (f(d_l) - f(d_r)) \, dx \end{aligned} \quad (6.5)$$

$$\begin{aligned} \int_0^\infty \int_{-\infty}^\infty (d \partial_t \gamma + f(d) \partial_x \gamma) \, dx dt &= - \int_{-\infty}^\infty \gamma(x, 0) d_0(x) \, dx + \\ &\quad + \int_0^\infty \gamma(x, x/u_s) \left( \frac{f(d_l) - f(d_r)}{u_s} - (d_l - d_r) \right) \, dx \end{aligned} \quad (6.6)$$



(6.6) is weak solution of the Riemann-problem, if

$$\frac{f(d_l) - f(d_r)}{u_s} - (d_l - d_r) = 0 \quad (6.7)$$

or

$$u_s = \frac{f(d_l) - f(d_r)}{d_l - d_r}. \quad (6.8)$$

We call  $u_s$  shock velocity and (6.8) Rankine-Hugoniot condition.

### 6.1.3 Diffusion Approximation

If the radiation field does not depend on the direction i.e. it is isotropic  $I_{\gamma,\text{diff}} = J_{\gamma,\text{diff}} \neq J_{\gamma,\text{diff}}(\mathbf{n})$ , the integration over the solid angle can be executed straightforward. Let be  $\mathbf{e}_r$  the normal vector  $\mathbf{n}$  in local spherical coordinates.

$$\begin{aligned} \mathbf{F}_{\gamma,\text{diff}} &= \int_0^{2\pi} \int_0^\pi I_\gamma \mathbf{e}_r \sin \vartheta \, d\vartheta d\varphi = I_\gamma \int_0^{2\pi} \int_0^\pi \sin \vartheta \begin{pmatrix} \cos \varphi \sin \vartheta \\ \sin \varphi \sin \vartheta \\ \cos \vartheta \end{pmatrix} d\vartheta d\varphi = \mathbf{0} \\ \mathbf{P}_{\gamma,\text{diff}} &= \frac{1}{c} \int_0^{2\pi} \int_0^\pi I_\gamma \mathbf{e}_r \mathbf{e}_r \sin \vartheta \, d\vartheta d\varphi = \frac{I_\gamma}{c} \int_0^{2\pi} \int_0^\pi \sin \vartheta \, d\vartheta d\varphi \cdot \\ &\quad \cdot \begin{pmatrix} \cos^2 \varphi \sin^2 \vartheta & \cos \varphi \sin \varphi \sin^2 \vartheta & \cos \varphi \cos \vartheta \sin \vartheta \\ \cos \varphi \sin \varphi \sin^2 \vartheta & \sin^2 \varphi \sin^2 \vartheta & \cos \vartheta \sin \varphi \sin \vartheta \\ \cos \varphi \cos \vartheta \sin \vartheta & \cos \vartheta \sin \varphi \sin \vartheta & \cos^2 \vartheta \end{pmatrix} = \\ &= \frac{I_\gamma}{c} \begin{pmatrix} \frac{4\pi}{3} & 0 & 0 \\ 0 & \frac{4\pi}{3} & 0 \\ 0 & 0 & \frac{4\pi}{3} \end{pmatrix} = \frac{1}{3} \mathbf{1} J_\gamma \end{aligned} \quad (6.9)$$

### 6.1.4 Strong Conservation Form on Adaptive Grids

In section 3.2.3 we outlined the strong conservation form for time dependent coordinates. Following Thompson, Warsi, Mastin [43] we present the full deduction of this conclusion.

The time derivative of a physical quantity  $\mathbf{d}$  in the non-steady coordinate system  $\Sigma_{(\beta)}$  relative to a coordinate system  $\Sigma_{(\alpha)}$  is given by  $\partial_t \mathbf{d}_{(\beta)} = \partial_t \mathbf{d}_{(\alpha)} + \nabla_{(\alpha)} \mathbf{d} \partial_t \mathbf{x}_{(\beta)}$  which is basically the Reynolds transport theorem. In system  $(\alpha)$  the time derivative of  $\mathbf{d}$  yields  $\partial_t \mathbf{d}_{(\alpha)} = \partial_t \mathbf{d}_{(\beta)} - \dot{\mathbf{x}} \nabla_{(\alpha)} \mathbf{d}$ . With  $\dot{\mathbf{x}}$  we introduced the grid velocity, the second term on the right hand side we also call grid advection. An advection term in a hyperbolic conservation law as we consider them usually gains the form

$$K = \mathbf{d}_t + \text{div}(\mathbf{u}\mathbf{d}) \quad (6.10)$$

## 6 Appendix

respectively in the transformed system

$$K = \mathbf{d}_t - \dot{\mathbf{x}} \cdot \nabla \mathbf{d} + \operatorname{div}(\mathbf{u}\mathbf{d}). \quad (6.11)$$

Applying the strong conservation form of our spatial differential operators we developed in section 3.2.2, this convection term yields

$$K = \mathbf{d}_t - \dot{\mathbf{x}} \cdot \frac{1}{\sqrt{|\mathbf{g}|}} \partial_i [\sqrt{|\mathbf{g}|} \mathbf{e}^i \mathbf{d}] + \frac{1}{\sqrt{|\mathbf{g}|}} \partial_i [\sqrt{|\mathbf{g}|} \mathbf{u} \cdot \mathbf{e}^i \mathbf{d}]. \quad (6.12)$$

Since we deal with non-steady coordinates both the base vectors and the metric are functions of time. We resort to an identity from tensor analysis for the metric tensor to consider the temporal derivative of  $\sqrt{|\mathbf{g}|}$

$$\begin{aligned} \partial_t \sqrt{|\mathbf{g}|} &= \partial_t [\mathbf{e}_1 \cdot (\mathbf{e}_2 \times \mathbf{e}_3)] \\ &= \partial_t \mathbf{e}_1 \cdot (\mathbf{e}_2 \times \mathbf{e}_3) + \partial_t \mathbf{e}_2 \cdot (\mathbf{e}_3 \times \mathbf{e}_1) + \dots \\ &= \sqrt{|\mathbf{g}|} \partial_t \mathbf{e}_i \cdot \mathbf{e}^i \end{aligned} \quad (6.13)$$

using  $\mathbf{e}^i = |\mathbf{g}|^{-1/2} (\mathbf{e}_j \times \mathbf{e}_k)$ . Moreover, we remember the definition of the covariant base vector

$$\mathbf{e}_{(\alpha)i} = \frac{\partial \mathbf{x}}{\partial x^i_{(\alpha)}} \quad (6.14)$$

which leads to an interesting conclusion for non-steady coordinates respectively adaptive grids.

$$\partial_t \sqrt{|\mathbf{g}|} = \sqrt{|\mathbf{g}|} \partial_i \dot{\mathbf{x}} \cdot \mathbf{e}^i \quad (6.15)$$

The variation of the volume element in time hence is connected with the derivatives of the grid velocity in all directions. Again we mention that even for solely radially adaptive grids the term  $\dot{\mathbf{x}}$  contains angular contributions, to wit  $\dot{\mathbf{x}} \neq \dot{r}$ .

We consider following expression in order to asses the temporal change of a *geometrically weighted* in comparison to a plain density function  $\mathbf{d}$

$$\begin{aligned} \frac{1}{\sqrt{|\mathbf{g}|}} \partial_t [\sqrt{|\mathbf{g}|} \mathbf{d}] &= \frac{1}{\sqrt{|\mathbf{g}|}} [\partial_t \sqrt{|\mathbf{g}|} \mathbf{d} + \sqrt{|\mathbf{g}|} \partial_t \mathbf{d}] \\ &= \frac{1}{\sqrt{|\mathbf{g}|}} [\sqrt{|\mathbf{g}|} \partial_i \dot{\mathbf{x}} \cdot \mathbf{e}^i \mathbf{d} + \sqrt{|\mathbf{g}|} \partial_t \mathbf{d}] \end{aligned}$$

and obtain

$$\partial_t \mathbf{d} = \frac{1}{\sqrt{|\mathbf{g}|}} \partial_t [\sqrt{|\mathbf{g}|} \mathbf{d}] - \partial_i \dot{\mathbf{x}} \cdot \mathbf{e}^i \mathbf{d}. \quad (6.16)$$

We compare that result with our convection term (6.12) to gain the strong conservation

form of the advection term in non-steady coordinates.

$$\begin{aligned}
K &= \frac{1}{\sqrt{|\mathbf{g}|}} \partial_t [\sqrt{|\mathbf{g}|} \mathbf{d}] - \partial_i \dot{\mathbf{x}} \cdot \mathbf{e}^i \mathbf{d} - \dot{\mathbf{x}} \cdot \frac{1}{\sqrt{|\mathbf{g}|}} \partial_i [\sqrt{|\mathbf{g}|} \mathbf{e}^i \mathbf{d}] + \frac{1}{\sqrt{|\mathbf{g}|}} \partial_i [\sqrt{|\mathbf{g}|} \mathbf{u} \cdot \mathbf{e}^i \mathbf{d}] \\
&= \frac{1}{\sqrt{|\mathbf{g}|}} \partial_t [\sqrt{|\mathbf{g}|} \mathbf{d}] - \frac{1}{\sqrt{|\mathbf{g}|}} \partial_i [\sqrt{|\mathbf{g}|} \dot{\mathbf{x}} \cdot \mathbf{e}^i \mathbf{d}] + \frac{1}{\sqrt{|\mathbf{g}|}} \partial_i [\sqrt{|\mathbf{g}|} \mathbf{u} \cdot \mathbf{e}^i \mathbf{d}] \\
\sqrt{|\mathbf{g}|} K &= \partial_t [\sqrt{|\mathbf{g}|} \mathbf{d}] + \partial_i [\sqrt{|\mathbf{g}|} \mathbf{e}^i \cdot (\mathbf{u} - \dot{\mathbf{x}}) \mathbf{d}]
\end{aligned} \tag{6.17}$$

If we define the contravariant velocity components relative to the moving grid by

$$U^i \equiv \mathbf{e}^i \cdot (\mathbf{u} - \dot{\mathbf{x}})$$

the upper equations yields

$$\sqrt{|\mathbf{g}|} K = \partial_t [\sqrt{|\mathbf{g}|} \mathbf{d}] + \partial_i [\sqrt{|\mathbf{g}|} U^i \mathbf{d}]. \tag{6.18}$$

## 6.2 Mathematica Files

On the following pages some examples of **Mathematica Notebooks** are presented that were used for tensor analytical computations in several coordinates and generation of strong conservation form equations. The analysis of the grid generation toy models presented in sections 4.4 and 4.6 conclude the Appendix.

Technical remark: in order to ensure that *integral* respectively conserved quantities are not divided automatically by the computer algebra system, we make use of **Patterns**. In this sense the partial derivatives act on braced expressions like  $\partial_i [\dots]$  that would be processed for the discretization.

**Spherical Coordinates** (`spherical_coordinates.nb`) Differential geometric definitions and relations for base vectors, metric components and Christoffel symbols, exemplarily executed with spherical coordinates. If the initial definition of the coordinate transformation gets modified to a nonorthogonal coordinate system, minor changes have to be made.

**Artificial Viscosity in Spherical Coordinates** (`artificial_viscosity.nb`) Using results from `spherical_coordinates.nb` we compute co- and contravariant components of the viscous pressure tensor in spherical coordinates. Symmetry of  $\mathbf{Q}$  and vanishing trace are evaluated explicitly.

**Equation of Motion in Spherical Coordinates** (`EOM_3D_sph.nb`) Using the previous definitions for geometric quantities and the viscous pressure we generate the equation of motion in spherical coordinates in strong conservation form for non-steady grids.

**Polynomial Coordinates Ansatz** (`poly_coordinates.nb`) Graphical analysis of a polynomial ansatz for orthogonal family of curves.

**Polar Non-Orthogonal Grid Ansatz** (`quasi_polar_grid.nb`) Generation of a non-orthogonal grid that in principle satisfies all postulations from 4.2 besides orthogonality. With the coordinate transformation determined one could go run through upper files and generate strong conservation form equations on non-steady non-orthogonal grids.

# Spherical Coordinates

## Differential Geometric Definitions and Relations

### ■ Coordinate Transformation

```
In[1]:= x := r Sin[theta] Cos[phi]
        y := r Sin[theta] Sin[phi]
        z := r Cos[theta]
```

```
In[4]:= lij = {{D[x, r], D[x, theta], D[x, phi]}, {D[y, r], D[y, theta], D[y, phi]},
              {D[z, r], D[z, theta], D[z, phi]}}; (* Jacobian of transformation *)
```

```
In[5]:= lijtransposed := Transpose[lij]
```

### ■ Covariant Components of Metric Tensor

```
In[6]:= gij = lijtransposed.lij // FullSimplify (* from gij=ei.ej *)
```

```
Out[6]:= {{1, 0, 0}, {0, r2, 0}, {0, 0, r2 Sin[theta]2}}
```

```
In[7]:= g = Det[gij]
```

```
Out[7]:= r4 Sin[theta]2
```

```
In[8]:= rootg = Assuming[{r > 0, Sin[theta] > 0}, Refine[Sqrt[g]]]
```

```
Out[8]:= r2 Sin[theta]
```

### ■ Covariant Base Vectors

```
In[9]:= er = lijtransposed[[1]] (* #-st row of Jacobian defines the #-st covariant base vector *)
```

```
Out[9]:= {Cos[phi] Sin[theta], Sin[phi] Sin[theta], Cos[theta]}
```

```
In[10]:= etheta = lijtransposed[[2]]
```

```
Out[10]:= {r Cos[phi] Cos[theta], r Cos[theta] Sin[phi], -r Sin[theta]}
```

```
In[11]:= ephi = lijtransposed[[3]]
```

```
Out[11]:= {-r Sin[phi] Sin[theta], r Cos[phi] Sin[theta], 0}
```

### ■ Contravariant Base Vectors

```
In[12]:= Er = 1 / rootg * Cross[etheta, ephi] // FullSimplify
        (* this identity is only satisfied for orthogonal coordinates;
           for nonorthogonal coordinats one needs to raise indices gijej *)
```

```
Out[12]:= {Cos[phi] Sin[theta], Sin[phi] Sin[theta], Cos[theta]}
```

```
In[13]:= E_theta = 1 / rootg * Cross[e_phi, e_r] // FullSimplify
```

$$\text{Out[13]= } \left\{ \frac{\cos[\phi] \cos[\theta]}{r}, \frac{\cos[\theta] \sin[\phi]}{r}, -\frac{\sin[\theta]}{r} \right\}$$

```
In[14]:= E_phi = 1 / rootg * Cross[e_r, e_theta] // FullSimplify
```

$$\text{Out[14]= } \left\{ -\frac{\csc[\theta] \sin[\phi]}{r}, \frac{\cos[\phi] \csc[\theta]}{r}, 0 \right\}$$

### ■ Covariant, Mixed and Contravariant Components of the Metric Tensor

```
In[15]:= Table[metricg[i, j] = e_i.e_j // FullSimplify, {i, {r, theta, phi}}, {j, {r, theta, phi}}]
```

$$\text{Out[15]= } \left\{ \{1, 0, 0\}, \{0, r^2, 0\}, \{0, 0, r^2 \sin^2[\theta]\} \right\}$$

```
In[16]:= Table[Metricg[i, j] = E_i.E_j // FullSimplify, {i, {r, theta, phi}}, {j, {r, theta, phi}}]
```

$$\text{Out[16]= } \left\{ \{1, 0, 0\}, \left\{0, \frac{1}{r^2}, 0\right\}, \left\{0, 0, \frac{\csc^2[\theta]}{r^2}\right\} \right\}$$

```
In[17]:= Table[delta[i, j] = E_i.e_j // FullSimplify, {i, {r, theta, phi}}, {j, {r, theta, phi}}]
```

$$\text{Out[17]= } \left\{ \{1, 0, 0\}, \{0, 1, 0\}, \{0, 0, 1\} \right\}$$

### ■ Christoffel Symbols

```
In[18]:= Table[Table[Table[Gammer[sigma, mu, nu] =
  1 / 2 * Sum[(E_sigma.E_rho) * (D[(e_nu.e_rho), mu] + D[(e_mu.e_rho), nu] - D[(e_mu.e_nu), rho]),
    {rho, {r, theta, phi}}] // FullSimplify,
  {sigma, {r, theta, phi}}], {mu, {r, theta, phi}}], {nu, {r, theta, phi}}]
```

$$\text{Out[18]= } \left\{ \left\{ \{0, 0, 0\}, \left\{0, \frac{1}{r}, 0\right\}, \left\{0, 0, \frac{1}{r}\right\} \right\}, \left\{ \left\{0, \frac{1}{r}, 0\right\}, \{-r, 0, 0\}, \{0, 0, \cot[\theta]\} \right\}, \right. \\ \left. \left\{ \left\{0, 0, \frac{1}{r}\right\}, \{0, 0, \cot[\theta]\}, \{-r \sin^2[\theta], -\cos[\theta] \sin[\theta], 0\} \right\} \right\}$$

# Artificial Viscosity

## Viscous Pressure Tensor

### ■ Definitions of Viscous Pressure

In order to proof consistency of our modified artificial viscosity we use different definitions and relations.

```
In[19]:= Table[
  qschlange[i, j] =
    1 / 2 * (d[i][u[j]] + d[j][u[i]] - Sum[Gammer[k, i, j] * u[k], {k, {r, theta, phi}}] -
      Sum[Gammer[k, j, i] * u[k], {k, {r, theta, phi}}]) - 1 / 3 * metricg[i, j] * div[u],
  {i, {r, theta, phi}}, {j, {r, theta, phi}}]; (* covariant componentes *)

In[20]:= Table[qschlangeoben[m, n] = Sum[(Metricg[m, k] * Metricg[n, l]) *
  (1 / 2 * (d[k][u[l]] + d[l][u[k]] - Sum[Gammer[o, k, l] * u[o], {o, {r, theta, phi}}] -
    Sum[Gammer[o, l, k] * u[o], {o, {r, theta, phi}}]) -
  1 / 3 * metricg[m, n] * div[u]), {k, {r, theta, phi}}, {l, {r, theta, phi}}],
  {m, {r, theta, phi}}, {n, {r, theta, phi}}]; (* contravariant components *)

In[21]:= Table[
  qoben[m, n] = Sum[(Metricg[m, i] * Metricg[n, j]) qschlange[i, j],
  {i, {r, theta, phi}}, {j, {r, theta, phi}}],
  {m, {r, theta, phi}}, {n, {r, theta, phi}}]; (* contravariant components *)

In[22]:= Table[
  qmix[i, j] = Sum[Metricg[l, i] * qschlange[l, j], {l, {r, theta, phi}}],
  {i, {r, theta, phi}}, {j, {r, theta, phi}}]; (* mixed components *)

In[23]:= Table[
  qmix2[i, n] = Sum[metricg[j, n] * qschlangeoben[i, j], {j, {r, theta, phi}}],
  {i, {r, theta, phi}}, {n, {r, theta, phi}}]; (* mixed components *)
```

## ■ Components Explicitly

```
In[24]:= Table[qmix[m, n], {m, {r, theta, phi}}, {n, {r, theta, phi}} // FullSimplify // Expand
```

$$\text{Out[24]= } \left\{ \left\{ -\frac{\text{div}[u]}{3} + d[r][u[r]], -\frac{u[\text{theta}]}{r} + \frac{1}{2} d[r][u[\text{theta}]] + \frac{1}{2} d[\text{theta}][u[r]], \right. \right.$$

$$\left. -\frac{u[\text{phi}]}{r} + \frac{1}{2} d[\text{phi}][u[r]] + \frac{1}{2} d[r][u[\text{phi}]] \right\},$$

$$\left\{ -\frac{u[\text{theta}]}{r^3} + \frac{d[r][u[\text{theta}]]}{2 r^2} + \frac{d[\text{theta}][u[r]]}{2 r^2}, -\frac{\text{div}[u]}{3} + \frac{u[r]}{r} + \frac{d[\text{theta}][u[\text{theta}]]}{r^2}, \right.$$

$$\left. -\frac{\text{Cot}[\text{theta}] u[\text{phi}]}{r^2} + \frac{d[\text{phi}][u[\text{theta}]]}{2 r^2} + \frac{d[\text{theta}][u[\text{phi}]]}{2 r^2} \right\},$$

$$\left\{ -\frac{\text{Csc}[\text{theta}]^2 u[\text{phi}]}{r^3} + \frac{\text{Csc}[\text{theta}]^2 d[\text{phi}][u[r]]}{2 r^2} + \frac{\text{Csc}[\text{theta}]^2 d[r][u[\text{phi}]]}{2 r^2}, \right.$$

$$\left. -\frac{\text{Cot}[\text{theta}] \text{Csc}[\text{theta}]^2 u[\text{phi}]}{r^2} + \right.$$

$$\left. \frac{\text{Csc}[\text{theta}]^2 d[\text{phi}][u[\text{theta}]]}{2 r^2} + \frac{\text{Csc}[\text{theta}]^2 d[\text{theta}][u[\text{phi}]]}{2 r^2}, \right.$$

$$\left. -\frac{\text{div}[u]}{3} + \frac{u[r]}{r} + \frac{\text{Cot}[\text{theta}] u[\text{theta}]}{r^2} + \frac{\text{Csc}[\text{theta}]^2 d[\text{phi}][u[\text{phi}]]}{r^2} \right\}$$

```
In[25]:= Do[Print[Q[m, n], " = ", qschlange[m, n] // FullSimplify // Expand],
  {m, {r, theta, phi}}, {n, {r, theta, phi}}
```

$$Q[r, r] = -\frac{\text{div}[u]}{3} + d[r][u[r]]$$

$$Q[r, \text{theta}] = -\frac{u[\text{theta}]}{r} + \frac{1}{2} d[r][u[\text{theta}]] + \frac{1}{2} d[\text{theta}][u[r]]$$

$$Q[r, \text{phi}] = -\frac{u[\text{phi}]}{r} + \frac{1}{2} d[\text{phi}][u[r]] + \frac{1}{2} d[r][u[\text{phi}]]$$

$$Q[\text{theta}, r] = -\frac{u[\text{theta}]}{r} + \frac{1}{2} d[r][u[\text{theta}]] + \frac{1}{2} d[\text{theta}][u[r]]$$

$$Q[\text{theta}, \text{theta}] = -\frac{1}{3} r^2 \text{div}[u] + r u[r] + d[\text{theta}][u[\text{theta}]]$$

$$Q[\text{theta}, \text{phi}] = -\text{Cot}[\text{theta}] u[\text{phi}] + \frac{1}{2} d[\text{phi}][u[\text{theta}]] + \frac{1}{2} d[\text{theta}][u[\text{phi}]]$$

$$Q[\text{phi}, r] = -\frac{u[\text{phi}]}{r} + \frac{1}{2} d[\text{phi}][u[r]] + \frac{1}{2} d[r][u[\text{phi}]]$$

$$Q[\text{phi}, \text{theta}] = -\text{Cot}[\text{theta}] u[\text{phi}] + \frac{1}{2} d[\text{phi}][u[\text{theta}]] + \frac{1}{2} d[\text{theta}][u[\text{phi}]]$$

$$Q[\text{phi}, \text{phi}] =$$

$$-\frac{1}{3} r^2 \text{div}[u] \text{Sin}[\text{theta}]^2 + r \text{Sin}[\text{theta}]^2 u[r] + \text{Cos}[\text{theta}] \text{Sin}[\text{theta}] u[\text{theta}] + d[\text{phi}][u[\text{phi}]]$$

```
In[26]:= Do[Print[Qcontra[m, n], " = ", qschlangeoben[m, n] // FullSimplify // Expand],
  {m, {r, theta, phi}}, {n, {r, theta, phi}}
```



$$\begin{aligned}
Q_{\text{contra}}[r, r] &= -\frac{\text{div}[u]}{3} + d[r][u[r]] \\
Q_{\text{contra}}[r, \text{theta}] &= -\frac{u[\text{theta}]}{r^3} + \frac{d[r][u[\text{theta}]]}{2 r^2} + \frac{d[\text{theta}][u[r]]}{2 r^2} \\
Q_{\text{contra}}[r, \text{phi}] &= -\frac{\text{Csc}[\text{theta}]^2 u[\text{phi}]}{r^3} + \frac{\text{Csc}[\text{theta}]^2 d[\text{phi}][u[r]]}{2 r^2} + \frac{\text{Csc}[\text{theta}]^2 d[r][u[\text{phi}]]}{2 r^2} \\
Q_{\text{contra}}[\text{theta}, r] &= -\frac{u[\text{theta}]}{r^3} + \frac{d[r][u[\text{theta}]]}{2 r^2} + \frac{d[\text{theta}][u[r]]}{2 r^2} \\
Q_{\text{contra}}[\text{theta}, \text{theta}] &= -\frac{\text{div}[u]}{3 r^2} + \frac{u[r]}{r^3} + \frac{d[\text{theta}][u[\text{theta}]]}{r^4} \\
Q_{\text{contra}}[\text{theta}, \text{phi}] &= \\
& -\frac{\text{Cot}[\text{theta}] \text{Csc}[\text{theta}]^2 u[\text{phi}]}{r^4} + \frac{\text{Csc}[\text{theta}]^2 d[\text{phi}][u[\text{theta}]]}{2 r^4} + \frac{\text{Csc}[\text{theta}]^2 d[\text{theta}][u[\text{phi}]]}{2 r^4} \\
Q_{\text{contra}}[\text{phi}, r] &= -\frac{\text{Csc}[\text{theta}]^2 u[\text{phi}]}{r^3} + \frac{\text{Csc}[\text{theta}]^2 d[\text{phi}][u[r]]}{2 r^2} + \frac{\text{Csc}[\text{theta}]^2 d[r][u[\text{phi}]]}{2 r^2} \\
Q_{\text{contra}}[\text{phi}, \text{theta}] &= \\
& -\frac{\text{Cot}[\text{theta}] \text{Csc}[\text{theta}]^2 u[\text{phi}]}{r^4} + \frac{\text{Csc}[\text{theta}]^2 d[\text{phi}][u[\text{theta}]]}{2 r^4} + \frac{\text{Csc}[\text{theta}]^2 d[\text{theta}][u[\text{phi}]]}{2 r^4} \\
Q_{\text{contra}}[\text{phi}, \text{phi}] &= -\frac{\text{Csc}[\text{theta}]^2 \text{div}[u]}{3 r^2} + \frac{\text{Csc}[\text{theta}]^2 u[r]}{r^3} + \\
& \frac{\text{Cot}[\text{theta}] \text{Csc}[\text{theta}]^2 u[\text{theta}]}{r^4} + \frac{\text{Csc}[\text{theta}]^4 d[\text{phi}][u[\text{phi}]]}{r^4}
\end{aligned}$$

### ■ Symmetry

In fact Q is symmetric in its co- and contravariant components.

```
In[27]= Table[qschlangeoben[m, n] === qschlangeoben[n, m], {m, {r, theta, phi}}, {n, {r, theta, phi}}]
```

```
Out[27]= {{True, True, True}, {True, True, True}, {True, True, True}}
```

```
In[28]= Table[qschlange[m, n] === qschlange[n, m], {m, {r, theta, phi}}, {n, {r, theta, phi}}]
```

```
Out[28]= {{True, True, True}, {True, True, True}, {True, True, True}}
```

```
In[29]= Table[qmix[m, n] === qmix[n, m], {m, {r, theta, phi}}, {n, {r, theta, phi}}]
```

```
Out[29]= {{True, False, False}, {False, True, False}, {False, False, True}}
```

### ■ Trace of Q

The trace vanishes as expected.

In[30]= `Sum[qmix[m, m], {m, {r, theta, phi}}`

$$\text{Out[30]= } -\frac{\text{div}[u]}{3} + \frac{1}{r^2} \text{Csc}[\text{theta}]^2 \left( -\frac{1}{3} r^2 \text{div}[u] \text{Sin}[\text{theta}]^2 + \frac{1}{2} (2 r \text{Sin}[\text{theta}]^2 u[r] + 2 \text{Cos}[\text{theta}] \text{Sin}[\text{theta}] u[\text{theta}] + 2 \text{d}[\text{phi}][u[\text{phi}]]) \right) + \frac{\text{d}[r][u[r]] + \frac{-\frac{1}{3} r^2 \text{div}[u] + \frac{1}{2} (2 r u[r] + 2 \text{d}[\text{theta}][u[\text{theta}]])}{r^2}}$$

In[31]= `Sum[qmix[m, m], {m, {r, theta, phi}}] /.`

$$\left\{ \text{div}[u] \rightarrow \frac{2 u[r]}{r} + \frac{\text{Cot}[\text{theta}] u[\text{theta}]}{r^2} + \frac{\text{Csc}[\text{theta}]^2 \text{d}[\text{phi}][u[\text{phi}]]}{r^2} + \text{d}[r][u[r]] + \frac{\text{d}[\text{theta}][u[\text{theta}]]}{r^2} \right\} // \text{FullSimplify} // \text{Expand}$$

Out[31]= 0

In[32]= `Sum[qmix2[m, m], {m, {r, theta, phi}}] /.`

$$\left\{ \text{div}[u] \rightarrow \frac{2 u[r]}{r} + \frac{\text{Cot}[\text{theta}] u[\text{theta}]}{r^2} + \frac{\text{Csc}[\text{theta}]^2 \text{d}[\text{phi}][u[\text{phi}]]}{r^2} + \text{d}[r][u[r]] + \frac{\text{d}[\text{theta}][u[\text{theta}]]}{r^2} \right\} // \text{FullSimplify} // \text{Expand}$$

Out[32]= 0

# Equation of Motion in Spherical Coordinates

## Generation of Strong Conservation Form Equation

### ■ Definition of Contravariant Components of Tensors

```

Table[rschlange[i, j] = rho * (u[i] - xdot[i]) * u[j] // FullSimplify,
      {i, {r, theta, phi}}, {j, {r, theta, phi}}]
Table[p[i, j] = p * Metricg[i, j] // FullSimplify, {i, {r, theta, phi}}, {j, {r, theta, phi}}]
Table[q[i, j] = Sum[(Metricg[i, m] * Metricg[j, n])
                    (1/2 * (d[n][u[m]] + d[n][u[m]] - Sum[Gammer[k, m, m] * u[k], {k, {r, theta, phi}}] -
                      Sum[Gammer[k, m, n] * u[k], {k, {r, theta, phi}}]) - 1/3 * metricg[n, m] * div[u]),
                    {n, {r, theta, phi}}, {m, {r, theta, phi}}] // FullSimplify,
      {i, {r, theta, phi}}, {j, {r, theta, phi}}]
(* note that there emerge covariant velocity components in Q due to its definition *)

```

```

Out[33]= {{rho u[r] (u[r] - xdot[r]), rho u[theta] (u[r] - xdot[r]), rho u[phi] (u[r] - xdot[r]),
          {rho u[r] (u[theta] - xdot[theta]), rho u[theta] (u[theta] - xdot[theta]),
          rho u[phi] (u[theta] - xdot[theta])}, {rho u[r] (u[phi] - xdot[phi]),
          rho u[theta] (u[phi] - xdot[phi]), rho u[phi] (u[phi] - xdot[phi])}}

```

```

Out[34]= {{p, 0, 0}, {0, p/r^2, 0}, {0, 0, p Csc[theta]^2/r^2}}

```

```

Out[35]= {{-div[u]/3 + d[r][u[r]],
          -u[theta]/(2 r^3) - 2 r d[theta][u[r]], -Csc[theta]^2 (u[phi] - 2 r d[phi][u[r]])/(2 r^3)},
          {r^2 u[r] - u[theta] + 2 r d[r][u[theta]], -r^2 div[u] + 3 (r u[r] + d[theta][u[theta]])/(2 r^3),
          Csc[theta]^2 (-Cot[theta] u[phi] + r u[r] + 2 d[phi][u[theta]])/(2 r^4)},
          {r^2 u[r] + r Cot[theta] u[theta] - Csc[theta]^2 (u[phi] - 2 r d[r][u[phi]])/(2 r^3),
          -Cot[theta] Csc[theta]^2 u[phi] + r u[r] + Cot[theta] u[theta] + 2 Csc[theta]^2 d[theta][u[phi]]/(2 r^4),
          Csc[theta]^2 (-r^2 div[u] + 3 (r u[r] + Cot[theta] u[theta] + Csc[theta]^2 d[phi][u[phi]]))/(3 r^4)}}

```

### ■ Equation of Motion in Spherical Coordinates and Strong Conservation Form

```

In[36]= Table[d[t][Sum[Sqrt[g] * rho * u[n] * e_n[[k]], {n, {r, theta, phi}}] + Sum[
          Sum[d[i][Sqrt[g] * (rschlange[i, j] + p[i, j] + Qkomp[i, j]) * e_j[[k]]], {i, {r, theta, phi}},
          {j, {r, theta, phi}}] + rho * Sum[d[l][Sqrt[g] * Phi * E_l[[k]]], {l, {r, theta, phi}}] -
          4 Pi / c * Sqrt[g] * (Sum[H[o] * e_o[[k]], {o, {r, theta, phi}}]) /
          {Sin[theta] -> Sqrt[1 - mu^2], d[theta] -> -Sqrt[1 - mu^2] d[mu],
          Csc[theta] -> 1 / Sqrt[1 - mu^2], Cos[theta] -> mu}, {k, {1, 2, 3}}]

```

$$\begin{aligned}
\text{Out[36]} = & \left\{ - \frac{4 \pi \sqrt{(1 - \mu^2) r^4} \left( \sqrt{1 - \mu^2} \cos[\phi] H[r] + \mu r \cos[\phi] H[\theta] - \sqrt{1 - \mu^2} r H[\phi] \sin[\phi] \right)}{c} + \right. \\
& \left( -\sqrt{1 - \mu^2} d[\mu] \right) \left[ -\sqrt{1 - \mu^2} r \sqrt{(1 - \mu^2) r^4} \sin[\phi] \right. \\
& \quad \left. \left( Q_{\text{komp}}[\theta, \phi] + \rho u[\phi] (u[\theta] - \dot{x}[\theta]) \right) \right] + \left( -\sqrt{1 - \mu^2} d[\mu] \right) \left[ \right. \\
& \quad \left. \sqrt{1 - \mu^2} \sqrt{(1 - \mu^2) r^4} \cos[\phi] \left( Q_{\text{komp}}[\theta, r] + \rho u[r] (u[\theta] - \dot{x}[\theta]) \right) \right] + \\
& \left( -\sqrt{1 - \mu^2} d[\mu] \right) \left[ \mu r \sqrt{(1 - \mu^2) r^4} \cos[\phi] \right. \\
& \quad \left. \left( \frac{p}{r^2} + Q_{\text{komp}}[\theta, \theta] + \rho u[\theta] (u[\theta] - \dot{x}[\theta]) \right) \right] + d[\phi] \left[ -\sqrt{1 - \mu^2} r \right. \\
& \quad \left. \sqrt{(1 - \mu^2) r^4} \sin[\phi] \left( \frac{p}{(1 - \mu^2) r^2} + Q_{\text{komp}}[\phi, \phi] + \rho u[\phi] (u[\phi] - \dot{x}[\phi]) \right) \right] \right] + \\
& d[\phi] \left[ \sqrt{1 - \mu^2} \sqrt{(1 - \mu^2) r^4} \cos[\phi] \left( Q_{\text{komp}}[\phi, r] + \rho u[r] (u[\phi] - \dot{x}[\phi]) \right) \right] + \\
& d[\phi] \left[ \mu r \sqrt{(1 - \mu^2) r^4} \cos[\phi] \left( Q_{\text{komp}}[\phi, \theta] + \rho u[\theta] (u[\phi] - \dot{x}[\phi]) \right) \right] + \\
& \rho \left( \left( -\sqrt{1 - \mu^2} d[\mu] \right) \left[ \frac{\mu \phi \sqrt{(1 - \mu^2) r^4} \cos[\phi]}{r} \right] + \right. \\
& \quad \left. d[\phi] \left[ -\frac{\phi \sqrt{(1 - \mu^2) r^4} \sin[\phi]}{\sqrt{1 - \mu^2} r} \right] + d[r] \left[ \sqrt{1 - \mu^2} \phi \sqrt{(1 - \mu^2) r^4} \cos[\phi] \right] \right) \right] + \\
& d[r] \left[ -\sqrt{1 - \mu^2} r \sqrt{(1 - \mu^2) r^4} \sin[\phi] \left( Q_{\text{komp}}[r, \phi] + \rho u[\phi] (u[r] - \dot{x}[r]) \right) \right] + \\
& d[r] \left[ \sqrt{1 - \mu^2} \sqrt{(1 - \mu^2) r^4} \cos[\phi] \left( p + Q_{\text{komp}}[r, r] + \rho u[r] (u[r] - \dot{x}[r]) \right) \right] + \\
& d[r] \left[ \mu r \sqrt{(1 - \mu^2) r^4} \cos[\phi] \left( Q_{\text{komp}}[r, \theta] + \rho u[\theta] (u[r] - \dot{x}[r]) \right) \right] + \\
& d[t] \left[ -\sqrt{1 - \mu^2} r \sqrt{(1 - \mu^2) r^4} \rho \sin[\phi] u[\phi] + \right. \\
& \quad \left. \sqrt{1 - \mu^2} \sqrt{(1 - \mu^2) r^4} \rho \cos[\phi] u[r] + \mu r \sqrt{(1 - \mu^2) r^4} \rho \cos[\phi] u[\theta] \right], \\
& \left. \frac{4 \pi \sqrt{(1 - \mu^2) r^4} \left( \sqrt{1 - \mu^2} r \cos[\phi] H[\phi] + \sqrt{1 - \mu^2} H[r] \sin[\phi] + \mu r H[\theta] \sin[\phi] \right)}{c} + \right. \\
& \left. \left( -\sqrt{1 - \mu^2} d[\mu] \right) \left[ \sqrt{1 - \mu^2} r \sqrt{(1 - \mu^2) r^4} \cos[\phi] \right] \right\}
\end{aligned}$$

$$\begin{aligned}
& \left( Q_{\text{komp}}[\text{theta}, \text{phi}] + \rho u[\text{phi}] (u[\text{theta}] - \text{xdot}[\text{theta}]) \right) + \left( -\sqrt{1 - \mu^2} d[\mu] \right) \left[ \right. \\
& \sqrt{1 - \mu^2} \sqrt{(1 - \mu^2) r^4} \text{Sin}[\text{phi}] \left( Q_{\text{komp}}[\text{theta}, r] + \rho u[r] (u[\text{theta}] - \text{xdot}[\text{theta}]) \right) \left. \right] + \\
& \left( -\sqrt{1 - \mu^2} d[\mu] \right) \left[ \mu r \sqrt{(1 - \mu^2) r^4} \text{Sin}[\text{phi}] \right. \\
& \left. \left( \frac{p}{r^2} + Q_{\text{komp}}[\text{theta}, \text{theta}] + \rho u[\text{theta}] (u[\text{theta}] - \text{xdot}[\text{theta}]) \right) \right] + d[\text{phi}] \left[ \sqrt{1 - \mu^2} r \right. \\
& \left. \sqrt{(1 - \mu^2) r^4} \text{Cos}[\text{phi}] \left( \frac{p}{(1 - \mu^2) r^2} + Q_{\text{komp}}[\text{phi}, \text{phi}] + \rho u[\text{phi}] (u[\text{phi}] - \text{xdot}[\text{phi}]) \right) \right] + \\
& d[\text{phi}] \left[ \sqrt{1 - \mu^2} \sqrt{(1 - \mu^2) r^4} \text{Sin}[\text{phi}] \left( Q_{\text{komp}}[\text{phi}, r] + \rho u[r] (u[\text{phi}] - \text{xdot}[\text{phi}]) \right) \right] + \\
& d[\text{phi}] \left[ \mu r \sqrt{(1 - \mu^2) r^4} \text{Sin}[\text{phi}] \left( Q_{\text{komp}}[\text{phi}, \text{theta}] + \rho u[\text{theta}] (u[\text{phi}] - \text{xdot}[\text{phi}]) \right) \right] + \\
& \rho \left( \left( -\sqrt{1 - \mu^2} d[\mu] \right) \left[ \frac{\mu \text{Phi} \sqrt{(1 - \mu^2) r^4} \text{Sin}[\text{phi}]}{r} \right] + \right. \\
& \left. d[\text{phi}] \left[ \frac{\text{Phi} \sqrt{(1 - \mu^2) r^4} \text{Cos}[\text{phi}]}{\sqrt{1 - \mu^2} r} \right] + d[r] \left[ \sqrt{1 - \mu^2} \text{Phi} \sqrt{(1 - \mu^2) r^4} \text{Sin}[\text{phi}] \right] \right) + \\
& d[r] \left[ \sqrt{1 - \mu^2} r \sqrt{(1 - \mu^2) r^4} \text{Cos}[\text{phi}] \left( Q_{\text{komp}}[r, \text{phi}] + \rho u[\text{phi}] (u[r] - \text{xdot}[r]) \right) \right] + \\
& d[r] \left[ \sqrt{1 - \mu^2} \sqrt{(1 - \mu^2) r^4} \text{Sin}[\text{phi}] \left( p + Q_{\text{komp}}[r, r] + \rho u[r] (u[r] - \text{xdot}[r]) \right) \right] + \\
& d[r] \left[ \mu r \sqrt{(1 - \mu^2) r^4} \text{Sin}[\text{phi}] \left( Q_{\text{komp}}[r, \text{theta}] + \rho u[\text{theta}] (u[r] - \text{xdot}[r]) \right) \right] + \\
& d[t] \left[ \sqrt{1 - \mu^2} r \sqrt{(1 - \mu^2) r^4} \rho \text{Cos}[\text{phi}] u[\text{phi}] + \right. \\
& \left. \sqrt{1 - \mu^2} \sqrt{(1 - \mu^2) r^4} \rho \text{Sin}[\text{phi}] u[r] + \mu r \sqrt{(1 - \mu^2) r^4} \rho \text{Sin}[\text{phi}] u[\text{theta}] \right], \\
& \frac{4 \pi \sqrt{(1 - \mu^2) r^4} \left( \mu H[r] - \sqrt{1 - \mu^2} r H[\text{theta}] \right)}{c} + \left( -\sqrt{1 - \mu^2} d[\mu] \right) [0] + \\
& \left( -\sqrt{1 - \mu^2} d[\mu] \right) \left[ \mu \sqrt{(1 - \mu^2) r^4} \left( Q_{\text{komp}}[\text{theta}, r] + \rho u[r] (u[\text{theta}] - \text{xdot}[\text{theta}]) \right) \right] + \\
& \left( -\sqrt{1 - \mu^2} d[\mu] \right) \left[ \right. \\
& \left. -\sqrt{1 - \mu^2} r \sqrt{(1 - \mu^2) r^4} \left( \frac{p}{r^2} + Q_{\text{komp}}[\text{theta}, \text{theta}] + \rho u[\text{theta}] (u[\text{theta}] - \text{xdot}[\text{theta}]) \right) \right] + \\
& d[\text{phi}] [0] + d[\text{phi}] \left[ \mu \sqrt{(1 - \mu^2) r^4} \left( Q_{\text{komp}}[\text{phi}, r] + \rho u[r] (u[\text{phi}] - \text{xdot}[\text{phi}]) \right) \right] + d[\text{phi}] \left[ \right.
\end{aligned}$$

$$\begin{aligned}
& -\sqrt{1-\mu^2} r \sqrt{(1-\mu^2) r^4} (Q_{\text{komp}}[\text{phi}, \text{theta}] + \rho u[\text{theta}] (u[\text{phi}] - \dot{x}[\text{phi}])) + d[r][0] + \\
& \rho \left( \left( -\sqrt{1-\mu^2} d[\mu] \right) \left[ -\frac{\sqrt{1-\mu^2} \text{Phi} \sqrt{(1-\mu^2) r^4}}{r} \right] + d[\text{phi}][0] + d[r] \left[ \mu \text{Phi} \sqrt{(1-\mu^2) r^4} \right] \right) + \\
& d[r] \left[ \mu \sqrt{(1-\mu^2) r^4} (p + Q_{\text{komp}}[r, r] + \rho u[r] (u[r] - \dot{x}[r])) \right] + \\
& d[r] \left[ -\sqrt{1-\mu^2} r \sqrt{(1-\mu^2) r^4} (Q_{\text{komp}}[r, \text{theta}] + \rho u[\text{theta}] (u[r] - \dot{x}[r])) \right] + \\
& d[t] \left[ \mu \sqrt{(1-\mu^2) r^4} \rho u[r] - \sqrt{1-\mu^2} r \sqrt{(1-\mu^2) r^4} \rho u[\text{theta}] \right]
\end{aligned}$$

### ■ EOM with Q explicitly

```

In[37]:= Table[d[t][Sum[Sqrt[g]*rho*u[n]*e_n[[k]], {n, {r, theta, phi}}]] +
  Sum[Sum[d[i][Sqrt[g]*(rschlang[e_i, j]+p[i, j]+q[i, j])*e_j[[k]], {i, {r, theta, phi}},
    {j, {r, theta, phi}}] - rho*Sum[d[1][Sqrt[g]*Phi*E_1[[k]], {1, {r, theta, phi}}]
    4 Pi/c*Sqrt[g]*(Sum[H[o]*e_o[[k]], {o, {r, theta, phi}})] /.
  {Sin[theta] -> Sqrt[1-mu^2], d[theta] -> -Sqrt[1-mu^2] d[mu],
  Csc[theta] -> 1/Sqrt[1-mu^2], Cos[theta] -> mu}, {k, {1, 2, 3}}]

```

$$\begin{aligned}
\text{Out[37]} = & \left\{ \left( -\sqrt{1-\mu^2} d[\mu] \right) \left[ \mu r \sqrt{(1-\mu^2) r^4} \cos[\text{phi}] \left( \frac{p}{r^2} + \rho u[\text{theta}] (u[\text{theta}] - \dot{x}[\text{theta}]) + \right. \right. \right. \\
& \left. \left. \left. \frac{-r^2 \text{div}[u] + 3 \left( r u[r] + \left( -\sqrt{1-\mu^2} d[\mu] \right) [u[\text{theta}]] \right)}{3 r^4} \right) \right] \right\} + \\
& \left( -\sqrt{1-\mu^2} d[\mu] \right) \left[ -\sqrt{1-\mu^2} r \sqrt{(1-\mu^2) r^4} \sin[\text{phi}] \right. \\
& \left. \left( \rho u[\text{phi}] (u[\text{theta}] - \dot{x}[\text{theta}]) + \frac{-\cot[\text{theta}] u[\text{phi}] + r u[r] + 2 d[\text{phi}][u[\text{theta}]]}{2 (1-\mu^2) r^4} \right) \right] + \\
& \left( -\sqrt{1-\mu^2} d[\mu] \right) \left[ \sqrt{1-\mu^2} \sqrt{(1-\mu^2) r^4} \cos[\text{phi}] \right. \\
& \left. \left( \rho u[r] (u[\text{theta}] - \dot{x}[\text{theta}]) + \frac{r^2 u[r] - u[\text{theta}] + 2 r d[r][u[\text{theta}]]}{2 r^3} \right) \right] +
\end{aligned}$$

$$\begin{aligned}
& d[\text{phi}] \left[ \mu r \sqrt{(1-\mu^2)} r^4 \cos[\text{phi}] \left( \rho u[\text{theta}] (u[\text{phi}] - \dot{x}[\text{phi}]) + \right. \right. \\
& \left. \left. - \frac{\cot[\text{theta}] u[\text{phi}]}{1-\mu^2} + r u[r] + \cot[\text{theta}] u[\text{theta}] + \frac{2 \left( -\sqrt{1-\mu^2} d[\mu] \right) [u[\text{phi}]]}{1-\mu^2} \right) \right] + \\
& \left. \frac{\phantom{d[\text{phi}]}}{2 r^4} \right] + \\
& d[\text{phi}] \left[ -\sqrt{1-\mu^2} r \sqrt{(1-\mu^2)} r^4 \sin[\text{phi}] \left( \frac{\rho}{(1-\mu^2) r^2} + \rho u[\text{phi}] (u[\text{phi}] - \dot{x}[\text{phi}]) + \right. \right. \\
& \left. \left. - r^2 \operatorname{div}[u] + 3 \left( r u[r] + \cot[\text{theta}] u[\text{theta}] + \frac{d[\text{phi}][u[\text{phi}]]}{1-\mu^2} \right) \right) \right] + \\
& \left. \frac{\phantom{d[\text{phi}]}}{3 (1-\mu^2) r^4} \right] + \\
& d[\text{phi}] \left[ \sqrt{1-\mu^2} \sqrt{(1-\mu^2)} r^4 \cos[\text{phi}] \left( \rho u[r] (u[\text{phi}] - \dot{x}[\text{phi}]) + \right. \right. \\
& \left. \left. \frac{r^2 u[r] + r \cot[\text{theta}] u[\text{theta}] - \frac{u[\text{phi}] - 2 r d[r][u[\text{phi}]]}{1-\mu^2}}{2 r^3} \right) \right] - \frac{1}{c} 4 \pi \sqrt{(1-\mu^2)} r^4 \\
& \rho \left( \sqrt{1-\mu^2} \cos[\text{phi}] H[r] + \mu r \cos[\text{phi}] H[\text{theta}] - \sqrt{1-\mu^2} r H[\text{phi}] \sin[\text{phi}] \right) \\
& \left( -\sqrt{1-\mu^2} d[\mu] \right) \left[ \frac{\mu \text{Phi} \sqrt{(1-\mu^2)} r^4 \cos[\text{phi}]}{r} \right] + d[\text{phi}] \left[ -\frac{\text{Phi} \sqrt{(1-\mu^2)} r^4 \sin[\text{phi}]}{\sqrt{1-\mu^2} r} \right] + \\
& \left. d[r] \left[ \sqrt{1-\mu^2} \text{Phi} \sqrt{(1-\mu^2)} r^4 \cos[\text{phi}] \right] \right] + d[r] \left[ \mu r \sqrt{(1-\mu^2)} r^4 \cos[\text{phi}] \right. \\
& \left. \left( \rho u[\text{theta}] (u[r] - \dot{x}[r]) - \frac{u[\text{theta}] - 2 r \left( -\sqrt{1-\mu^2} d[\mu] \right) [u[r]]}{2 r^3} \right) \right] + d[r] \left[ \right. \\
& \left. -\sqrt{1-\mu^2} r \sqrt{(1-\mu^2)} r^4 \sin[\text{phi}] \left( \rho u[\text{phi}] (u[r] - \dot{x}[r]) - \frac{u[\text{phi}] - 2 r d[\text{phi}][u[r]]}{2 (1-\mu^2) r^3} \right) \right] +
\end{aligned}$$

$$\begin{aligned}
& d[r] \left[ \sqrt{1-\mu^2} \sqrt{(1-\mu^2) r^4} \cos[\phi] \left( p - \frac{\text{div}[u]}{3} + \rho u[r] (u[r] - \dot{x}) + d[r][u[r]] \right) \right] + \\
& d[t] \left[ -\sqrt{1-\mu^2} r \sqrt{(1-\mu^2) r^4} \rho \sin[\phi] u[\phi] + \right. \\
& \quad \left. \sqrt{1-\mu^2} \sqrt{(1-\mu^2) r^4} \rho \cos[\phi] u[r] + \mu r \sqrt{(1-\mu^2) r^4} \rho \cos[\phi] u[\theta] \right], \\
& \left( -\sqrt{1-\mu^2} d[\mu] \right) \left[ \mu r \sqrt{(1-\mu^2) r^4} \sin[\phi] \left( \frac{p}{r^2} + \rho u[\theta] (u[\theta] - \dot{x}) + \right. \right. \\
& \quad \left. \left. \frac{-r^2 \text{div}[u] + 3 \left( r u[r] + \left( -\sqrt{1-\mu^2} d[\mu] \right) [u[\theta]] \right)}{3 r^4} \right) \right] + \\
& \left( -\sqrt{1-\mu^2} d[\mu] \right) \left[ \sqrt{1-\mu^2} r \sqrt{(1-\mu^2) r^4} \cos[\phi] \right. \\
& \quad \left. \left( \rho u[\phi] (u[\theta] - \dot{x}) + \frac{-\cot[\theta] u[\phi] + r u[r] + 2 d[\phi][u[\theta]]}{2 (1-\mu^2) r^4} \right) \right] + \\
& \left( -\sqrt{1-\mu^2} d[\mu] \right) \left[ \sqrt{1-\mu^2} \sqrt{(1-\mu^2) r^4} \sin[\phi] \right. \\
& \quad \left. \left( \rho u[r] (u[\theta] - \dot{x}) + \frac{r^2 u[r] - u[\theta] + 2 r d[r][u[\theta]]}{2 r^3} \right) \right] + \\
& d[\phi] \left[ \mu r \sqrt{(1-\mu^2) r^4} \sin[\phi] \left( \rho u[\theta] (u[\phi] - \dot{x}) + \right. \right. \\
& \quad \left. \left. \frac{-\frac{\cot[\theta] u[\phi]}{1-\mu^2} + r u[r] + \cot[\theta] u[\theta] + \frac{2 \left( -\sqrt{1-\mu^2} d[\mu] \right) [u[\phi]]}{1-\mu^2}}{2 r^4} \right) \right] + \\
& d[\phi] \left[ \sqrt{1-\mu^2} r \sqrt{(1-\mu^2) r^4} \cos[\phi] \left( \frac{p}{(1-\mu^2) r^2} + \rho u[\phi] (u[\phi] - \dot{x}) + \right. \right. \\
& \quad \left. \left. \frac{-r^2 \text{div}[u] + 3 \left( r u[r] + \cot[\theta] u[\theta] + \frac{d[\phi][u[\phi]]}{1-\mu^2} \right)}{3 (1-\mu^2) r^4} \right) \right] +
\end{aligned}$$



$$\begin{aligned}
& d[\text{phi}] \left[ \sqrt{1-\mu^2} \sqrt{(1-\mu^2) r^4} \text{Sin}[\text{phi}] \left( \rho u[r] (u[\text{phi}] - \text{xdot}[\text{phi}]) + \right. \right. \\
& \quad \left. \left. \frac{r^2 u[r] + r \text{Cot}[\text{theta}] u[\text{theta}] - \frac{u[\text{phi}] - 2 r d[r][u[\text{phi}]]}{1-\mu^2}}{2 r^3} \right) \right] - \frac{1}{c} 4 \pi \sqrt{(1-\mu^2) r^4} \\
& \rho \left( \sqrt{1-\mu^2} r \text{Cos}[\text{phi}] \text{H}[\text{phi}] + \sqrt{1-\mu^2} \text{H}[r] \text{Sin}[\text{phi}] + \mu r \text{H}[\text{theta}] \text{Sin}[\text{phi}] \right) \\
& \left( -\sqrt{1-\mu^2} d[\mu] \right) \left[ \frac{\mu \text{Phi} \sqrt{(1-\mu^2) r^4} \text{Sin}[\text{phi}]}{r} \right] + d[\text{phi}] \left[ \frac{\text{Phi} \sqrt{(1-\mu^2) r^4} \text{Cos}[\text{phi}]}{\sqrt{1-\mu^2} r} \right] + \\
& \quad d[r] \left[ \sqrt{1-\mu^2} \text{Phi} \sqrt{(1-\mu^2) r^4} \text{Sin}[\text{phi}] \right] \left. \right) + d[r] \left[ \mu r \sqrt{(1-\mu^2) r^4} \text{Sin}[\text{phi}] \right. \\
& \quad \left. \left( \rho u[\text{theta}] (u[r] - \text{xdot}[r]) - \frac{u[\text{theta}] - 2 r \left( -\sqrt{1-\mu^2} d[\mu] \right) [u[r]]}{2 r^3} \right) \right] + d[r] \left[ \right. \\
& \quad \left. \sqrt{1-\mu^2} r \sqrt{(1-\mu^2) r^4} \text{Cos}[\text{phi}] \left( \rho u[\text{phi}] (u[r] - \text{xdot}[r]) - \frac{u[\text{phi}] - 2 r d[\text{phi}][u[r]]}{2 (1-\mu^2) r^3} \right) \right] + \\
& d[r] \left[ \sqrt{1-\mu^2} \sqrt{(1-\mu^2) r^4} \text{Sin}[\text{phi}] \left( \text{p} - \frac{\text{div}[u]}{3} + \rho u[r] (u[r] - \text{xdot}[r]) + d[r][u[r]] \right) \right] + \\
& d[t] \left[ \sqrt{1-\mu^2} r \sqrt{(1-\mu^2) r^4} \rho \text{Cos}[\text{phi}] u[\text{phi}] + \sqrt{1-\mu^2} \sqrt{(1-\mu^2) r^4} \rho \text{Sin}[\text{phi}] u[r] + \right. \\
& \quad \left. \mu r \sqrt{(1-\mu^2) r^4} \rho \text{Sin}[\text{phi}] u[\text{theta}] \right], \left( -\sqrt{1-\mu^2} d[\mu] \right) [0] + \\
& \left( -\sqrt{1-\mu^2} d[\mu] \right) \left[ -\sqrt{1-\mu^2} r \sqrt{(1-\mu^2) r^4} \left( \frac{\text{p}}{r^2} + \rho u[\text{theta}] (u[\text{theta}] - \text{xdot}[\text{theta}]) + \right. \right. \\
& \quad \left. \left. \frac{-r^2 \text{div}[u] + 3 \left( r u[r] + \left( -\sqrt{1-\mu^2} d[\mu] \right) [u[\text{theta}]] \right)}{3 r^4} \right) \right] + \left( -\sqrt{1-\mu^2} d[\mu] \right) \left[ \right. \\
& \quad \left. \mu \sqrt{(1-\mu^2) r^4} \left( \rho u[r] (u[\text{theta}] - \text{xdot}[\text{theta}]) + \frac{r^2 u[r] - u[\text{theta}] + 2 r d[r][u[\text{theta}]]}{2 r^3} \right) \right] +
\end{aligned}$$

$$\begin{aligned}
& d[\text{phi}][0] + d[\text{phi}]\left[-\sqrt{1-\mu^2} r \sqrt{(1-\mu^2) r^4} \left( \rho u[\text{theta}] (u[\text{phi}] - \text{xdot}[\text{phi}]) + \right. \right. \\
& \quad \left. \left. - \frac{\text{Cot}[\text{theta}] u[\text{phi}]}{1-\mu^2} + r u[r] + \text{Cot}[\text{theta}] u[\text{theta}] + \frac{2(-\sqrt{1-\mu^2} d[\mu]) [u[\text{phi}]]}{1-\mu^2} \right) \right] + \\
& \quad \left. \frac{2 r^4}{2 r^4} \right] + \\
& d[\text{phi}]\left[\mu \sqrt{(1-\mu^2) r^4} \left( \rho u[r] (u[\text{phi}] - \text{xdot}[\text{phi}]) + \right. \right. \\
& \quad \left. \left. \frac{r^2 u[r] + r \text{Cot}[\text{theta}] u[\text{theta}] - \frac{u[\text{phi}] - 2 r d[r] [u[\text{phi}]]}{1-\mu^2}}{2 r^3} \right) \right] + \\
& d[r][0] - \frac{1}{c} 4 \pi \sqrt{(1-\mu^2) r^4} \rho \left( \mu H[r] - \sqrt{1-\mu^2} r H[\text{theta}] \right) \\
& \quad \left( \left( -\sqrt{1-\mu^2} d[\mu] \right) \left[ -\frac{\sqrt{1-\mu^2} \text{Phi} \sqrt{(1-\mu^2) r^4}}{r} \right] + d[\text{phi}][0] + d[r]\left[\mu \text{Phi} \sqrt{(1-\mu^2) r^4} \right] \right) + \\
& d[r]\left[-\sqrt{1-\mu^2} r \sqrt{(1-\mu^2) r^4} \right. \\
& \quad \left. \left( \rho u[\text{theta}] (u[r] - \text{xdot}[r]) - \frac{u[\text{theta}] - 2 r (-\sqrt{1-\mu^2} d[\mu]) [u[r]]}{2 r^3} \right) \right] + \\
& d[r]\left[\mu \sqrt{(1-\mu^2) r^4} \left( p - \frac{\text{div}[u]}{3} + \rho u[r] (u[r] - \text{xdot}[r]) + d[r][u[r]] \right) \right] + \\
& d[t]\left[\mu \sqrt{(1-\mu^2) r^4} \rho u[r] - \sqrt{1-\mu^2} r \sqrt{(1-\mu^2) r^4} \rho u[\text{theta}] \right] \}
\end{aligned}$$

# Polynomial Coordinates Ansatz

## Grid Generation via Orthogonal Curves

### ■ Ansatz for Polynomial Curves

```
In[1]:=  $\eta[x_, r_, t_] = a0[r, t] + a1[r, t] * x + a2[r, t] * x^2 + a3[r, t] * x^3$   
      ( $++a4[r, t] * x^4 + a5[r, t] * x^5$ );
```

First derivative to determine slope

```
In[2]:=  $g[x_, r_, t_] = D[\eta[x, r, t], x];$ 
```

Second derivative

```
In[3]:=  $h[x_, r_, t_] = D[\eta[x, r, t], x, x];$ 
```

### ■ Rotation Matrix to Rotate Coordinate System

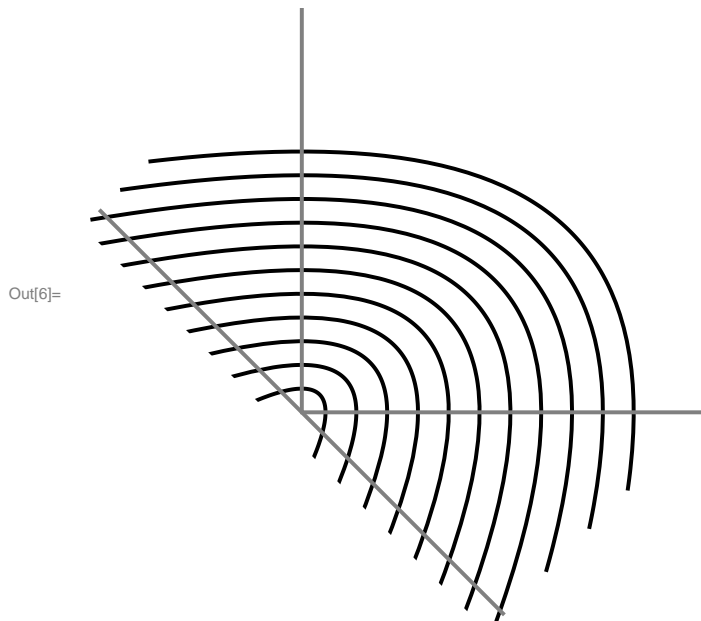
Since infinite slope cannot be requirement for linear equation system, the whole coordinate system gets rotated by 45 degree. So the slopes are +1 and -1.

```
In[4]:=  $A[\alpha] = \{\{\text{Cos}[\alpha], -\text{Sin}[\alpha]\}, \{\text{Sin}[\alpha], \text{Cos}[\alpha]\}\};$ 
```

```
In[5]:=  $\text{coeff} = \text{Table}[$   
       $P1 = A[\text{Pi} / 4].\{0.1 + n * 0.13, 0\};$   
       $P2 = A[\text{Pi} / 4].\{0, 0.1 + n * 0.1\};$   
       $\text{Solve}[\{\eta[P1[[1]], r, t] == P1[[2]], \eta[P2[[1]], r, t] == P2[[2]],$   
       $g[P1[[1]], r, t] == -1, g[P2[[1]], r, t] == 1(*, f[0, r, t] == 0.1 + n * 0.12, g[0, r, t] == 0*)\},$   
       $\{a0[r, t], a1[r, t], a2[r, t], a3[r, t] (*, a4[r, t], a5[r, t] *)\}, \{n, 0, 10\}]$   
      ( $* \text{generation of polynomials intersecting with two equidistant points at x-}$   
       $\text{and y-axis} *$ )
```

```
Out[5]= {{{a0[r, t] → 0.106066, a1[r, t] → 0., a2[r, t] → -7.07107, a3[r, t] → 0.},  
  {{a0[r, t] → 0.226564, a1[r, t] → 0.173909, a2[r, t] → -3.24084, a3[r, t] → -1.5093}},  
  {{a0[r, t] → 0.346169, a1[r, t] → 0.226146, a2[r, t] → -2.08962, a3[r, t] → -0.834794}},  
  {{a0[r, t] → 0.465575, a1[r, t] → 0.251258, a2[r, t] → -1.54026, a3[r, t] → -0.510661}},  
  {{a0[r, t] → 0.584904, a1[r, t] → 0.266012, a2[r, t] → -1.21921, a3[r, t] → -0.341655}},  
  {{a0[r, t] → 0.704197, a1[r, t] → 0.27572, a2[r, t] → -1.00877, a3[r, t] → -0.243865}},  
  {{a0[r, t] → 0.823468, a1[r, t] → 0.282592, a2[r, t] → -0.860221, a3[r, t] → -0.182541}},  
  {{a0[r, t] → 0.942727, a1[r, t] → 0.287713, a2[r, t] → -0.749781, a3[r, t] → -0.141659}},  
  {{a0[r, t] → 1.06198, a1[r, t] → 0.291675, a2[r, t] → -0.664457, a3[r, t] → -0.113079}},  
  {{a0[r, t] → 1.18122, a1[r, t] → 0.294833, a2[r, t] → -0.59656, a3[r, t] → -0.0923307}},  
  {{a0[r, t] → 1.30046, a1[r, t] → 0.297408, a2[r, t] → -0.541248, a3[r, t] → -0.0768}}}
```

```
In[6]:= Rotate[
  Show[Plot[{Evaluate[η[x, r, t] /. {coeff}]*, Evaluate[f[x, r, t] /. {ergmore2}]*], Abs[x], 0],
    {x, -1.2, 1.2}, PlotRange → {-0.1, 1.5}, AspectRatio → Automatic, Background → White,
    Axes → None, PlotStyle → {{Black, Thick}, {Gray, Thick}, {Gray, Thick}}], (*,
  Graphics[{Thick, Red, Arrow[{{0, 0}, {1, 0}]}, Thick, Blue, Arrow[{{0, 0}, {0, 1}]},
    Thick, Black, Dashed, Arrow[{{0, 0}, 1*{1, 0}+1*{0, 1}}]}], -45 Degree]
```



## ■ Orthogonal Curves

```
In[7]:= po1[x_] = η[x, r, t] /. {coeff[[1]]}; (* define polynomial functions *)
po2[x_] = η[x, r, t] /. {coeff[[2]]};
po3[x_] = η[x, r, t] /. {coeff[[3]]};
po4[x_] = η[x, r, t] /. {coeff[[4]]};
po5[x_] = η[x, r, t] /. {coeff[[5]]};
po6[x_] = η[x, r, t] /. {coeff[[6]]};
po7[x_] = η[x, r, t] /. {coeff[[7]]};
po8[x_] = η[x, r, t] /. {coeff[[8]]};
```

```
In[15]:= ort4[x0_, x_] = -1 / (D[po4[x], x]) * (x - x0) + po7[x0];
(* orthogonal curves to polynomial # *)
ort7[x0_, x_] = -1 / (D[po7[x], x]) * (x - x0) + po7[x0];
ort8[x0_, x_] = -1 / (D[po8[x], x]) * (x - x0) + po8[x0];
```

```
In[18]:= Table[
  intersectort8po7[m] =
  FindInstance[{Evaluate[ort8[0.25 + 0.1 * m, x]] == po7[x], x > 0.18, x < 0.8}, x, Reals][[1]][[
  1]] (* determine intersections *)
,
  {m,
  0,
  4}]
```

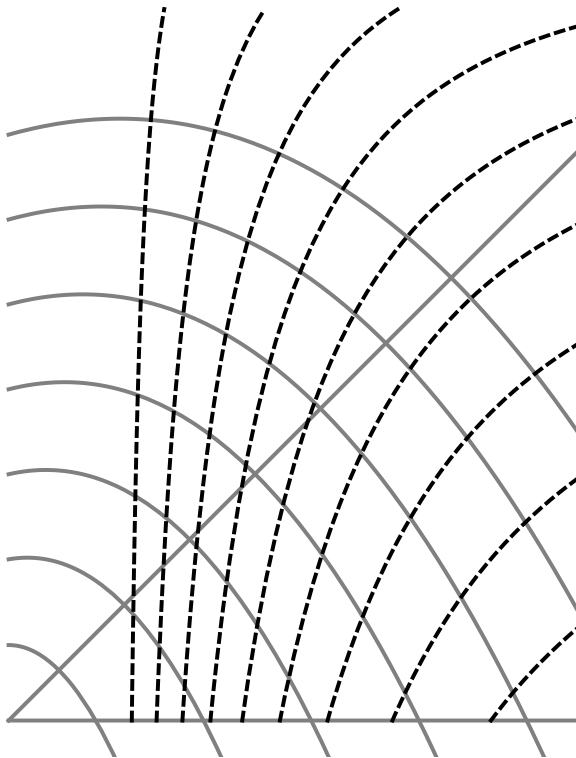
```
Out[18]= {x → 0.2382, x → 0.320295, x → 0.403032, x → 0.487458, x → 0.574101}
```

```
In[19]:= Table[
  intersectort7po8old[n] =
    FindInstance[{Evaluate[ort7[0.25 + 0.1 * n, x]] == po8[x], x > 0.18, x < 0.8}, x, Reals][[1]][[
      1]]
  ,
  {n,
    0,
    4}]
```

```
Out[19]= {x → 0.279988, x → 0.409555, x → 0.530964, x → 0.645, x → 0.754393}
```

```
In[20]:= Show[Plot[({*neu8[x], neu7[x], *}po7[x], po6[x], po5[x], po4[x],
  po3[x], po2[x], po1[x], Abs[x], 0), {x, 0, 0.8}, PlotRange → {-0.05, 1.},
  AspectRatio → Automatic, Background → White, PlotStyle → {{Gray, Thick}}, Axes → False],
  Table[Plot[Evaluate[ort7[0.2 + 0.09 * m, x]], {x, 0.17, 0.8},
  AspectRatio → Automatic, Background → White, PlotRange → {0., 1.},
  PlotStyle → {Black, Dashed, Thick}, Axes → False], {m, 0, 8}]
  (*Table[Plot[Evaluate[y8[x/.Schnitty7mitneu8[n], x]], {x, 0.2, 0.8}, AspectRatio → Automatic,
  Background → White, PlotRange → {0.4, 1.2}, PlotStyle → {Blue}, Axes → False], {n, 0, 3}], *)
]
```

```
Out[20]=
```



## ■ Normal Vectors

```
In[21]:= slope7[x_] = -1 / (D[po7[x], x])
```

```
Out[21]= {{- 1 / (0.282592 - 1.72044 x - 0.547624 x^2)}}
```

```
In[22]:= vecend[n_] = {0.25 + 0.1 * n, po7[0.25 + 0.1 * n][[1]][[1]]} +
  {0.25 + 0.1 * n + 1, po7[0.25 + 0.1 * n][[1]][[1]] + slope7[0.25 + 0.1 * n][[1]][[1]]}
```

```
Out[22]= {1.5 + 0.2 n, 1.64694 -  $\frac{1}{0.282592 - 1.72044 (0.25 + 0.1 n) - 0.547624 (0.25 + 0.1 n)^2 + 0.565184 (0.25 + 0.1 n) - 1.72044 (0.25 + 0.1 n)^2 - 0.365083 (0.25 + 0.1 n)^3}$ }
```

```
In[23]:= slope8[x_] = -1 / (D[po8[x], x])
```

```
Out[23]= {{ -  $\frac{1}{0.287713 - 1.49956 x - 0.424976 x^2}$  }}
```

```
In[24]:= Table[
  intersectort7po8[n] = x /. FindInstance[
    {Evaluate[ort7[0.25 + 0.1 * n, x]] == po8[x], x > 0.18, x < 0.8}, x, Reals][[1]][[1]]
  ,
  {n,
  0,
  4}]
```

```
Out[24]= {0.279988, 0.409555, 0.530964, 0.645, 0.754393}
```

```
In[25]:= Table[vecend8[m] =
  {intersectort7po8[m], po8[intersectort7po8[m]][[1]][[1]]} + {intersectort7po8[m] + 1,
  po8[intersectort7po8[m]][[1]][[1]] + slope8[intersectort7po8[m]][[1]][[1]]}, {m, 0, 3}]
```

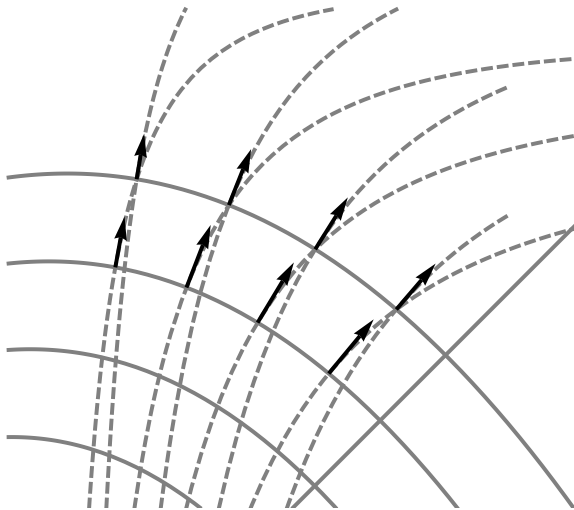
```
Out[25]= {{1.55998, 7.9665}, {1.81911, 4.36444}, {2.06193, 3.31738}, {2.29, 2.72453}}
```

```

In[26]:= Show[Plot[{po8[x], po7[x], po6[x], po5[x], Abs[x]}, {x, 0.1, 0.9}, PlotRange -> {0.5, 1.3},
  AspectRatio -> Automatic, Background -> White, PlotStyle -> {{Gray, Thick}}, Axes -> False],
  Table[Plot[Evaluate[ort7[0.25 + 0.1 * m, x]], {x, 0.2, 0.9},
    AspectRatio -> Automatic, Background -> White, PlotRange -> {0.5, 1.2},
    PlotStyle -> {Gray, Dashed, Thick}, Axes -> False], {m, 0, 3}],
  Table[Plot[Evaluate[ort8[x /. intersectort7po8old[n], x]], {x, 0.2, 0.8},
    AspectRatio -> Automatic, Background -> White, PlotRange -> {0.5, 1.2},
    PlotStyle -> {Gray, Dashed, Thick}, Axes -> False], {n, 0, 3}],
  Table[Graphics[{Thick, Black, Arrow[{{0.25 + 0.1 * n, po7[0.25 + 0.1 * n][[1]][[1]]},
    {0.25 + 0.1 * n + 0.7 / Norm[vecend[n]]^2 * 1, po7[0.25 + 0.1 * n][[1]][[1]] +
    0.7 / Norm[vecend[n]]^2 * slope7[0.25 + 0.1 * n][[1]][[1]]}}}], {n, 0, 3}],
  Table[Graphics[{Thick, Black, Arrow[{{intersectort7po8[n],
    po8[intersectort7po8[n]][[1]][[1]]},
    {intersectort7po8[n] + 0.7 / Norm[vecend8[n]]^2 * 1, po8[intersectort7po8[n]][[1]][[1]] +
    0.7 / Norm[vecend8[n]]^2 * slope8[intersectort7po8[n]][[1]][[1]]}}}], {n, 0, 3}]
]

```

Out[26]=



# Polar Non-Orthogonal Grid Ansatz

## Generation of Quasi-Polar Grid in 2D

---

### Ansatz for Quasi-Polar Coordinates

#### ■ Coordinate Transformation with Product Ansatz

We define a coordinate transformation with product ansatz, which is reasonable for any kind of coordinate system.

```
In[1]:= x = X[ξ, η];  
       y = Y[ξ, η];  
  
In[3]:= X[ξ_, η_] = a[ξ] * α[η];  
       Y[ξ_, η_] = b[ξ] * β[η];  
  
In[5]:= α[η_] = (1 + alpha1 * η + alpha2 * η^2 + alpha3 * η^3) * Cos[η];  
       β[η_] = (1 + beta1 * η + beta2 * η^2 + beta3 * η^3) * Sin[η];  
       a[ξ_] = (a1 * ξ + a2 * ξ^2);  
       b[ξ_] = (b1 * ξ + b2 * ξ^2);
```

We calculate the Jacobian of this transformation to get the base vectors in the new coordinate system.

```
In[9]:= lij = {{D[x, ξ], D[x, η]}, {D[y, ξ], D[y, η]}};  
  
In[10]:= lijtransposed := Transpose[lij]
```

#### ■ Covariant Components of Metric Tensor

For trivial signatures, the metric tensor is simply given by the Jacobian times its transpositon. The off diagonal elements contain the information about the non-orthogonality (angles), the diagonal elements are measures of lenght in the coordinate directions.

```
In[11]:= gij = lijtransposed.lij;  
  
In[12]:= g11[ξ_, η_] = gij[[1, 1]];  
       g12[ξ_, η_] = gij[[1, 2]];  
       g21[ξ_, η_] = gij[[2, 1]];  
       g22[ξ_, η_] = gij[[2, 2]];
```

#### ■ Covariant Base Vectors

The base vectors yield

```
In[16]:= eξ[ξ_, η_] = lijtransposed[[1]]  
  
Out[16]= { (1 + alpha1 η + alpha2 η^2 + alpha3 η^3) (a1 + 2 a2 ξ) Cos[η],  
          (1 + beta1 η + beta2 η^2 + beta3 η^3) (b1 + 2 b2 ξ) Sin[η] }
```



```
In[17]:= eη[ξ-, η-] = lijtransposed[[2]]
```

```
Out[17]= { (alpha1 + 2 alpha2 η + 3 alpha3 η2) (a1 ξ + a2 ξ2) Cos[η] -
  (1 + alpha1 η + alpha2 η2 + alpha3 η3) (a1 ξ + a2 ξ2) Sin[η],
  (1 + beta1 η + beta2 η2 + beta3 η3) (b1 ξ + b2 ξ2) Cos[η] +
  (beta1 + 2 beta2 η + 3 beta3 η2) (b1 ξ + b2 ξ2) Sin[η] }
```

## PDEs + Boundary Conditions

### ■ Controlling the Grid

In order to control the shape of the grid by a manageable number of parameters and for reasons of symmetry we impose geometrically motivated boundary conditions. Since some of them are either redundant or exclusive, the following list is somewhat heuristic.

```
In[18]:= ESSol = Solve[ {
  (*g12[ξ,η]==0,*) (* orthogonality *)
  eξ[ξ, 0][[1]] == 1, (* scaling *)
  eξ[ξ, 0][[2]] == 0, (* in "x"-axis *)
  eξ[ξ, Pi / 2][[1]] == 0, (* in "y"-axis *)
  eξ[ξ, Pi / 2][[2]] == 1, (* scaling *)
  eη[ξ, 0][[1]] == 0, (* normal to "x"-axis *)
  eη[ξ, 0][[2]] == ξ, (* scaling *)
  eη[ξ, Pi / 2][[1]] == -ξ, (* orientation *)
  eη[ξ, Pi / 2][[2]] == 0, (* normal to "y"-axis *)
  X[0, 0] == 0, (* set origin *)
  Y[0, 0] == 0, (* set origin *)
  X[ξ, 0] == X[ξ, 2 * Pi], (* periodicity *)
  Y[ξ, 0] == Y[ξ, 2 * Pi], (* periodicity *)
  X[ξ, 0] == ξ * X[1, 0] (* scaling *)
},
  {alpha1, alpha2, beta1, beta2, , alpha3, beta3, a1, a2}]
```

Solve::svars : Equations may not give solutions for all "solve" variables. >>

```
Out[18]= { {beta1 →  $\frac{\text{beta3 } \pi^3 - 16 \text{ b2 } \xi + \text{b2 beta3 } \pi^3 \xi}{4 \pi (1 + \text{b2 } \xi)}$ ,
  beta2 →  $\frac{-\text{beta3 } \pi^3 + 4 \text{ b2 } \xi - \text{b2 beta3 } \pi^3 \xi}{\pi^2 (1 + \text{b2 } \xi)}$ , alpha2 → 0, alpha1 → 0, alpha3 → 0, a1 → 1, a2 → 0} }
```

```
In[19]:= Xnew[ξ-, η-] = Evaluate[X[ξ, η] /. ESSol[[1]]] // Simplify
Ynew[ξ-, η-] = Evaluate[Y[ξ, η] /. ESSol[[1]]] // Simplify
```

```
Out[19]= ξ Cos[η]
```

```
Out[20]=  $\frac{1}{4 \pi^2 (1 + \text{b2 } \xi)}$  ξ (b1 + b2 ξ)
  (-16 b2 π η ξ + 16 b2 η2 ξ + beta3 π4 η (1 + b2 ξ) - 4 beta3 π3 η2 (1 + b2 ξ) + 4 π2 (1 + beta3 η3) (1 + b2 ξ) )
  Sin[η]
```

### ■ Plots

This example for a quasi-polar mesh is being controlled by three parameters.

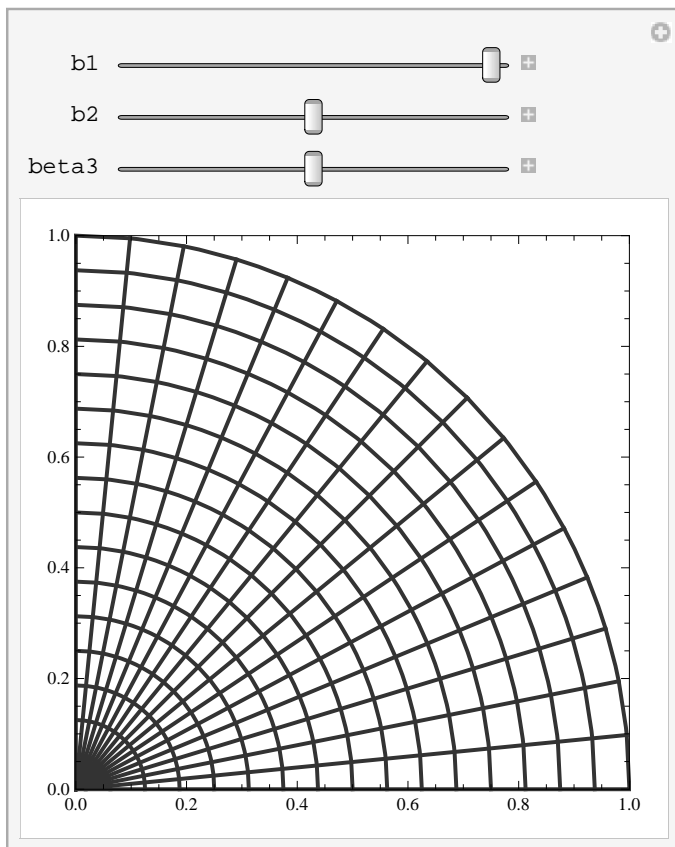
In[21]= Manipulate[

```

ParametricPlot[{{ξ Cos[η],  $\frac{1}{4 \pi^2 (1 + b_2 \xi)}$  ξ (b1 + b2 ξ) (-16 b2 π η ξ + 16 b2 η2 ξ + beta3 π4 η (1 + b2 ξ) -
4 beta3 π3 η2 (1 + b2 ξ) + 4 π2 (1 + beta3 η3) (1 + b2 ξ)) Sin[η]},
{ξ, 0, 1}, {η, 0, Pi / 2}, AspectRatio → 1, PlotRange → {0, 1}, Axes → None,
BoundaryStyle → {RGBColor[.2, .2, .2], Thick},
MeshStyle → {{RGBColor[.2, .2, .2], Thick}}, MeshFunctions → Automatic,
MeshShading -> {{White, White}, {White, White}}, Background → White(*, LabelStyle->*)],
{{b1, 1}, -1, 1}, {{b2, 0}, -1, 1}, {{beta3, 0}, -1, 1}]

```

Out[21]=




---

## Geometrical Characteristics of Toy Models

Determination of maximal relative volumes respectively off-diagonal metric elements.

```
In[22]= lijnew = {{D[Xnew[ξ, η], ξ], D[Xnew[ξ, η], η]}, {D[Ynew[ξ, η], ξ], D[Ynew[ξ, η], η]}};
```

```
In[23]= gijnew = Transpose[lijnew].lijnew;
```

```
In[24]= grida = {b1 → 1, b2 → 0, beta3 → 0};
gridb = {b1 → 0.8, b2 → 0, beta3 → 0};
gridc = {b1 → 0.8, b2 → 0, beta3 → 0.5};
gridd = {b1 → 0.8, b2 → 0.2, beta3 → 0.5};
```

```

In[28]:= deta[ξ_, η_] = Evaluate[Det[gijnew] /. grida];
          detb[ξ_, η_] = Evaluate[Det[gijnew] /. gridb];
          detc[ξ_, η_] = Evaluate[Det[gijnew] /. gridc];
          detd[ξ_, η_] = Evaluate[Det[gijnew] /. gridd];

In[32]:= offa[ξ_, η_] = Evaluate[gijnew[[1, 2]] /. grida];
          offb[ξ_, η_] = Evaluate[gijnew[[1, 2]] /. gridb];
          offc[ξ_, η_] = Evaluate[gijnew[[1, 2]] /. gridc];
          offd[ξ_, η_] = Evaluate[gijnew[[1, 2]] /. gridd];

```

## ■ Maxima

```

In[36]:= FindMaximum[{deta[ξ, η] / ξ^2, ξ ≥ 0 && η ≥ 0 && ξ ≤ 1 && η ≤ Pi / 4}, {ξ, η}]
Out[36]= {1., {ξ → 0.899989, η → 0.706847}}

In[37]:= FindMaximum[{Abs[offa[ξ, η] / ξ], ξ ≥ 0 && η ≥ 0 && ξ ≤ 1 && η ≤ Pi / 4}, {ξ, η}]
Out[37]= {0., {ξ → 0., η → 0.}}

In[38]:= FindMaximum[{detb[ξ, η] / ξ^2, ξ ≥ 0 && η ≥ 0 && ξ ≤ .8 && η ≤ Pi / 4}, {ξ, η}]
Out[38]= {0.64, {ξ → 0.719994, η → 0.706852}}

In[39]:= FindMaximum[{Abs[offb[ξ, η] / ξ], ξ ≥ 0 && η ≥ 0 && ξ ≤ 1 && η ≤ Pi / 4}, {ξ, η}]
Out[39]= {0.179999, {ξ → 0.851429, η → 0.783879}}

In[40]:= FindMaximum[{detc[ξ, η] / ξ^2, ξ ≥ 0 && η ≥ 0 && ξ ≤ 1 && η ≤ Pi / 4}, {ξ, η}]
Out[40]= {1.19161, {ξ → 0.860374, η → 0.327134}}

In[41]:= FindMaximum[{Abs[offc[ξ, η] / ξ], ξ ≥ 0 && η ≥ 0 && ξ ≤ 1 && η ≤ Pi / 4}, {ξ, η}]
Out[41]= {0.128795, {ξ → 0.899702, η → 0.785398}}

In[42]:= FindMaximum[{detd[ξ, η] / ξ^2, ξ ≥ 0 && η ≥ 0 && ξ ≤ 1 && η ≤ Pi / 4}, {ξ, η}]
Out[42]= {1.62084, {ξ → 1., η → 0.293574}}

In[43]:= FindMaximum[{Abs[offd[ξ, η] / ξ], ξ ≥ 0 && η ≥ 0 && ξ ≤ 1 && η ≤ Pi / 4}, {ξ, η}]
Out[43]= {0.248654, {ξ → 0.999999, η → 0.424638}}

```

## ■ Minima

```

In[44]:= FindMinimum[{deta[ξ, η] / ξ^2, ξ ≥ 0 && η ≥ 0 && ξ ≤ 1 && η ≤ Pi / 4}, {ξ, η}]
Out[44]= {1., {ξ → 0.899989, η → 0.706847}}

In[45]:= FindMinimum[{Abs[offa[ξ, η] / ξ], ξ ≥ 0 && η ≥ 0 && ξ ≤ 1 && η ≤ Pi / 4}, {ξ, η}]
Out[45]= {0., {ξ → 0., η → 0.}}

In[46]:= FindMinimum[{detb[ξ, η] / ξ^2, ξ ≥ 0 && η ≥ 0 && ξ ≤ .8 && η ≤ Pi / 4}, {ξ, η}]
Out[46]= {0.64, {ξ → 0.719994, η → 0.706852}}

```

```
In[47]:= FindMinimum[{Abs[offb[ξ, η] / ξ], ξ ≥ 0 && η ≥ 0 && ξ ≤ 1 && η ≤ Pi / 4}, {ξ, η}]
```

```
Out[47]= {8.29014 × 10-8, {ξ → 0.772027, η → 2.30282 × 10-7}}
```

```
In[48]:= FindMinimum[{detc[ξ, η] / ξ2, ξ ≥ 0 && η ≥ 0 && ξ ≤ 1 && η ≤ Pi / 4}, {ξ, η}]
```

```
Out[48]= {0.757631, {ξ → 0.897993, η → 0.785396}}
```

```
In[49]:= FindMinimum[{Abs[offc[ξ, η] / ξ], ξ ≥ 0 && η ≥ 0 && ξ ≤ 1 && η ≤ Pi / 4}, {ξ, η}]
```

```
Out[49]= {2.46448 × 10-8, {ξ → 0.734207, η → 6.84577 × 10-8}}
```

```
In[50]:= FindMinimum[{detd[ξ, η] / ξ2, ξ ≥ 0 && η ≥ 0 && ξ ≤ 1 && η ≤ Pi / 4}, {ξ, η}]
```

```
Out[50]= {0.75763, {ξ → 5.89009 × 10-7, η → 0.785398}}
```

```
In[53]:= FindMinimum[{Abs[offd[ξ, η] / ξ], ξ ≥ 0 && η ≥ 0 && ξ ≤ 1 && η ≤ Pi / 4}, {ξ, η}]
```

```
FindMinimum::eit :
```

```
The algorithm does not converge to the tolerance of 4.806217383937354-6
in 500 iterations. The best estimated solution, with
feasibility residual, KKT residual, or complementary residual
of {0.000658608, 0.100761, 0.000246563}, is returned. >>
```

```
Out[53]= {3.42416 × 10-6, {ξ → 0.709494, η → 0.716048}}
```

## Bibliography

- [1] R. Adams. *Sobolev Spaces, Pure and Applied Mathematics*. Academic Press, Boston, MA, 1975.
- [2] D. A. Anderson. Equidistribution schemes, poisson generators, and adaptive grids. *Applied Mathematics and Computation*, 24(3):211 – 227, 1987.
- [3] D. J. Benson and S. Schoenfeld. A total variation diminishing shock viscosity. *Computational Mechanics*, 11:107 – 121, 1993.
- [4] O. P. Bhutani and P. Dewanwala. Invariance and conservation laws for physical systems. *Journal of Mathematical and Physical Sciences*, 15:225–237, June 1981.
- [5] T. J. Bridges. Conservation laws in curvilinear coordinates: A short proof of vinokur’s theorem using differential forms. *Applied Mathematics and Computation*, 202(2):882 – 885, 2008.
- [6] J. R. Buchler. Radiation hydrodynamics in the fluid frame. *Journal of Quantitative Spectroscopy and Radiative Transfer*, 22(3):293 – 300, 1979.
- [7] J. R. Buchler. Radiation transfer in the fluid frame. *Journal of Quantitative Spectroscopy and Radiative Transfer*, 30(5):395 – 407, 1983.
- [8] J. Castillo, editor. *Mathematical Aspects of Numerical Grid Generation*. Society for Industrial and Applied Mathematics, 1991.
- [9] G. Delzanno, L. Chacon, J. Finn, Y. Chung, and G. Lapenta. An optimal robust equidistribution method for two-dimensional grid adaptation based on monge-kantorovich optimization. *Journal of Computational Physics*, 227(23):9841 – 9864, 2008.
- [10] R. d’Inverno. *Einführung in die Relativitätstheorie*. WILEY-VCH, 2009.
- [11] E. Dorfi and L. Drury. Simple adaptive grids for 1 - d initial value problems. *Journal of Computational Physics*, 69(1):175 – 195, 1987.
- [12] E. Dorfi, H. Pikall, A. Stökl, and A. Gautschy. Towards a more consistent discretization scheme for adaptive implicit rhd computations. *Computer Physics Communications*, 174(10):771 – 782, 2006.
- [13] E. A. Dorfi. Implicit radiation hydrodynamics for 1d-problems. *Journal of Computational and Applied Mathematics*, 109(1-2):153 – 171, 1999.
- [14] L. C. Evans. *Partial Differential Equations*. American Mathematical Society, Chelsea, 1998.

## Bibliography

- [15] R. Furzeland, J. Verwer, and P. Zegeling. A numerical study of three moving-grid methods for one-dimensional partial differential equations which are based on the method of lines. *Journal of Computational Physics*, 89(2):349 – 388, 1990.
- [16] E. Godlewski and P. Raviart. Numerical approximation of hyperbolic systems of conservation laws. *Applied Mathematical Sciences*, 18(18), 1992.
- [17] S. I. Goldberg and R. L. Bishop. *Tensor Analysis on Manifolds*. Dover Publications, December 1980.
- [18] A. Harten. High resolution schemes for hyperbolic conservation laws,. *Journal of Computational Physics*, 135(2):260 – 278, 1997. Reprinted from Volume 49, Number 3, March 1983, pages 357 to 393.
- [19] A. Harten, J. Hyman, P. Lax, and B. Keyfitz. On finite-difference approximations and entropy conditions for shocks. *Communications on Pure and Applied Mathematics*, XXIX:297 – 322, 1976.
- [20] W. Huang and D. M. Sloan. A simple adaptive grid method in two dimensions. *SIAM Journal on Scientific Computing*, 15(4):776–797, 1994.
- [21] T. Kambe. Gauge principle and variational formulation for ideal fluids with reference to translation symmetry. *Fluid Dynamics Research*, 39(1-3):98 – 120, 2007. In memoriam: Professor Isao Imai, 1914-2004.
- [22] P. Knupp and S. Steinberg. *Fundamentals of Grid Generation*. CRC Press, 1993.
- [23] L. Landau and E. Lifschitz. *Lehrbuch der theoretischen Physik, 10 Bde., Bd.6, Hydrodynamik*. Akademie Verlag, Berlin, 1974.
- [24] R. Landshoff. A numerical method for treating fluid flow in the presence of shocks. *Los Alamos National Laboratory Report*, LA-1930, 1955.
- [25] R. LeVeque, D. Mihalas, E. Dorfi, and E. Müller. *Computational Methods for Astrophysical Fluid Flow*. Springer, 1997. Saas-Fee Advanced Courses.
- [26] R. J. LeVeque. Numerical methods for conservation laws. *Lectures in Mathematics, ETH-Zurich*, 1990.
- [27] C. D. Levermore. Relating eddington factors to flux limiters. *Journal of Quantitative Spectroscopy and Radiative Transfer*, 31(2):149 – 160, 1984.
- [28] A. Lichnerowicz. *Einführung in die Tensoranalysis*. Bibliographisches Institut AG, Mannheim, 1966.
- [29] R. W. Lindquist. Relativistic transport theory. *Annals of Physics*, 37(3):487 – 518, 1966.
- [30] V. D. Liseikin. *Grid Generation Methods*. Springer-Verlag, Berlin Heidelberg, 1999.
- [31] V. D. Liseikin. *A Computational Differential Geometry Approach to Grid Generation*. Springer-Verlag, Berlin Heidelberg, 2004.

- [32] D. Mihalas and B. W. Mihalas. *Foundations of Radiation Hydrodynamics*. Oxford University Press, 1984.
- [33] D. Mihalas, K.-H. A. Winkler, and M. L. Norman. Adaptive-mesh radiation hydrodynamics–ii. the radiation and fluid equations in relativistic flows. *Journal of Quantitative Spectroscopy and Radiative Transfer*, 31(6):479 – 489, 1984.
- [34] E. Müller and M. Steinmetz. Simulating self-gravitating hydrodynamic flows. *Computer Physics Communications*, 89(1-3):45 – 58, 1995. Numerical Methods in Astrophysical Hydrodynamics.
- [35] J. A. Pons, J. M. Ibanez, and J. A. Miralles. Hyperbolic character of the angular moment equations of radiative transfer and numerical methods. *Monthly Notices of the Royal Astronomical Society*, 317(3):550–562, 2000.
- [36] R. D. Richtmyer and K. W. Morton. *Difference Methods for Initial-Value Problems*. Krieger Pub Co, 1994.
- [37] B. Schutz. *Geometrical Methods of Mathematical Physics*. Press Syndicate of the University of Cambridge, 1980.
- [38] S. P. Spekreijse. Elliptic grid generation based on laplace equations and algebraic transformations. *Journal of Computational Physics*, 118(1):38 – 61, 1995.
- [39] V. Springel. E pur si muove: Galilean-invariant cosmological hydrodynamical simulations on a moving mesh. *Monthly Notices of the Royal Astronomical Society*, 401(2):791 – 851, 2009.
- [40] A. Stökl. *Implicit Radiation Hydrodynamics on Adaptive Grids*. PhD thesis, University of Vienna, Vienna, 2006.
- [41] M. Sulman, J. F. Williams, and R. D. Russell. Monge-Kantorovich Approach for Grid Generation. In T. E. Simos, G. Psihoyios, & C. Tsitouras, editor, *American Institute of Physics Conference Series*, volume 1168, pages 25–28, Sept. 2009.
- [42] L. H. Thomas. The Radiation Field in a Fluid in Motion. *Quarterly Journal of Mathematics*, os-1(1):239–251, 1930.
- [43] J. F. Thompson, Z. U. Warsi, and C. W. Mastin. *Numerical grid generation: foundations and applications*. Elsevier North-Holland, Inc., New York, NY, USA, 1985.
- [44] W. M. Tscharnuter and K. H. Winkler. A method for computing selfgravitating gas flows with radiation. *Computer Physics Communications*, 18(2):171 – 199, 1979.
- [45] B. van Leer. Towards the ultimate conservative difference scheme. v. a second-order sequel to godunov’s method. *Journal of Computational Physics*, 32(1):101 – 136, 1979.
- [46] M. Vinokur. Conservation equations of gasdynamics in curvilinear coordinate systems. *Journal of Computational Physics*, 14(2):105 – 125, 1974.
- [47] J. VonNeumann and R. D. Richtmyer. A method for the numerical calculation of hydrodynamic shocks. *Journal of Applied Physics*, 21(3):232–237, 1950.

## Bibliography

- [48] Z. U. A. Warsi. Conservation form of the navier-stokes equations in general non-steady coordinates. *AIAA Journal*, 19:240–242, 1981.
- [49] M. L. Wilkins. Use of artificial viscosity in multidimensional fluid dynamic calculations,. *Journal of Computational Physics*, 36(3):281 – 303, 1980.
- [50] K.-H. A. Winkler. *Über ein numerische Verfahren zur Berechnung instationärer sphärischer Stossfronten mit Strahlung*. PhD thesis, Max-Planck Institut für Physik und Astrophysik, München, 1977.
- [51] K.-H. A. Winkler, M. L. Norman, and D. Mihalas. Adaptive-mesh radiation hydrodynamics–i. the radiation transport equation in a completely adaptive coordinate system. *Journal of Quantitative Spectroscopy and Radiative Transfer*, 31(6):473 – 478, 1984.
- [52] A. M. Winslow. Numerical solution of the quasilinear poisson equation in a nonuniform triangle mesh. *Journal of Computational Physics*, 1(2):149 – 172, 1966.
- [53] Y. Zhang, Y. Jia, and S. S. Wang. 2d nearly orthogonal mesh generation with controls on distortion function. *Journal of Computational Physics*, 218(2):549 – 571, 2006.



## Abstract

We study conservative numerical methods for implicit radiation hydrodynamics (RHD) in general non-steady coordinates in 2D and 3D.

We discuss fundamental mathematics and physics of RHD with special focus on differential geometric consistency and study numerical methods for nonlinear conservation laws. We apply Vinokurs theorem to obtain the strong conservation form for conservation laws in general curvilinear coordinates. Differential geometric derivations in this context lead to a reformulation of artificial viscosity in such general coordinates.

A non-static gravitation equation in order to avoid solving the Poisson equation for the gravitational potential is suggested.

It is shown that there is no coordinate system in 2D and 3D that contains the polar respectively spherical coordinates and allows multi-dimensionally adaptiveness. We suggest an ansatz to generate non-orthogonal non-steady coordinates that contain these orthogonal reference frames.

## Zusammenfassung

Wir untersuchen konservative, implizite numerische Methoden im Rahmen der Strahlungshydrodynamik (SHD) in allgemeinen Koordinaten.

Grundlegende mathematische und physikalische Konzepte werden mit speziellem Fokus auf geometrische Konsistenz diskutiert und numerische Methoden für nichtlineare Erhaltungssätze untersucht. Mit Hilfe des Vinokurschen Theorems lässt sich die konservative Form der Erhaltungssätze auf allgemeinen Koordinaten formulieren. Differentialgeometrische Überlegungen in diesem Zusammenhang führen zu einer Umformulierung der künstlichen Viskosität für solch allgemeine Koordinatensysteme.

Wir schlagen eine nicht-statische Gleichung für die Eigengravitation vor, um die Lösung der Poisson-Gleichung für das Gravitationspotential zu umgehen.

Es wird gezeigt, dass kein Koordinatensystem in 2D und 3D existiert, das die Polar- bzw. Kugelkoordinaten beinhaltet und mehrdimensionale Adaptivität des Gitters erlaubt. Wir schlagen einen Ansatz für nicht-orthogonale zeitabhängige Koordinaten vor, der diese Referenzgitter enthält.

## Curriculum Vitae

Name: **Harald HÖLLER Bakk.rer.nat**  
Datum und Ort der Geburt: **04. März 1983** in Villach, Österreich  
Eltern: Anna HÖLLER und Engelbert Viktor HÖLLER  
  
Adresse: Alszeile 119, 1170 Wien  
E-Mail: [harald.hoeller@univie.ac.at](mailto:harald.hoeller@univie.ac.at)  
Homepage: <http://homepage.univie.ac.at/harald.hoeller/>

### Stationen

- 2009, 2010** Lektor an der Fakultät für Physik - Lehrveranstaltungen aus Theoretischer Physik und Mathematischer Methoden.
- 08/2007-01/2010** Projektmitarbeiter bei *eLearnPhysik* - E-Learning an der Fakultät für Physik. Schwerpunkte waren die redaktionelle und technische Betreuung des Wiki der Fakultät für Physik, Content und Usability Fragen, sowie E-Learning im Bereich Theoretische Physik und der Einsatz von Computeralgebra in der Lehre.
- 2007, 2008** eTutor an der Fakultät für Physik - Lehrveranstaltungen aus Experimentalphysik sowie Theoretischer Physik und Mathematischer Methoden.
- 2007, 2008, 2009** Seminare und Workshops im Rahmen der KinderUni Wien, des Wissenschaftsclub für Jugendliche sowie der StauneLaune Forschungswochen.
- Sommer 2005, 2006** Ferialpraktikant bei Infineon Technologies Austria AG am Standort Villach im Bereich Forschung und Entwicklung.

## Schule und Studium

- seit 2005 Magisterstudium Astronomie.
- seit 2003 Diplomstudium Physik (Zweitstudium) an der Universität Wien.
- 2002, 2005 Zuerkennung von Leistungsstipendium.
- 2005 Abschluss des Bakkalaureatsstudiums Astronomie mit ausgezeichnetem Erfolg.
- 2005 Unterstellung in neuen Studienplan; Bakkalaureatsstudium Astronomie.
- 2001-2005 Diplomstudium Astronomie an der Universität Wien.
- 2001 Matura am BORG Klagenfurt mit ausgezeichnetem Erfolg.

## Publikation

- **Wiki Based Teaching and Learning Scenarios at the University of Vienna**, Harald Höller und Peter Reisinger, Vortrag auf der *World Conference on Educational Multimedia, Hypermedia & Telecommunications* (ED-MEDIA 30.06.-04.07.08, Technische Universität Wien), in den Proceedings erschienen.

## Eingeladene Vorträge

- **Hearing zum Finale des *Medida Prix 2009***, Franz Embacher, Harald Höller, Christian Primetshofer, Peter Reisinger, Brigitte Wolny - Vorstellung des Projekts *eLearnPhysik*, 15.09.2009, Berlin.
- **Phaidra, Wiki und die Content-Strategie der Fakultät für Physik**, Harald Höller, Peter Reisinger im Rahmen des *Phaidra Day an der Fakultät für Physik* am 01.10.2009 .
- **eLearnPhysik**, Franz Embacher, Harald Höller, Christian Primetshofer, Peter Reisinger - Vorstellung des Projekts im Rahmen der *Friday Lectures* am Projektzentrum Lehrentwicklung am 07.12.2007.